Broadcast and Multicast Communication Enablers for the Fifth-Generation of Wireless Systems

Deliverable D3.2

Air Interface

Version v3.00 Date: 2019/07/25

Document properties:

Grant Number:	761498
Document Number:	D3.2
Document Title:	Air Interface
Editors:	Eduardo Garro, Manuel Fuentes (UPV), Jordi Joan Gimenez (IRT), Jose Luis Carcel (SEUK)
Authors:	Eduardo Garro, Manuel Fuentes, David Gomez-Barquero (UPV); Jordi Joan Gimenez (IRT); Jose Luis Carcel (SEUK); De Mi, Hongzhi Chen, Ibrahim Hemadeh (UNIS); David Vargas (BBC); Dani Korpi (Nokia).
Reviewers	Lachlan Michael (SONY), Samuel Atsungiri (SONY)
Contractual Date of Delivery:	2019/07/25
Dissemination level:	Public
Status:	Final
Version:	3.00
File Name:	5G-Xcast_WP3_D3.2_v3.00

Abstract

This report investigates the 3GPP Release'15 (Rel'15) of 5G New Radio (NR), and extends the air interface to point-to-multipoint (PTM) communications. Two modes have been proposed in order to fulfil the different 3GPP requirements needed for broadcast and multicast. The 5G-Xcast Mixed Mode enables a dynamic and seamless switching between Point-to-Point (PTP) and PTM transmissions both in the downlink and the uplink. It reuses the NR Rel'15 air interface specification. The 5G-Xcast Terrestrial Broadcast Mode enables the reception of the service to users without uplink capabilities, i.e. being a downlink-only mode. One of its design principles is the transmission over large coverage areas in order to enable High-Power High-Tower (HPHT) network configurations. This deliverable also provides an evaluation of the 5G NR Rel'15 unicast specifications. In addition, the two 5G-Xcast PTM solutions are evaluated in order to demonstrate the more efficient use of the radio resources and their advantages over PTP for the scenarios considered in 5G-Xcast.

Keywords

5G New Radio, Point-to-Multipoint, Multicast, Broadcast, Radio Access Network, Key Performance Indicators, Link Level Simulations, System Level Simulations, Coverage Simulations, IMT-2020 evaluation.

Revision History

Revision	Date	Issued by	Description
V1.00	31/05/2018	Eduardo Garro	Interim version
V2.00	2018/11/30	Eduardo Garro	Final version
V3.00	2019/07/25	Eduardo Garro	Terrestrial Broadcast, new KPIs added

Disclaimer

Executive Summary

This report investigates the 3GPP Release'15 (Rel'15) of 5G New Radio (NR), and extends the air interface to point-to-multipoint (PTM) communications. Two specific 5G PTM technologies are proposed in order to fulfil the different 3GPP requirements needed for broadcast and multicast, as well as those derived from the 5G-Xcast use cases defined in Deliverable D2.1. These technologies are the Mixed Mode and the Terrestrial Broadcast Mode. 5G-Xcast partners have been contributing to the 3GPP Rel'16 discussions in order to detect missing functionalities that are needed to fulfill the agreed PTM requirements.

The 5G-Xcast Mixed Mode enables a dynamic and seamless switching between Point-to-Point (PTP) and PTM transmissions both in the downlink and the uplink. This solution is envisaged for the different verticals of the 5G-Xcast project, i.e. media and entertainment, automotive, internet of things (IoT) and public warning. It reuses the NR Rel'15 air interface specification as much as possible to ensure the maximum compatibility with PTP. However, some modifications are included such as the discovery of the scheduling information to a group of users is enabled by the introduction of a Group Radio Network Identifier (G-RNTI), and a multiple cell coordination that is enabled by forcing the same cell scrambling sequence to the neighbouring Next Generation NodeBs (gNB). Negative numerologies as well as the concept of mini-slots are also included to support SFN areas and larger deployments.

The 5G-Xcast Terrestrial Broadcast Mode enables the reception of the service to users without uplink capabilities, i.e. being a downlink-only mode. The key design principle is the reuse of the existing 5G-NR design for Mixed-Mode operation with the necessary extensions to deliver Terrestrial Broadcast services. This includes enabling transmission over small, medium and large coverage areas including from Low-Power Low-Tower (LPLT) to High-Power High-Tower (HPHT) stations. To make this possible, different configurations are enabled to operate Multi-Frequency Network (MFN) and Single Frequency Network (SFN) deployments. In particular, the necessity to cope with large delay spread (in HPHT MFN due to natural echoes and in HPHT SFN due to large inter-site distance) impose important changes in the air-interface design. To allow very large Inter-Site Distances (ISDs) in Single Frequency Networks (SFNs), as required by the 3GPP requirements, very narrow carrier spacing (more than those provided in the Mixed Mode), new cyclic-prefix values and reference signals are include in NR. In addition, special attention is given to the LTE Cell Acquisition Subframe (CAS) taking into account new design possibilities in NR

This deliverable also provides an evaluation of the 5G NR Rel'15 unicast specifications against specific Key Performance Indicators (KPIs), as defined in the IMT-2020 guidelines. It includes analysis, inspection and link-level simulations. In addition, the two 5G-Xcast PTM solutions are evaluated in order to demonstrate the more efficient use of the radio resources and their advantages over PTP for the scenarios considered in 5G-Xcast.

Table of Contents

List of Figures

List of Tables

List of Acronyms and Abbreviations

3GPP	3rd Generation Partnership Project
5G	5th Generation
ACK	Acknowledgment
AL	Aggregation Level
AMC	Adaptive Modulation and Coding
ATSC	Advanced Television Systems Committee
AWGN	Additive White Gaussian Noise
BER	Bit Error Rate
BICM	Bit-Interleaved Coded Modulation
BLER	Block Error Rate
BW	Bandwidth
CA	Carrier Aggregation
CB	Coded Block
CAS	Cell Acquisition Subframe
CCE	Control-Channel Elements
CNR	Carrier-to-Noise Ratio
CQI	Channel Quality Indicator
CoMP	Coordinated MultiPoint
CORESET	Control-resource Sets
CP	Cyclic Prefix
CR	Coding Rate
CRC	Cyclic Redundancy Check
C-RNTI	Cell-Radio Network Temporary Identifier
CSI	Channel State Information
CSI-RS	Channel State Information Reference Signals
DCI	Downlink Control Indicator
DL	Downlink
DMRS	Demodulation Reference Signals
DTT	Digital Terrestrial Television
eMBB	enhanced Mobile Broadband
eMBMS	evolved Multimedia Broadcast Multicast Service
eNB	eNodeB
FEC	Forward Error Correction
FFT	Fast Fourier Transform
FR	Frequency Range
G-RNTI	Group-Radio Network Temporary Identifier
HARQ	Hybrid Automatic Repeat Request
HPHT	High Power High Tower
ICI	Inter-Carrier Interference
i.i.d.	independent and identically distributed
IMT	International Mobile Telecommunication
IoT	Internet of Things
ISD	Inter-Site Distance
ITU	International Telecommunication Union
KPI	Key Performance Indicator
LDPC	Low Density Parity Check
LoS	Line-of-Sight
LPLT	Low-Power Low-Tower
LTE	Long Term Evolution
LTE-M	LTE for Machines
MAC	Medium Access Control
MBSFN	MBMS over Single Frequency Networks
MC-MM	Multiple Cell Mixed Mode
MCS	Modulation and Coding Scheme
MIB	Master Information Block

MIMO	Multiple Input Multiple Output
ML	Maximum Likelihood
mMTC	massive Machine Type Communications
M&E	Media and Entertainment
NB-IoT	NarrowBand IoT
NLoS	Non-LoS
NR	New Radio
NSA	Non-Standalone
NUC	Non-Uniform Constellation
OFDM	Orthogonal Frequency Division Multiplexing
OH	Overhead
PBCH	Physical Broadcast Channel
PDCCH	Physical Downlink Control Channel
PDSCH	Physical Downlink Shared Channel
PHICH	Physical HARQ Indicator Channel
PRACH	Physical Random Access Channel
PSS	Primary Synchronization Signal
PTM	Point-to-Multipoint
PTP	Point-to-Point
PT-RS	Phase Tracking Reference Signals
PUCCH	Physical Uplink Control Channel
PUSCH	Physical Uplink Shared Channel
PW	Public Warning
QAM	Quadrature Amplitude Modulation
QoS	Quality of Service
QPSK	Quadrature Phase Shift Keying
RAN	Radio Access Network
RB	Resource Block
RE	Resource Element
REG	Resource Element Group
Rel	Release
RF	Radio Frequency
RLC-UM	Radio Link Control-Unacknowledged Mode
RMSI	Remaining System Information
ROM	Receive Only Mode
RRM	Radio Resource Management
RS	Reference Signals
SA	Stand-Alone
SC-MM	Single Cell Mixed Mode
SC-PTM	Single Cell – Point-to-Multipoint
SCS	Subcarrier Spacing
SFI	Slot Format Indicator
SFN	Single Frequency Networks
SIB	System Information Block
SISO	Single Input Single Output
SoA	State of the Art
SRS	Sounding Reference Signals
SSS	Secondary Synchronization Signals
SS/PBCH	Synchronization Signals/PBCH
TDL	Tapped Delay Line
TM	Transmission Mode
TR	Technical Report
TS	Technical Specification
TU-6	Typical Urban 6 taps
TV	Television
UE	User Equipment
UL	Uplink

URLLC	Ultra Reliable and Low Latency Communications
V2X	Vehicular to everything
WP	Work Package

1 Introduction

1.1 5G Development Status

The first 3GPP release of 5G, i.e. Release'15 (Rel'15) has been structured in three phases. An early drop non-standalone (NSA) version was initially approved in December 2017. This version relies on both Long Term Evolution (LTE) and New Radio (NR) air interfaces and reuses the LTE core network. It also focuses on the user plane and makes use of LTE for the control plane. In June 2018, a 5G stand-alone (SA) version was specified. It additionally includes a fully 5G core network and has full user and control plane capabilities. The last drop of Rel'15 is expected to be released at the end of 2018 and it will enable the 5G core to inter-work equally with both LTE RAN and NR RAN.

The NR air interface brings a large number of improvements compared to LTE to address the new IMT-2020 requirements of enhanced mobile broadband (eMBB) and ultra-reliable low-latency communication (URLLC) services[1], as well as to cover an extensive number of use cases for the digitalization of new industries (also known as verticals). The main improvements in the air interface are more efficient Forward Error Correction (FEC) codes, large bandwidths, new OFDM waveform numerologies that adapt to the new spectrum bands and bandwidth allocations, dynamic frame structures, or massive MIMO (Multiple-Input Multiple-Output) schemes, among others [1]. However, NR Rel'15 only supports point-to-point (PTP), which may be inefficient when transmitting the same content to a large number of users simultaneously [2]. In fact, the deliverable D2.1 of 5G-Xcast [3] describes a series of use cases from 4 verticals where point-to-multipoint (PTM) would improve the overall performance in 5G: media and entertainment (M&E), vehicle-to-everything (V2X) communications, Internet-of-Things (IoT) and public warning. PTM transmissions are also useful in other verticals such as airborne communications (e.g. use of drones).

3GPP identified a flexible broadcast/multicast service as a basic feature to be used in 5G systems [4] and reference [5] sets out multicast/broadcast requirements in 3GPP for next-generation access technologies. The support of broadcast and multicast capabilities in 5G was discussed in Rel'16 and a new Study Item (SI) called "*LTE-based 5G Terrestrial Broadcast*" was approved. Although this SI is highly related to the project, it is based on LTE enTV solutions. Therefore, it has been included as part of deliverable D3.1. There are no plans in 3GPP for the use of PTM in 5G NR Rel'16. This study has been postponed, at least, to Rel'17.

1.2 Objectives of the document

This deliverable presents the 5G-Xcast air interface that enables the use of multicast and broadcast in 5G NR. In addition to the 3GPP requirements provided in [4] and [5], it also considers the limitations of eMBMS Rel'14 analysed in D3.1 [6] and published in [7]. This deliverable also leverages on D3.3 and D3.4, which define the RAN logical architecture and RAT protocols to enable PTM in NR respectively.

3GPP has followed an approach in which two different tracks are identified for PTM in 5G: a NR mixed mode with multicast capabilities [8] and a terrestrial broadcast mode based on LTE enTV for Rel'16 [9]. With the approach in 5G-Xcast, the transmission of linear TV/radio services is not relegated to LTE but included in 5G-NR as a configuration

[1] IMT-2020 requirements for massive Machine-Type Communications (mMTC) will be addressed with LTE IoT (Internet-of-Things) solutions LTE-M (LTE for Machines) and NB-IoT (Narrow-Band IoT).

option over the Mixed-Mode approach. For downlink-only LPLT or HPHT MFN deployments, the design is similar to that for the Mixed-Mode. The main difference between both modes come from the support of large delay spread in large-area SFN.

1.3 Structure of the document

This document is structured as follows. Chapter 2 provides a high-level description of the 5G NR air interface as specified in 3GPP for unicast. Chapter 3 describes in detail the extensions considered in 5G-Xcast for the use of broadcast in 5G. NR Rel'15 unicast is evaluated in Chapter 4 against the IMT-2020 Key Performance Indicators (KPIs) and requirements. The 5G-Xcast PTM air interfaces are also evaluated in Chapter 5 in order to demonstrate their potential benefits and improvements compared to unicast. Chapter 6 summarises the findings of this work. Additionally, Annex A describes in detail the block diagrams of the NR physical downlink channels that have been evaluated. Annex B provides the calibration results obtained to validate the simulators used in this deliverable.

2 5G Point-to-Point Air Interface Overview

This section provides a brief description about the physical layer of the NR Point-to-Point (PTP) solution. Frame structure, physical downlink channels as well as acquisition and feedback procedures are described in the following subsections.

2.1 Frame Structure

Both downlink and uplink physical channels in NR are organized into frames with 10 ms duration each. Frames are divided in turn into 10 subframes, with each subframe having a fixed duration of 1 ms. The number of OFDM symbols in a subframe will depend on the carrier spacing in the frequency domain, which is directly linked to the term **numerology**, and the **type of cyclic prefix (CP)**. Multiple numerology options are defined by μ, a positive integer factor. OFDM symbols are also grouped in slots. With normal CP each slot conveys 14 OFDM symbols. With extended CP (only available with numerology μ=2), there are 12 OFDM symbols per slot. An illustrative example of framing structure for numerology μ=0 is shown in Figure 1.

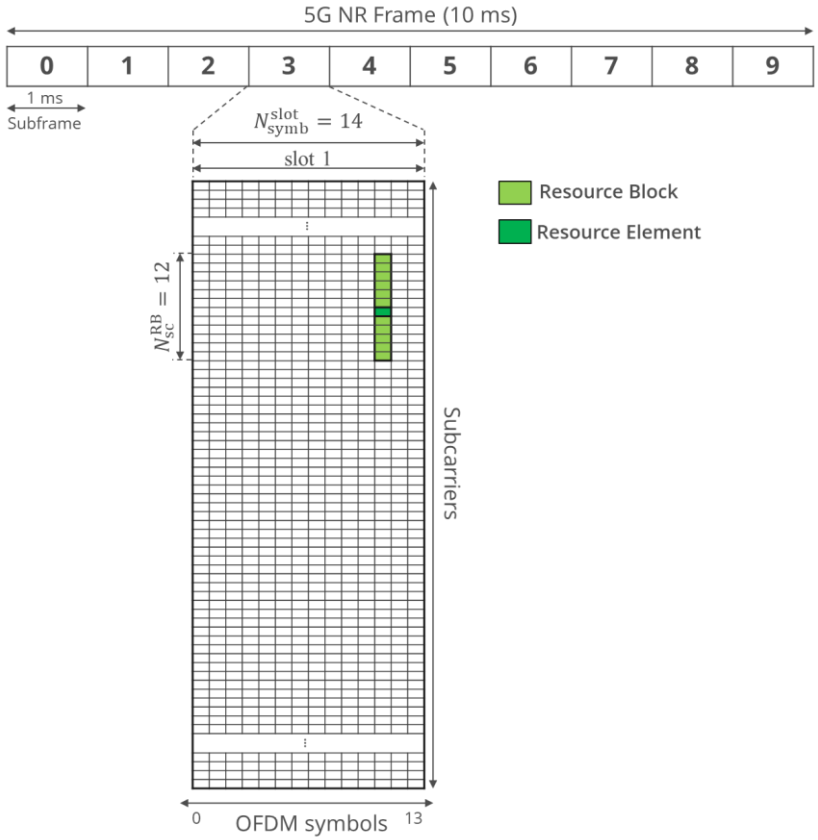

Figure 1. NR Framing structure (μ = 0).

In the frequency domain, each OFDM symbol contains a fixed number of subcarriers. This number also depends on the numerology selected, but also on the total bandwidth. Note that each OFDM symbol can be assigned to downlink or uplink transmissions depending on the Slot Format Indicator (SFI), which allows flexible assignment for Time Division Duplex (TDD) or Frequency Division Duplex (FDD) operation modes. In any case, a **Resource Element (RE)** is defined as 1 subcarrier in a OFDM symbol, and a

Resource Block (RB) is defined as a group of 12 REs in frequency. The REs are separated with a specific carrier spacing (SCS), calculated as follows:

$$SCS = 2^{\mu} \cdot 15\ kHz \quad (1)$$

The influence of different numerologies on the framing parameters is shown in Table 1.

Table 1. 5G air interface parameters: numerology (μ), subcarrier spacing, useful symbol duration (T_U), CP duration (T_{CP}) and slots per subframe.

μ	SCS (kHz)	T_U (μs)	Type CP	T_{CP} (μs)[2]	Slot (μs)	slots/subframe
0	15	66.66	Normal	5.21/4.69	1000	1
1	30	33.33	Normal	2.60/2.34	500	2
2	60	16.66	Normal	1.30/1.17	250	4
			Extended	4.16	250	4
3	120	8.33	Normal	0.65/0.59	125	8
4	240	4.17	Normal	0.33/0.29	62.5	16

Different bandwidths are available depending on the different frequency ranges [10]. While FR1 (450 MHz - 6 GHz) allows bandwidths from 5 MHz up to 100 MHz, FR2 (24.25 GHz - 52.6 GHz) offers values from 50 MHz up to 400 MHz. A more detailed explanation is provided in Section 3.

2.2 Physical Channels and Signals

Channels are known as flows of information transmitted between different protocol layers. Thanks to them, the different types of data are separated and transported across different layers. Whereas physical channels carry MAC layer information, physical signals are only used by the physical layer. The physical channels and signals for downlink and uplink transmissions are described next.

2.2.1 Physical Downlink Channels and Signals

Different physical channels and signals are used in downlink transmissions depending on its functionality:

- **Physical Broadcast Channel (PBCH):** Transmits the static part of the System Information (SI), known as the Master Information Block (MIB), to all the UEs requiring to access the network.
- **Physical Downlink Control Channel (PDCCH):** Specifies the scheduling and allocation of the data content for every UE that requests it. It also configures HARQ retransmission, link adaptation and MIMO parameters.
- **Physical Downlink Shared Channel (PDSCH):** Transmits the data content to the UE and the System Information Blocks (SIBs).
- **Primary and Secondary Synchronization Signals (PSS, SSS):** Together with PBCH they are needed for allowing the UE network access. Specifically, provide radio frame timing information and Cell ID at the initial cell search. In addition, they are also used for the beam management in IDLE state.
- **Demodulation Reference Signals (DMRS):** Used for the channel estimation in order to allow the proper demodulation of PBCH, PDCCH and PDSCH.

[2] For Normal CP, two CP lengths are (first OFDM symbol / rest of OFDM symbols).

- **Phase Tracking Reference Signals (PT-RS):** Used to estimate the phase noise in the PDSCH. They are only used at high frequency ranges (FR2).
- **Channel State Information Reference Signals (CSI-RS):** Used to provide channel state information (CSI) needed for link adaptation. It is also used for beam management in CONNECTED state.

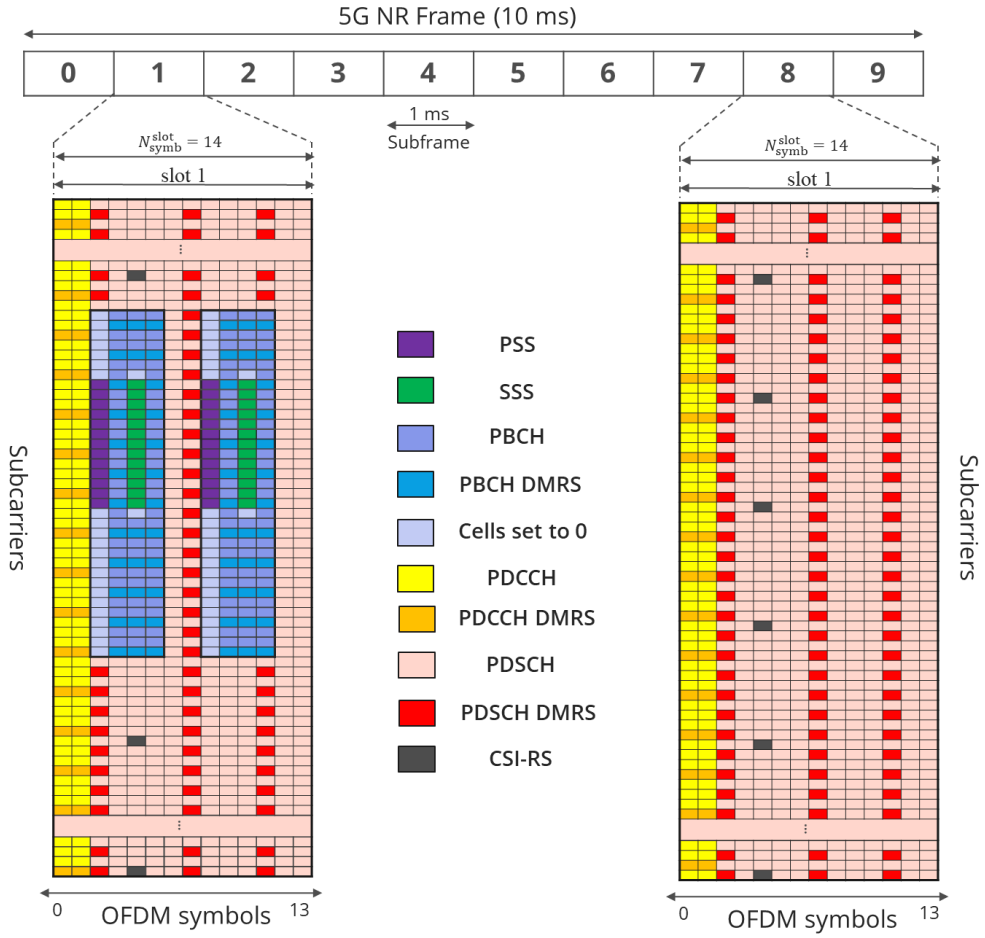

Figure 2. Framing structure for SFI=0 (10 subframes, 100% downlink).

Physical channels and signals are allocated in a frame as shown in Figure 2. In this particular case, the SFI value is 0, which means that the 14 OFDM symbols are allocated to the downlink. From this figure, the physical channels and physical signals are allocated as follows:

PSS / SSS / PBCH / PBCH-DMRS:

Grouped in SS/PBCH blocks, where each SS/PBCH block consists of 240 subcarriers and 4 OFDM symbols [11]. PSS signals are allocated in the first OFDM symbol within a SS/PBCH block, while SSS signals are distributed across the third OFDM symbol. The PBCH and PBCH-DMRS signals are transmitted in the second, third and fourth OFDM symbol. Cells set to 0s are used as padding to complete the block structure. There are four available numerology options within the block, μ = {0,1,3,4}, which are selected depending on the frequency range. The allocation of SS/PBCH blocks in the frequency domain is specified by the higher-layer parameter *ssb-subcarrierOffset*. In the time domain, SS/PBCH blocks are sent in periodical burst sets, where the number of SS/PBCH blocks transmitted in each burst (number of antenna beams) depends on the

numerology and the frequency band of operation [12]. An example of SS/PBCH block allocation within a slot is given in Figure 3.

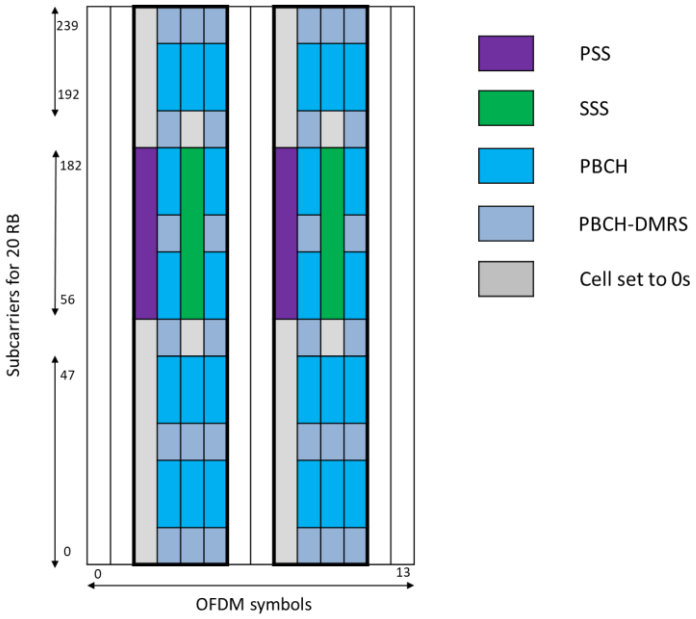

Figure 3. SS/PBCH block allocation within a slot

PDCCH:

The control information specifies the data scheduling and allocation for each UE by means of the Downlink Control Information (DCI). This information is mapped within the PDCCH in one or more control-channel elements (CCE). The number of CCEs allocated in the PDCCH depends on the Aggregation Level (AL), which has five possible values {1,2,4,8,16}. Each CCE consists of 6 REGs, where a REG is defined as one RB allocated in one OFDM symbol. REGs are mapped in control-resource sets (CORESETs) for a given numerology. The total number of REGs associated to each UE is mapped within PDCCH in CORESETs packets allocated in a specific control region. Hence, the minimum CORESET length is equal to 6 RBs x 12 REs/RB = 72 REs (1.2 MHz for μ = 0). The allocation of CORESETs in the frequency domain is specified by higher-layer parameters. Regarding the time domain allocation, CORESETs can be transmitted at OFDM symbols 0,1 or 2 of subframes which do not contain SS/PBCH blocks. CORESET content can be distributed at most over three consecutive OFDM symbols, depending on high layer parameters. CORESET also includes DMRS signals to allow the correct demodulation of the PDCCH. Figure 4 (left) illustrates a possible CORESET allocation with AL = 1.

PDSCH:

It contains SIBs and data content from the DL-SCH transport channel. In particular, PDSCH is distributed in the remaining REs where the SS/PBCH and PDCCH are not allocated. The number of RBs associated to PDSCH transmissions depends on the available bandwidth and numerology. As for PBCH and PDCCH, PDSCH also includes DMRS in order to ease the demodulation process. DMRS allocation depends on the selected DMRS pattern. In addition, PDSCH also includes PT-RS and CSI-RS. An example of PDCCH and PDSCH allocation as well as RS is shown in Figure 4 (right).

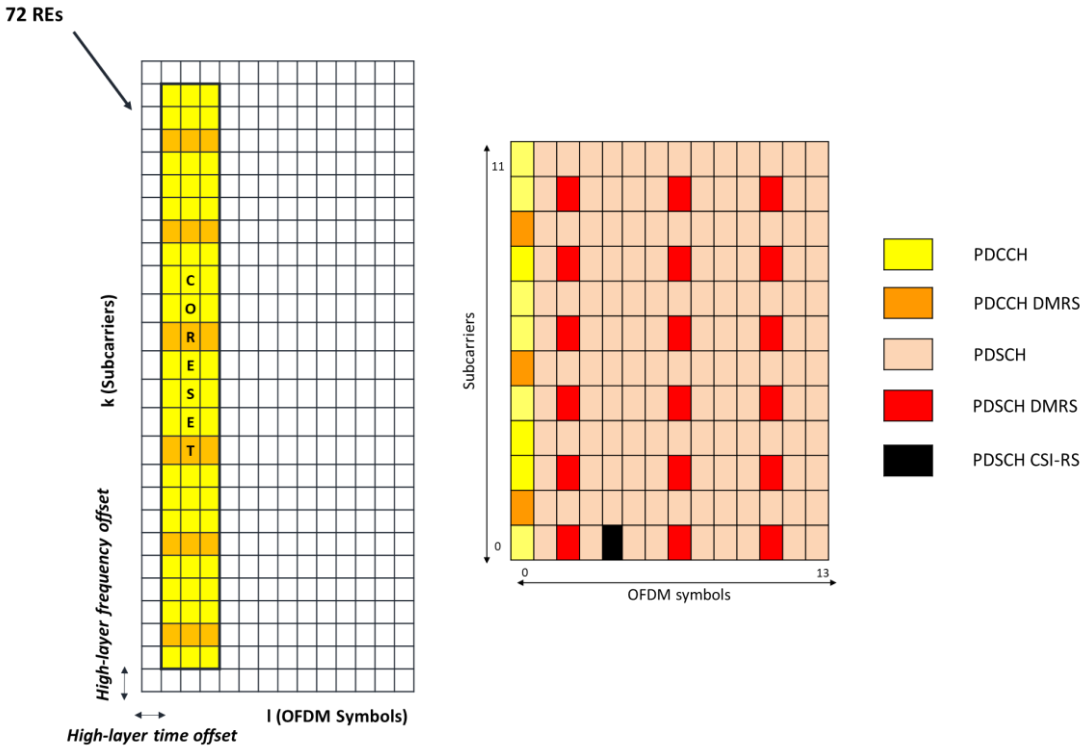

Figure 4. CORESET allocation with AL = 1 (left). PDSCH resources in a slot (right).

2.2.2 Physical Uplink Channels and Signals

Different physical channels and signals are also used in the uplink:

- **Physical Random Access Channel (PRACH):** Used by the UE to request the uplink initial access. It is also used during the beam management process.
- **Physical Uplink Control Channel (PUCCH):** Carries Uplink Control Information (UCI). UCI contains different information such as CSI, HARQ retransmission and scheduling requests.
- **Physical Uplink Shared Channel (PUSCH):** Transmits the data content to the gNB. Optionally, it can also convey UCI transmissions.
- **Demodulation Reference Signals (DMRS):** Used for the channel estimation in order to allow the proper demodulation of PUCCH and PUSCH.
- **Phase Tracking Reference Signals (PT-RS):** Used for the same functionality than in downlink case.
- **Sounding Reference Signals (SRS):** It is equivalent to CSI-RS for uplink. Therefore, it provides CSI to the gNB in order to configure link adaptation and scheduling at the UL.

2.3 Acquisition Procedure

Acquisition is a basic procedure that enables the connection of UEs to the network and provides basic information required to receive the data information carried in the PDSCH. The acquisition procedure involves the use of PSS, SSS, PBCH, PDCCH, PDSCH and PRACH as shown in Figure 5.

The acquisition procedure starts when the UE receives the SS/PBCH block. It includes PSS and SSS, which provide frame synchronization and information of the physical cell identity. Both synchronization signals are transmitted together with the PBCH. PBCH

payload contains a Master Information Block (MIB), which provides minimum system information to all UEs. It also specifies the parameter configuration needed to access the Remaining System Information (RMSI) CORESET, which is sent over the PDCCH. An RMSI CORESET carries a special DCI to provide the System Information Block 1 (SIB1) scheduling. SIB1 contains information related to the availability and scheduling of other SIBs within the cell (whether they are provided via periodic broadcast basis or only on-demand basis) [13]. SIB1 is sent over PDSCH.

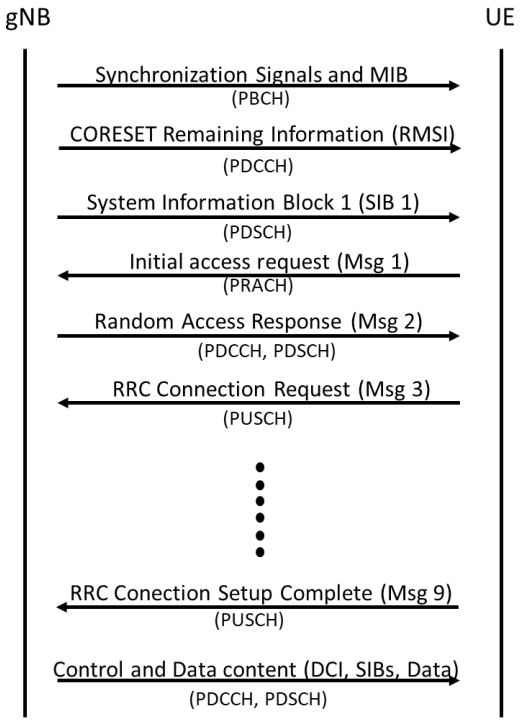

Figure 5. NR Rel'15 acquisition procedure.

When UEs request a particular SIB, the PRACH uplink channel starts the initial access with message 1 (Msg 1). Following the initial access request, gNB sends a random access response (Msg 2) through PDCCH and PDSCH. Then, the UE requests the RRC connection with Msg 3, sent via PUSCH. RRC Connection is carried through a message exchange process. Once RRC Connection has been completed, the UE acquires the Cell-Radio Network Temporary Identifier (C-RNTI), which uniquely identifies the link between the gNB and the UE. Afterwards, gNB sends in the PDCCH the DCI, which is CRC encoded and specifies where specific data is scheduled. The CRC sequence is scrambled by the C-RNTI, which disables the reception of the serving UE content for the rest of UEs. Once the DCI is decoded, the UE obtains the data allocation inside the PDSCH. Finally, the UE accedes to its corresponding data region, which is also scrambled with the C-RNTI.

2.4 Feedback

Feedback procedures are possible thanks to the uplink. They are also known as link adaptation schemes. The three main link adaptation schemes are: Hybrid Automatic Repeat Request (HARQ), Adaptive Modulation and Coding (AMC), and Close-Loop MIMO.

- **HARQ:** used to perform physical layer retransmissions enabling transmitters to use higher code rates for a fixed MCS selection while decreasing the number of received errors. HARQ ACK are transmitted in PUCCH, while data retransmissions are sent via PDSCH.
- **AMC**: adaptive MCS selection mechanisms that provide significant spectral efficiency gains by means of CSI, Channel Quality Indicator (CQI) and HARQs. [14]. The UE feedback is typically utilized by two adaptation mechanisms: inner loop link adaptation (ILLA), and outer loop link adaptation (OLLA). ILLA adjusts the modulation and coding scheme (MCS) explicitly based on the CQI feedback, using a predefined MCS table. Since it is unusual that ILLA alone can ensure the desired block error rate (BLER), due to various inaccuracies in the CQI measurement and reporting, OLLA is used to fine-tune the MCS selection. Essentially, it observes the HARQ feedback provided by the UE and calculates a correction factor for the CQI accordingly. ILLA then uses this corrected CQI to determine the optimal MCS, and the desired BLER is thereby achieved.

3 5G Point-to-Multipoint Air Interface Design

3.1 Introduction

Deliverable D3.1 [6] of this project analysed a series of limitations from the air-interface perspective in Release 14 LTE-Advanced Pro. This technology provides two broadcast mechanisms, i.e. Single-Cell Point to Multipoint (SC-PTM) and Multicast Broadcast SFN (MBSFN). D3.2 will consider these limitations in order to overcome them. Although a more efficient and advanced air-interface in Rel'15 will improve some of the limitations found in LTE, other limitations should be overcome through the design of specific solutions for the use of broadcast and multicast.

3.1.1 Summary of RAN Technical Requirements

The 5G-Xcast solution should provide a flexible and optimized RAN, able to adapt to the specific constrains of the relevant four vertical sectors considered in the project. In particular, the 5G-Xcast RAN should allow optimizing radio resources as well as providing further interactivity through enhanced PTM (broadcast/multicast) transmissions and feedback mechanisms from the users. The RAN solution should provide flexibility on the available waveform parameters (OFDM parameters such as CP and inter-carrier spacing) to allow different types of network deployments such as HPHT and LPLT. This would allow the system to efficiently use the best network to provide better coverage in different environments, such as indoor, outdoor, fixed or vehicular.

A flexible RAN would also facilitate the orchestration of the network to provide a seamless experience when the users move across environments. With the increased quality of video formats (e.g., UHDTV) and new experiences such as Virtual Reality (VR) broadcast, the new RAN requires significantly larger data rates from both physical layer (i.e., advanced signal processing algorithms and use of MIMO) and network deployment point of views (i.e., efficient frequency reuse).

Efficient PTP/PTM multiplexing techniques in the same frequency band as well as the ability to switch between them can unlock the potential of the use cases identified in WP2. It is key that the new PTM configuration does not imply significant changes neither to the radio air interface nor to the radio technology protocols. This will facilitate the integration of PTM transmissions in 5G.

New use cases such as VR broadcast and remote live production require Gbps communications and extremely low latencies. Furthermore, they may require the use of new frequency bands with wide bandwidth allocations. The 5G-Xcast RAN solution should not be restrictive on the type of frequency bands to allow these use cases. On the other hand, PW and IoT use cases require significantly less data rates than the previous aforementioned cases. Instead, they require high reliability and low energy consumption requirements, and the 5G-Xcast RAN solution should support them thanks to a flexible frame configuration.

3.1.2 Summary of Potential Limitations of LTE Broadcast RAN

The LTE eMBMS RAN is configured with rigid OFDM numerology parameters that limit the type of network deployment. Both MBSFN and SC-PTM Rel'14 solutions suffer these limitations. This naturally hinders LTE eMBMS in supporting the requirements of different network deployments, such as high coverage and high mobility in large area deployments for the hybrid broadcast service. Note that some of the requirements are challenging even for 5G Rel'15 PTP technology, such as the extremely high data rate and low end-to-end latency required in the virtual/augmented reality broadcast or in the

remote live production scenarios. In addition, the lack of feedback channels in some of the LTE eMBMS modes, e.g. LTE enTV, may disable the essential features of the network, e.g., supporting dynamic optimisation of resource allocation or providing useful audience metrics. Compared to ATSC 3.0 and DVB technologies such as DVB-NGH, where spatial multiplexing techniques, longer CPs and high constellation sizes are available, eMBMS Rel'14 is very limited and unable to support certain network deployments, e.g., large area deployment with high spectral efficiencies.

The setup of an MBSFN area and related radio parameter configurations within the RAN is done statically, thereby limiting the dynamic provisioning of such services based on real-time traffic demands. Additionally, eMBMS requires a separate user-plane infrastructure for connectivity of the RAN with the core network as well as for special MBSFN subframes over the air interface. While SC-PTM enables scheduling of data using PDSCH, the infrastructure requirements are similar to MBSFN. These aspects lead to a significantly large footprint in added infrastructure investments for the network operator as well as additional implementation complexity in the UE. Furthermore, this prompts the requirement of special middleware for reliable reception of such data.

One of the key design principles adopted for the 5G RAN design would be to limit the added footprint for delivering PTM services over the existing PTP infrastructure and physical layer design. This would limit investment costs and implementation complexity. The LTE eMBMS radio session setup procedure is complex and time-consuming. This requires simplification in 5G for enabling fast and efficient 5G-Xcast RAN sessions.

3.2 Single Cell Mixed Mode (SC-MM)

The 5G-Xcast project has designed an extension of the 5G Rel'15 air-interface to enable the dynamic allocation of unicast and multicast resources within a single cell. This extension is called Single-Cell Mixed Mode (SC-MM). SC-MM has been designed considering the 5G NR Rel'15 unicast air interface as a reference. It reuses as much as possible the existing air interface components, i.e. coding, framing, scheduling and physical channels employed, but also includes some mandatory modifications to enable PTM services and transmit them in the most efficient way.

Only some changes are introduced in the physical control channels, i.e. PDCCH and PUCCH. Regarding the PDCCH, in addition to the C-RNTI already provided for unicast, a new temporary identifier defined as Group-RNTI (G-RNTI) is proposed in order to enable scheduling and channel acquisition for entire groups of users. This modification leads to the definition of a new DCI format for PTM. The potential use of only one CORESET in order to minimize the PDCCH overhead and therefore maximize the PDSCH resources is also analysed. In the uplink, an efficient use of feedback for group communications may also be needed in the PUCCH to efficiently ensure adequate QoS per group of users (e.g. via link adaptation schemes and HARQ retransmissions).

3.2.1 Modifications Introduced in the Downlink (PDCCH)

The C-RNTI plays a key role in the reception of scheduling information and de-scrambling of data. Based on this mechanism, it is possible to define a common identifier, G-RNTI, so that several UEs interested in the same content transmitted over a single cell can be easily grouped. The G-RNTI should be acquired during the RRC connection, as done with the C-RNTI. When UEs acquire a G-RNTI, the corresponding CRC is descrambled and the DCI is decoded. DCIs can be configured with different formats. The 5G-Xcast project has considered the use of the DCI Format 1_0 for the SC-MM, which is based on the PTP downlink format and offers a useful payload of 30 bits. However,

new DCI formats particularly designed for PTM communications could additionally be considered.

The introduction of the G-RNTI enables a dynamic scheduling between PTP and PTM within the PDSCH channel, thus allowing to create a flexible and scalable air interface solution. The basic mechanism behind this process is illustrated in Figure 6.

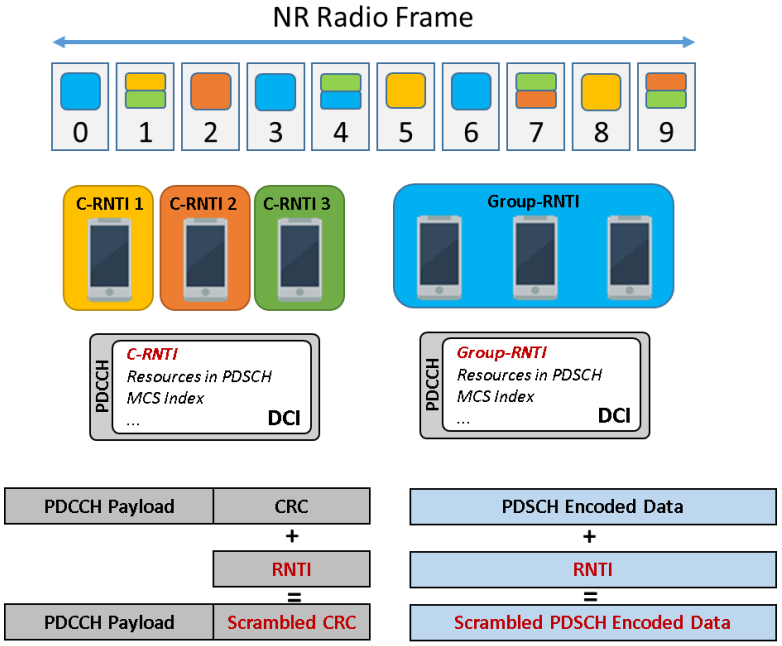

Figure 6. C-RNTI for PTP versus G-RNTI for PTM communications.

In PTM transmissions, a DCI could be transmitted within a single CORESET for a group of UEs interested in the same content. This solution avoids replication and a transmission where several CORESETs announce the same data to all users. This modification reduces considerably the PDCCH overhead within a NR frame. As an example, Table 2 shows the number of REs in CORESETs needed for PTP with different numbers of UEs, and compares the results to the SC-MM solution proposed. Naturally, the larger the number of users, the higher the overhead reduction introduced. For instance, when 10 UEs request the same content, the PDCCH overhead is reduced a 90%.

Table 2. Number of Resource Elements (REs) allocated for PDCCH CORESET with different number of UEs for PTP and SC-MM.

Number of UEs	Number of REs PTP	Number of REs SC-MM	Overhead Reduction (%)
2	144	72	50%
3	216		66%
5	360		80%
10	720		90%

3.2.2 Modifications Introduced in the Uplink (PUCCH)

Additionally, new uplink mechanisms such as AMC link adaptation or HARQ retransmissions can be adopted to enable a more efficient SC-MM. Link adaptation is

performed over groups of users depending on the number of requests. If few UEs demand the same content in the same cell, AMC is performed based on CSI feedback. However, if the number of UE requests is fairly large, it is assumed that the selected MCS fulfils the majority of UEs requirements. It can be shown that if the number of UEs is sufficiently large, at least one of them experiences very poor link quality, and thereby only a more robust MCS needs to be considered. In the simplest case with a very large number of UEs requesting the same content, a fixed MCS can be chosen based on a statistical BLER requirement. In such a case, no feedback is therefore necessarily required. The use of link adaptation schemes can be considered as one of the most efficient feedback solutions in multicast contexts [15]. Section 5.2.2.1 of D3.4 [16] conducts link adaptation analysis for PTM transmission with heuristic fixed offsets as well as adaptive MCS via CQI report from a UE that has the worst radio link, SU-MIMO Precoding Matrix Indicator (PMI) and Rank Indicator (RI) settings. It was found that the cyclic PMI outperforms 95% coverage as compared to fixed PMI for rank 1 and the diversity benefits of rank 2 are exhibited at lower packet loss rates for the same PMI setting, but saturate at higher packet loss rates. In addition, it was also shown that for adaptive MCS the worst-UE PMI settings outperform cyclic PMI settings.

Group HARQs can be additionally considered for the SC-MM solution. When several UEs request a HARQ/ACK retransmission via PUCCH, gNB sends a joint retransmission via PDSCH to all of them. Different studies have proved that HARQ feedback provides noticeable performance improvements in SC-PTM systems. However, the use of HARQ may also introduce some limitations depending on the number of UE requests. Considerable overheads and latency may be introduced when large numbers of UEs ask for retransmissions [17]. In addition, the use of HARQ also requires an increase of the buffer capacity at the transmitter and the receiver to store the different packet retransmissions.

3.3 Multiple Cell Mixed Mode (MC-MM)

One of the main drawbacks in SC-MM is the inefficiency to cover multiple cell areas due to inter-cell interferences encountered at the cell edge. The coverage can be drastically extended by means of multiple cell coordination. Two different mechanisms can be adopted in this case. The first one is called Coordinated MultiPoint (CoMP), and its study is studied in task 3.4 (Radio Resource Management). The second mechanism is a Single Frequency Network (SFN) deployment, which affects the air-interface. This mechanism is considered in this section and has been included as part of the Multi-Cell Mixed Mode (MC-MM). MC-MM takes the SC-MM air interface design as a baseline and adds some modifications on the cell specific scrambling sequence to support SFN capabilities. This section additionally analyses the coverage improvements that this additional mode could bring, as well as the potential benefits of a feedback coordination between serving cells.

3.3.1 Common Cell Scrambling Sequence

A cell specific scrambling sequence is a pseudo-random process used to determine the control, data and DMRS positions. The initialization of the scrambling sequence depends on the $N_{ID}^{n_{SCID}}$ parameter and can be performed in two ways. It can be defined as the physical layer cell ID, $N_{ID}^{n_{SCID}} = N_{ID}^{cell}$. N_{ID}^{cell} , which depends on the PSS and SSS chosen by the network operator for a specific cell. From a MC-MM perspective, with this option each cell will have a different scrambling sequence and cell coordination will not be achieved. Alternatively, the scrambling sequence initialization $N_{ID}^{n_{SCID}}$ can be forced to a certain value, $N_{ID}^{n_{SCID}} \in \{0, 1., \dots, 65535\}$, which is given by the higher-layer parameter *DL-DMRS-Scrambling-ID*. 5G-Xcast has selected this method to allow multi-cell

synchronized transmissions, since MC-MM initializes the same scrambling sequence for all serving cells.

3.3.2 Negative Numerologies and Extended CP

SFN scenarios are limited by the CP length, which in turn depends on the numerology. The CP is directly related to the maximum inter-site distance (ISD) permitted between transmitters. As Table 3 shows, only ISDs of up to 1.4 km can be reached if the numerologies from 5G NR Rel'15 unicast are reused for MC-MM.

Table 3. Maximum ISD with 5G NR Rel'15 unicast numerologies.

μ	SCS (kHz)	Type CP	CP (μs)	ISD (km)
0	15	Normal	4.69	**1.41**
1	30	Normal	2.34	**0.70**
2	60	Normal	1.17	**0.35**
		Extended	4.16	**1.25**
3	120	Normal	0.59	**0.18**
4	240	Normal	0.29	**0.09**

Although these ISD values are suitable for some specific scenarios such as stadiums, campuses or malls, other larger scenarios such as urban and rural environments require higher ISD values not fulfilled with Rel-15 numerologies. Naturally, a set of different enhancements may be introduced to introduce longer ranges in SFN operations.

The use of **negative numerologies** combined with **extended CPs** represent one of the main improvements to achieve this goal, as it was introduced in [18]. Negative numerologies are selected through negative integer values for μ. A negative μ implies a narrower subcarrier spacing, longer OFDM symbol length and therefore a longer cyclic prefix, directly equivalent to larger ISD distances in SFN environments. The combination of this concept with the use of an extended CP of 1/4 (only available in PTP for $\mu = 2$), may increase even more the SFN coverage.

The main problem encountered with negative numerologies is the framing limitation. Since 5G framing defines a fixed duration per subframe of 1 ms with a fixed number of OFDM symbols per slot, the number and duration of slots are affected by the numerology (See Section 2.1). With negative numerologies, the slot duration increases and **slots span over more than one subframe** in the time domain. Due to the slot expansion, small changes would need to be introduced in the framing structure to create a solution compatible with negative integer numerologies. According to [18], a mini-slot structure would enable the use of negative numerologies, with slots spanning over different subframes or even frames. Mini-slots are a small framing unit formed by a group of 2, 4 or 7 OFDM symbols (normal frames are formed by 14 symbols). They offer a better granularity and flexibility, as well as lower latencies that may benefit some 5G scenarios [19].

An example of compatible solution to integrate mini-slots in 5G negative numerology framing is shown in Figure 7. When numerology $\mu = -1$ and extended CP are selected, mini-slots cover two OFDM symbols. In order to occupy the whole slot length, six mini-slots are required. With $\mu = -2$, mini-slots can group up to four OFDM symbols with three mini-slots filling each slot.

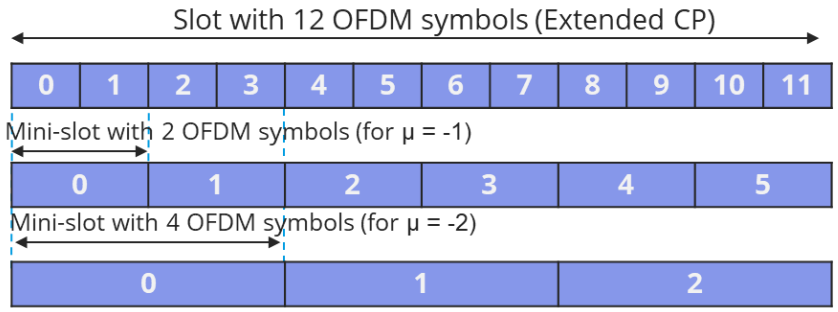

Figure 7. Mini-slots considered for numerologies -1 and -2.

As Figure 8 shows, if larger numerology values are considered, the number of mini-slots required to fill the slot structure is not an integer. This limits the use of negative numerologies to the value -2. In 5G-Xcast, only **numerologies μ = 0, μ = - 1 and μ = - 2 are considered** as compatible solutions with a mini-slot frame structure.

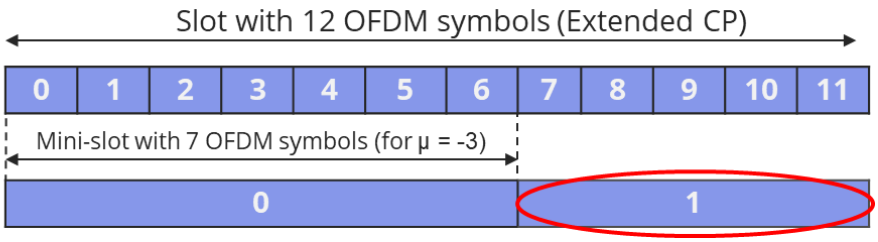

Figure 8. Mini-slot for numerology -3 and incompatibility with 5G Rel'15.

Table 4 shows the symbol duration, extended CP duration and ISD obtained when using negative numerologies with values down to μ = - 2.

Table 4. Extended cyclic prefixes for 5G negative numerologies.

μ	SCS (kHz)	T_U (μs)	T_{CP} (μs)	ISD (km)	CP overhead (%)
0	15	66,6	16,6	5	20
-1	7,5	133,3	33,3	10	
-2	3.75	266,6	66,6	20	

The use of an extended CP allows to deploy SFNs in small, medium and large cells for LPLT environments with a constant CP overhead (OH_{CP}):

$$OH_{CP} = \frac{T_U}{T_U + T_{CP}} = 0.2 \quad (2)$$

Negative numerologies can bring additional restrictions such as a narrower subcarrier spacing and therefore longer OFDM symbol duration. This aspect may limit the mobility conditions, introducing noticeable vulnerability to high-speed scenarios due to Doppler shifts. Furthermore, large FFT sizes are required and consequently the complexity of the system increases.

Based on the scalable numerology solution, specific control regions and reference signal patterns need to be defined for the different subcarrier spacing configurations. With 5G PTP Rel'15, the PDCCH can be allocated at the first three OFDM symbols in every slot.

Considering the reduction in the number of OFDM symbols obtained as a result of the negative numerologies, PDCCH will be allocated at the first one or two OFDM symbols, depending on the new numerology configuration.

3.3.3 Channel Estimation

New DMRS signals need to be designed as well to enable the channel estimation process in large SFN areas. Patterns can be defined by D_x, which is the separation of reference signals along different OFDM symbols in frequency domain, and D_y, which specifies the separation of reference signals for the same subcarrier in time domain. D_x and D_y directly influence the Nyquist limit (T_P) of the multipath channel delay spread and the maximum mobility tolerance ($f_{D_{limit}}$), which at the same time affects the SFN operation performance. This impact is shown as follows:

$$T_P = \frac{T_U}{D_x} \tag{3}$$

$$f_{D_{limit}} = \frac{1}{2D_y(T_U + T_{CP})} \tag{4}$$

MC-MM maintains the same physical channels in order to keep a backwards compatible philosophy with 5G NR Rel'15 and the SC-MM defined in Section 3.2. As a consequence, the DMRS patterns from 5G NR unicast are reused as shown in Figure 9. It additionally shows an example of the control region allocation.

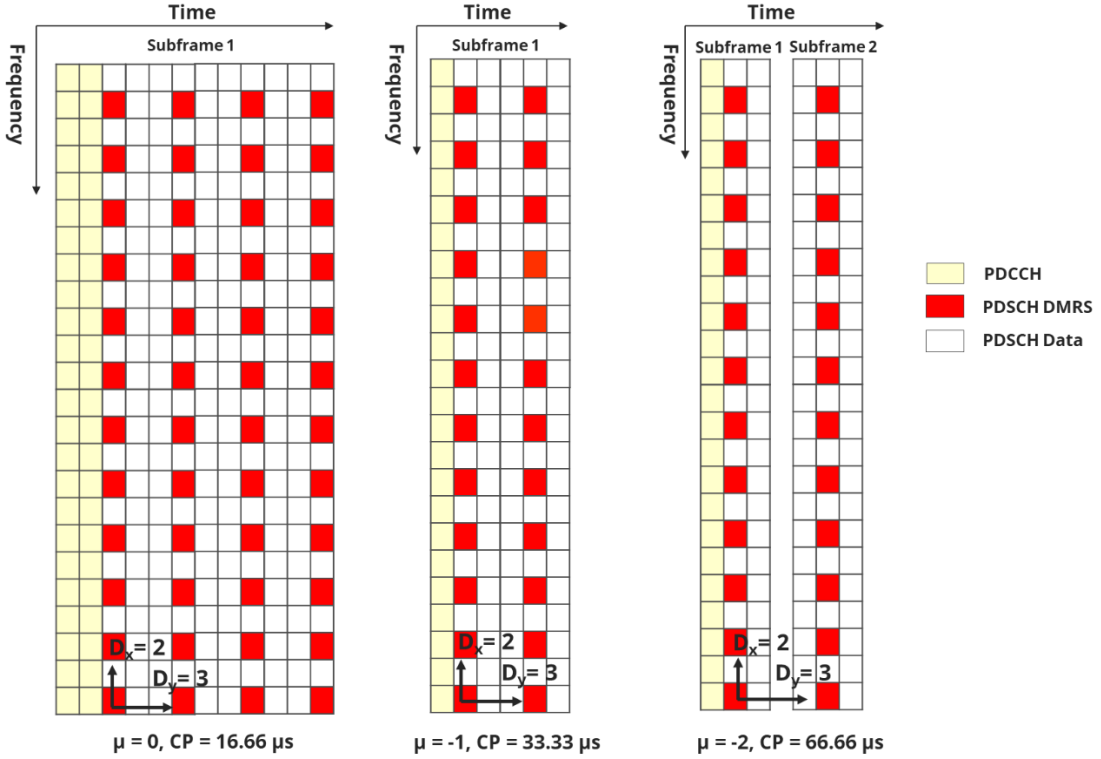

Figure 9. MC-MM Control region and DMRS patterns for negative numerologies.

The use of the same DMRS pattern for all numerology configurations logically leads to the same DMRS overhead ($OH_{DMRS} = \frac{1}{D_x D_y} = 0.1666$). More details about the DMRS patterns considered for the MC-MM solution are given in Table 5.

Table 5. MC-MM Reference Signal Patterns

μ	SCS (kHz)	D_x	D_y	Overhead (%)	T_u (µs)	CP (µs)	T_p(µs)	$f_{D_{limit}}(Hz)$
0	15	2	3	16.66	66.66	16.66	33.33	2000
-1	7.5				133.33	33.33	66.66	1000
-2	3.75				266.66	66.66	133.33	500

The obtained Nyquist limits do not imply a limitation in the SFN operation since they are larger than the corresponding CP. Regarding the maximum mobility conditions, the obtained speed limit is set up to 771 km/h (µ = -2) and 3085 km/h (µ = 0) in a frequency range of 700 MHz and up to 135 km/h (µ = -2) and 540 km/h (µ = -2) in the range of 4 GHz.

3.3.4 Feedback

Link adaptation schemes used in SC-MM are here reused. Moreover, this mode considers feedback coordination between cells in multi-cell environments. While in SC-MM HARQ retransmissions are done via PDSCH from a single gNB, MC-MM may require coordinated retransmissions from more than one gNB depending on the UE location. For example, HARQ efficiency for one UE located between multiple serving cells may be increased if coordinated retransmissions are received from multiple gNBs. Nevertheless, in a multi-cell scenario, it is very likely to have reliable delivery calls for a very robust fixed MCS when a large number of UEs receive the same content. In that case, the role of feedback might not be crucial. Similar to SC-MM, a fixed MCS chosen in a statistical manner could be used, rendering any uplink feedback unnecessary.

3.4 Terrestrial Broadcast Mode

The Terrestrial Broadcast (TB) mode in this deliverable refers to the air interface configuration that enables a dedicated transmission for media delivery (e.g. TV/radio services) in a static manner (defined by the network operator without user involvement) and without the need for UEs to register/attach to the network (DL-only).

The starting point to develop an NR-based Terrestrial Broadcast system is the definition of a number of new transmission modes to provide flexibility to cater for a wide range of deployment scenarios. The following main design principles are taken into account:

- Minimization of the footprint with respect to unicast transmission and scheduling processes. Reuse of unicast scheduling mechanism with one RNTI per service.
- Numerology options adequate for diverse scenarios including Multiple Frequency Network (MFN) and SFN configurations and topologies from low-power low-tower (LPLT) up to high-power high-tower (HPHT), with different inter-site distances.
- Transmission modes adequate for mobile (improving Doppler performance for high speed reception) and static reception (reducing capacity overheads at the expense of Doppler tolerance).
- Leveraging of 5G-NR bandwidth configuration and spectrum utilization efficiency to transmit large bandwidth signals instead of bandwidth-limited (to a few MHz) carriers, if desired.

- Efficient multiplexing in time and frequency domain of local, regional and nation-wide services targeting mobile and fixed reception.

3.4.1 Waveform and Numerology options

The diverse nature of networks that may be used for transmitting Terrestrial Broadcast services (with network topologies ranging from LPLT to HPHT and from single-cell, MFN to nationwide SFN coverage areas) make highly desirable to provide a range of new numerologies to better cater for the different types of transmission networks that could be used. Whereas numerology μ=0 is already suitable for single-cell or MFN Terrestrial Broadcast operation, particularly from LPLT networks, and the negative numerologies proposed for MC-MM can cover LPLT SFN deployments, an extensive set of numerologies must be derived for SFN deployments with large-ISD (e.g. HPHT). However, following similar negative numerology methodology as in MC-MM would require of longer OFDM symbol durations, leading to non-integer multiples of NR subframes (see Section 3.3.2). A second method introduced in [20] by re-defining the number of SCs per RB has been addressed. The equation below provides the means to derive the new number of SC per RB as a function of the OFDM symbol duration and a CP fraction, which needs to be selected so that the number of SC per RB is an integer.

$$SC_{RB} = 12 \cdot 15kHz \cdot \boldsymbol{T_S} \cdot (\boldsymbol{1} - \boldsymbol{CP}) \qquad (5)$$

By this method, it is possible to derive multiple combinations of T_{CP} and T_U[3]. Therefore, it is possible to select the appropriate combinations according to the deployment scenario and the receiving environment. Table 6 provides a set of numerologies that may be considered for Terrestrial Broadcast operation with different SCS, overhead and CP duration. Note that OFDM symbol durations (T_U+T_{CP}) of 0.5, 1, 2, 2.5, 5 and 10 ms are particularly interesting as an integer number of them fit into a 10 ms frame.

Table 6. Terrestrial Broadcast numerologies and extended CP combinations.

	μ	Δ_f (Hz)	T_U (μs)	CP Fraction	T_{CP} (μs)	T_S (ms)	SC_{RB}	ISD (km)
A	0	15000	66.67	~7%	4.7/5.1	0.07	12	1.4
E	-	2500	400.00	20%	100.00	0.50	72	30
G	-	1250	800.00	20%	200.00	1.0	144	60
H	-	625	1600.00	20%	400.00	2.0	288	120
I	-	3333	300.00	10%	33.33	0.33	54	10
J	-	2045.45	488.88	2.22%	11.11	0.50	88	3.3
K	-	1022.72	977.78	2.22%	22.22	1.0	176	6.6
L	-	511.36	1955.56	2.22%	44.44	2.0	352	13.2
M	-	416.67	2400	4%	100	2.5	432	30
N	-	208.33	4800	4%	200	5.0	864	60
O	-	104.67	9600	4%	400	10.0	1728	120
p	-	217.39	4600	8%	400	5.0	828	120

[3] It should be noted that although decreasing the TCP/TU ratio reduces CP overhead, increasing the FFT size may cause significant impact in receiver complexity, which would need to be considered, along with other practical aspects of the receiver design.

According to the considered deployments assumed for this project, three numerology options from the table can be adopted for Terrestrial Broadcast mode: E, G, and H. Numerology E could be useful for LPLT SFNs with a compromise between SFN gain in short/medium ISD deployments, while retaining high mobility. Numerology G corresponds to the one specified in LTE Rel'14 enTV that can be applied to MPMT. Numerology H would allow SFN deployments with ISD of up to 120 km, fulfilling with the Req. 7 of [5].

3.4.2 Channel Estimation

DMRS defined for unicast may be used for single-cell or MFN deployments. However, the introduction of new SCS configurations leads to the design of specific DMRS patterns to address the channel estimation process in large-scale SFN scenarios[4]. It is possible to create specific patterns able to optimize the equalization interval length and the maximum mobility tolerance easily. Dense patterns increase the SFN equalization interval and mobility tolerance at the expense of introducing larger overheads.

Table 7 shows the proposed DMRS patterns for the Terrestrial Broadcast adopted numerologies. These patterns permit longer equalization intervals while keeping the same overhead, i.e. 16.66 %, with all possible configurations.

Table 7. Terrestrial Broadcast DMRS patterns

SCS (kHz)	D_x	D_y	Overhead (%)	T_u (μs)	CP (μs)	T_p(μs)	$f_{D_{limit}}(Hz)$
2.5 (E)	3	2	16.66	400	100	166.66	500
1.25 (G)				800	200	266.66	250
0.625 (H)				1600	400	533.33	125

The Terrestrial Broadcast mode is also able to cope with high mobility conditions due to the dense pattern design in time domain ($D_y = 2$). In particular, the introduction of a CP of 100 μs (E) supposes a good alternative when high mobility requirements are needed. According to the obtained Doppler limits using (4), speeds up to 192 km/h (SCS = 0.625 kHz) and 771 km/h (SCS = 2.5 kHz) for 700 MHz and up to 33 km/h (SCS = 0.625 kHz) and 135 km/h (SCS = 2.5 kHz) for 4 GHz are supported. The DMRS allocation is shown in Figure 10.

[4] Also for SFN, a common DMRS scrambling sequence for the stations involved in an SFN area is required.

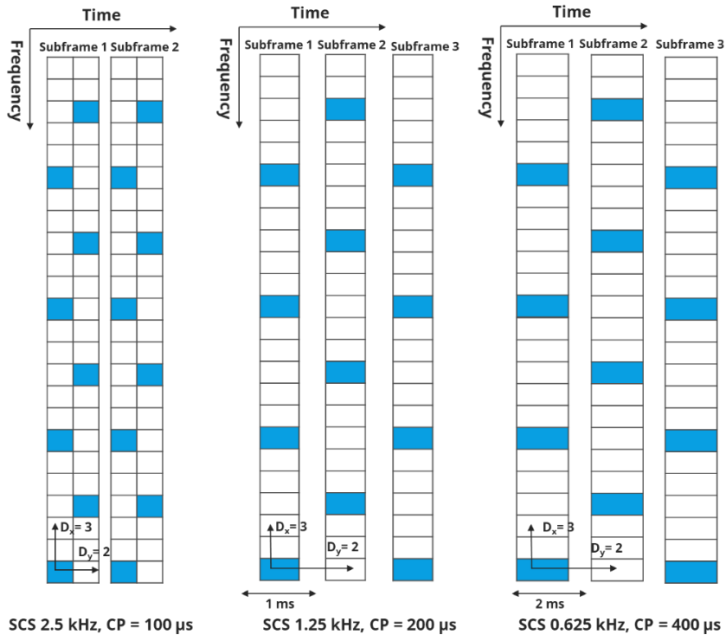

Figure 10. DMRS Patterns for large-scale HPHT SFN. DRMS (blue), data (white).

3.4.3 Bandwidth, Multiplexing and Spectrum Utilization

For Terrestrial Broadcast deployments in frequencies below 1 GHz, NR FR1 provides the following options regarding bandwidth: 5, 10, 15, 20, 25, 40, 50, 60, 80 or 100 MHz. Note that with numerology 15 kHz a 50 MHz carrier can be configured with 270 RBs (97.2% bandwidth utilization). For 10 MHz the bandwidth utilization is 93.6% (52 RBs). Note that the total allocated bandwidth can be extended via Carrier Aggregation, which in NR supports the bundling of up to 16 carriers. The combination of large bandwidth transmission with robust modulation and coding could also enable the introduction of Wideband Broadcasting transmission as presented in Deliverable D3.1.

The potential application of the Channel Bandwidth Part (CBP) concept to Terrestrial Broadcast distribution is proposed next. The use of CBPs is considered as an option for the FDM multiplexing of single-cell or MFN services with those intended for SFN areas within the same carrier. In this case, a single wideband carrier can multiplex not only services addressing different reception conditions, but also different coverage areas and network deployments thanks of allowing the use of different numerologies within one carrier[5]. Figure 11 shows a wideband carrier that allocates three different CBPs, each one with different numerology (see OFDM A, B and C). For instance, part of the BW can be reserved to schedule services for nationwide SFN coverage (OFDM A) alongside services intended for regional (OFDM B) or local (OFDM C) areas. A receiver would only demodulate the specific resources containing a desired service. Following this approach, a single 5G-NR carrier can transmit services intended for different reception conditions and coverage targets without the need of transmitting isolated multiplexes as currently done in Terrestrial Broadcast systems.

[5] Note that different numerologies can also be multiplexed in TDM.

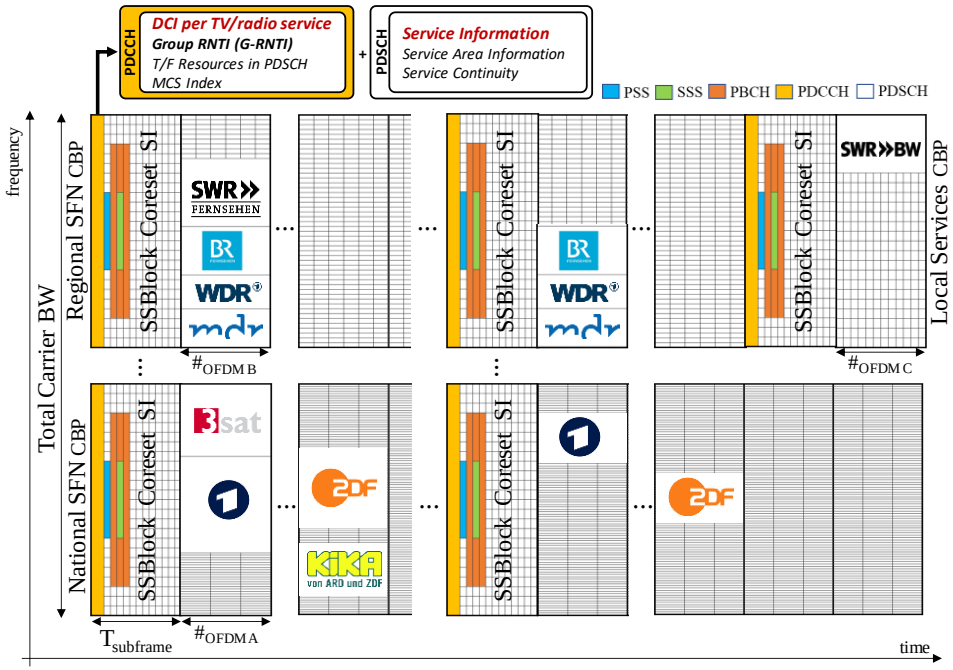

Figure 11. Carrier Bandwidth Parts could be used for the provision of Terrestrial Broadcast services, where each one is transmitted in a different resource region according to the desired numerology. Each service can be assigned a distinct DCI (C-RNTI, resource mapping and MCS index) so that each TV/radio service is treated in a similar way as user data in regular unicast frames.

3.4.4 Control Channel, Synchronization, Acquisition and Scheduling mechanism

Signalling and synchronization mechanisms may be simplified with respect to LTE enTV, i.e. by reducing the amount of signalling to only that necessary for the correct reception and discovery of services. As system preambles, control channels are assumed to convey SS/PBCH Block, MIB signalling via the PDCCH and a series of SIBs via the PDSCH. Additional service announcement information may be allocated over the PDSCH so that physical channels and procedures do not require major modifications.

These control channels are proposed to be transmitted using regular unicast numerology as they may contain information, which is intended to be transmitter-specific. By means of network planning, the control channel resources for each transmitter can be scheduled so that co-channel interferences are avoided. Although the mismatch between numerologies of the control channels and SFN data may still exist, it may be possible to detect the signal at the expense of larger detection time by means of an increase number of repetitions i.e., with longer aggregation levels. For single-cell or MFN transmissions as well as for SFN, coordinated frame scheduling is required in order to avoid overlaps between adjacent time/frequency resources that may create interference (in the first case) and to provide synchronous SFN transmission (in the latter case).

Regarding data scheduling, a reuse of the procedures existing for unicast are desired in order to minimize implementation impact and to exploit flexible resource allocation. Hence, the G-RNTI proposed for the Mixed Mode is also employed for Terrestrial Broadcast. Furthermore, scheduling each TV/radio service in a similar way to unicast traffic, would allow defining specific TV/radio service parameters. The transmitted service information would enable identification of time/frequency resource allocation in the

frame, the corresponding MCS (with a corresponding DCI format), as well as service area information or service continuity information (by means of SIBs). With dynamic scheduling, TV/radio services can be transmitted according to operator demands, exploiting better statistical multiplexing and spectral efficiency. Services could also be switched on and off or created (e.g. introduction of local services) over time, therefore only consuming the resources of the 5G NR carrier when required.

Figure 11 shows an illustrative example of a potential framing configuration. Note that some of the contents addressing different coverage areas (nationwide SFN, regional SFNs and local areas) are multiplexed within the same carrier.

3.5 MIMO Techniques

In this section, a general overview of the MIMO precoding for multicast and broadcast is given, in the context of physical layer techniques for PTM transmissions, aiming to provide some insightful guidelines for the implementation of MIMO techniques in broadcasting and multicasting. The first subsection considers the situation when the transmitter has channel state information (CSI) of the channel coefficients experienced by the UEs, while the second subsection considers the situation where the transmitter has no knowledge of the CSI.

3.5.1 MIMO precoding with CSI at the Transmitter

In general, precoding techniques aim for achieving PHY multicasting, where multiple information is conveyed for multiple groups of users. This translates to PTP transmission, when each group has a single user and to PTM when multiple users belong to a single multicast group. Different studies categorised precoding techniques based on different characteristics; however here we divide them into two main categories: linear/non-linear techniques as well as optimisation-based techniques, which are presented in what follows.

3.5.1.1 Linear and Non-Linear Precoding Techniques

Closed-form precoding techniques are generally divided into two main categories, namely into linear techniques [21] and non-linear techniques [22]. Linear techniques mainly constitute three precoding types, namely Maximum Ratio Transmission (MRT) precoding [23], Zero-Forcing (ZF) [24] and Minimum Mean Square Error (MMSE) [25]. More specifically, MRT aims for maximising the transmission power towards the desired receiver under a transmit power constraint. Its precoding matrix is typically expressed as the conjugate transpose of the channel response. On the other hand, both ZF and MMSE remove interference at the receiver by decoupling multi-user channels into distinct subchannels. Furthermore, ZF performs best at the high SNR regime with a precoding matrix of the pseudo-inverse of the channel response, while MMSE incorporates the noise level into its precoder in order to boost system's performance at low SNR values. In the case of unicast transmission, linear approaches were utilised for communicating with single-antenna receivers [21-26] and multi-antenna receivers [27-28]. By contrast, both ZF and MMSE precoding schemes were used for multicast transmission in [29].

The main drawback of the aforementioned closed-form precoding techniques is their limitations in terms of specific objective optimisation. Furthermore, linear techniques would incur some restrictions on the multi-user system, such as for the number of users as well as for the number of transmit and receive antennas. Nonlinear techniques on the other hand include a wide range of algorithms and techniques. One of the most common nonlinear techniques is the optimal Dirty Paper Coding (DPC) technique [30], which aims for cancelling interference prior to transmission and is known for achieving MIMO

capacity. Another example is the Tomlinson-Harashima Precoding (THP) technique [31], which is a sub-optimal derivative of DPC.

3.5.1.2 Optimisation-Based Precoding Techniques

In practice, optimisation-based precoding techniques are more desirable, since they can be designed for optimising a specific system metric. In this context, various optimisation approaches have been proposed in the literature, which are mainly based on the Quality of Service (QoS) [32] as well as the min-max fair problems [33-34]. In the context of PHY multicasting, both problems are considered NP-hard. The QoS optimisation problem can be optimally solved using the Semi-Definite Relaxation (SDR)-based approach. SDR solutions are mainly based on optimising the average transmit power maintaining a specific QoS at each user [33], while in [35] a max-min fairness optimisation solution aims for maximising the minimum SINR between all users in the context of multi-group multicast in massive MIMO systems. Furthermore, the multigroup transmission problem was approximated by Sidiropoulos et al. [32] as an NP-hard problem using SDR-based optimisation. Christopoulos et al. [36] proposed a per-antenna power constrained multicasting precoding technique, which is based on QoS and min-max fairness solutions. The SDR-based optimisation was also utilised for multicast transmission by [37]. Furthermore, an iteration-based method was proposed by Demir and Tuncer in [38], which relies on antenna selection and hybrid beamforming for communicating with multiple groups of users. In the case of broadcast transmission, which translates to a single multicast group, interference effect is ignored since all users receive a single message. This was approximated again by Sidiropoulos et al. [32] as an NP-hard broadcast problem by SDR and Gaussian randomisation.

3.5.2 MIMO Precoding without CSI at the Transmitter

In the situation where the transmitter does not have CSI, the MIMO precoding cannot be designed according to the specific channel conditions experienced by the UEs but it has to be designed to enhance the spatial diversity of the system and/or to accommodate different deployment scenarios. DVB-NGH and ATSC 3.0 include precoding with spatial multiplexing for MIMO 2x2 (i.e. two transmit and receive antennas) based mainly on rotation matrices [39-40]. The rotation matrix linearly combines the information streams of each transmit antenna, according to a rotation angle, increasing the spatial diversity of the transmitted signal. Optimal rotation angles for MIMO 2x2 with cross-polar antennas was investigated in [41] where it was shown that the optimal rotation angle mainly depends on the physical layer code-rate. The concept of rotation matrices can be extended to accommodate more general antenna configuration arrangements with different number of transmit and receive antennas. This is especially important for the design of the NR air interface where the base-stations can have large antenna arrays. Hence, an important research area is to investigate MIMO precoding techniques without CSI at the base-station for large antenna arrays. Other MIMO precoding stages can include stream-power-allocation and power-imbalance matrices. The stream-power-allocation matrix allows designing the power allocation to each of the information streams that can be modulated with constellations with different cardinality. On the other hand, the power-allocation matrix allows to design the final output power per transmit antenna that can be useful to accommodate different deployment scenarios that may have specific restrictions on the total power radiated per polarisation. As for the rotation matrices, the extension of these precoding stages to larger antenna arrays is also an important area of research.

4 Performance Evaluation of 5G PTP against IMT-2020 Requirements

This section evaluates the 5G New Radio air interface as specified in 3GPP Rel'15 [11-12, 42-43] towards the use cases and test environments defined in IMT-2020 [44]. This deliverable evaluates some KPIs defined in the IMT-2020 guidelines and includes an additional KPI that better defines some of the verticals and scenarios considered within this project. The aforementioned KPIs were already introduced in D3.1 [6]. The main outcomes of this section have been used as a **contribution to the 5G PPP IMT-2020 Evaluation Group**.

The methodology in this deliverable is structured around the different evaluation types considered. Three methodologies are followed in Section 4: inspection, analysis and link-level simulations [44]. Table 8 shows the KPIs evaluated in D3.2, as well as their related IMT-2020 scenarios and 5G-Xcast verticals. Each of the scenarios considered can be easily mapped to a 5G-Xcast vertical as defined in WP2 [3]. KPIs defined in Table 8 are related to three usage scenarios from IMT-2020: Enhanced Mobile Broadband (**eMBB**), Ultra-Reliable Low Latency Communications (**URLLC**) and Massive Machine-Type Communications (**mMTC**). While eMBB is usually related to the M&E vertical, URLLC is linked to public warning, and automotive (V2X), and mMTC englobes de IoT vertical of the project.

Table 8. Assessment method used per KPI and associated 5G-Xcast verticals.

KPI	IMT-2020 Scenario	Vertical	Methodology
Bandwidth	eMBB, URLLC	M&E, PW, V2X	Inspection
Peak data rate	eMBB	M&E	Analytical
Peak spectral efficiency	eMBB	M&E	Analytical
BICM spectral efficiency	eMBB	M&E	Link Level
Mobility	URLLC, eMBB	PW, V2X, M&E	Link Level
User Plane Latency	URLLC, eMBB	PW, V2X	Analytical
Control Plane Latency	URLLC, eMBB	PW, V2X	Analytical
Energy Efficiecy	mMTC, eMBB	PW, IoT	Analytical

It is worth saying that the importance of a KPI highly depends on the scenario under evaluation. As Table 8 shows, eMBB is the most demanding scenario in terms of data rate, spectral efficiency, bandwidth, latency or mobility. These KPIs are needed for the successful transmission of high throughputs in M&E use cases. URLLC scenarios demand for reliable communications with very short latency but most importantly very high user speeds. Finally, the most important KPI for mMTC is the energy efficiency.

The next subsection introduces the first scenario, eMBB, and evaluates the most important KPIs related to it.

4.1 Enhanced Mobile Broadband for Media & Entertainment

4.1.1 Bandwidth

Bandwidth is defined as the maximum aggregated system bandwidth in Hz (including frequency guard bands). The maximum supported bandwidth may be composed of either a single or multiple radio frequency (RF) carriers. It is calculated by inspection.

Depending on the frequency range (FR) selected, a single component carrier supports the following bandwidths and guard bands [45]:

- FR1 (*450 MHz - 6 GHz*):
  - 5, 10, 15, 20, 25, 40, 50, 60, 80 or 100 MHz.
  - Guard band ratio from 2 to 20%.
- FR2 (*24.25 GHz - 52.6 GHz*):
  - 50, 100, 200 or 400 MHz.
  - Guard band ratio from 5 to 8%.

The minimum amount of paired spectrum is 2 x 5 MHz, while the minimum amount of unpaired spectrum is 5 MHz.

From these possible values, NR defines different maximum bandwidths depending on the numerology and frequency band used [8]. In any case, carrier aggregation of up to **16 carriers** is permitted, as specified in [12]. The maximum bandwidth supported is shown in Table 9.

Table 9. NR maximum supported bandwidth.

Frequency range	μ	BW_{max} (MHz)	N_{RB}	CA	CA BW_{max} (GHz)
FR1 (450 MHz - 6 GHz)	0	50	270	16	**0.8**
	1	100	273		**1.6**
	2	100	135		**1.6**
FR2 (24.25 GHz - 52.6 GHz)	2	200	264		**3.2**
	3	400	264		**6.4**

By aggregating multiple component carriers, transmission bandwidths up to **6.4 GHz** are supported to provide high data rates. As explained in [45], component carriers can be either contiguous or non-contiguous in the frequency domain. The number of component carriers transmitted and/or received by the user equipment can vary over time depending on the instantaneous data rate.

4.1.2 Peak data rate

Peak data rate is the maximum achievable data rate (bit/s) under ideal conditions. It is defined as the received data bits assuming error-free conditions assignable to a single mobile station, when all assignable radio resources for the corresponding link direction are utilized (i.e. excluding radio resources that are used for physical layer synchronization, reference signals or pilots, control region, guard bands and guard times). The peak data rate expression in NR is defined for DL (Downlink) and UL (Uplink) transmissions combined with TDD (Time Division Duplex) and FDD (Frequency Division Duplex) techniques as:

$$\gamma_p = \sum_{j=1}^{J} \left(\alpha^{(j)} \cdot v_{Layers}^{(j)} \cdot Q_m^{(j)} \cdot f^{(j)} \cdot R_{max} \cdot \frac{N_{PRB}^{BW(j),\mu} \cdot 12}{T_s^{\mu}} \cdot \left(1 - OH^{(j)}\right) \right) \quad (6)$$

where:

- $\boldsymbol{J}$ is the number of aggregated component carriers in a frequency band. It has integer values from 1 to 16.
- $\boldsymbol{\alpha^{(j)}}$ is the normalized scaling factor related to the ratio of resources used in the DL/UL for the j component carrier. In FDD, $\alpha^{(j)} = 1$ for both DL and UL. In TDD and other duplexing techniques, both for DL and UL, $\alpha^{(j)}$ is calculated based on the frame structure and the SFI.
    - For TDD, $\alpha^{(j)}$ includes the presence of Guard Period (GP) symbols as part of the effective BW. Consequently, the impact of GP is considered in the overhead ($OH^{(j)}$) calculation.
- $\boldsymbol{v_{Layers}^{(j)}}$ is the number of layers when multiple antennas are used. For the DL, it has integer values from 1 to 8. For the UL, it goes from 1 to 4.
- $\boldsymbol{Q_m^{(j)}}$ is the maximum modulation order, i.e. 8.
- $\boldsymbol{f^{(j)}}$ is the scaling factor used to reflect the capability mismatch between baseband and RF for both types of standalone and non-standalone UEs. Its use is also proposed to scale down the maximum throughput of NR UEs where there is LTE and NR hardware sharing. $f^{(j)}$ is signalled per band and per band per band combination as per UE capability signalling. There are two possible values, 1 or 0.75.
- $\boldsymbol{R_{max}}$ is the maximum CR of 948/1024.
- $\boldsymbol{\mu}$ is the numerology.
- $\boldsymbol{T_s^{\mu}}$: is the average OFDM symbol duration in a subframe for numerology, μ, i.e. $T_s^{\mu} = \frac{10^{-3}}{14 \cdot 2^{\mu}}$. It includes the impact of the CP insertion.
- $\boldsymbol{N_{PRB}^{BW(j),\mu}}$ is the maximum RB allocation in the available system bandwidth with numerology μ. TR 38.817-01 [10], in section 4.5.1, provides the maximum bandwidth supported by a UE for a given band.
- $\boldsymbol{OH^{(j)}}$ is the overhead calculated as the average ratio of REs occupied by L1/L2 control, synchronization signals, PBCH, reference signals, guard bands and guard period (only for TDD), compared to the total number of REs available in the effective bandwidth and a frame time product.

4.1.2.1 Peak data rate calculation

A. Downlink

This section provides the DL peak data rate for both FDD and TDD modes. For FDD, only the FR1 is evaluated to ensure minimum efficiency levels. For TDD, the peak data rate is calculated in both FR1 and FR2. The values have been calculated for both SISO and MIMO schemes, as well as the use of aggregated component carriers. An extensive and detailed parameter selection for all evaluated configurations is described in Annex B.

FDD

Considering a FDD configuration where all resources are assigned to DL transmissions, the obtained peak date rate values are shown in Table 10:

Table 10. FDD DL peak data rate values

μ	BW_{max} (MHz)	γ_p SISO (Gbit/s)	Layers	γ_p MIMO (Gbit/s)	CA	γ_p SISO+CA (Gbit/s)	γ_p MIMO+CA (Gbit/s)	Req. (Gbit/s)
0	50	0.30	8	2.40	16	4.81	**38.54**	20
1	100	0.60		4.87		9.75	**78.05**	
2		0.59		4.78		9.57	**76.62**	

TDD

Following the same procedure, TDD DL peak data rate values are:

Table 11. TDD DL peak data rate values

μ		BW_{max} (MHz)	γ_p SISO (Gbit/s)	Layers	γ_p MIMO (Gbit/s)	CA	γ_p SISO+CA (Gbit/s)	γ_p MIMO+CA (Gbit/s)	Req. (Gbit/s)
FR1	**0**	50	0.22	8	1.80	16	3.61	**28.94**	20
	1	100	0.45		3.66		7.32	**58.62**	
	2		0.44		3.59		7.19	**57.52**	
FR2	**2**	200	0.89	6	5.39		14.38	**86.31**	
	3	400	1.80		10.85		28.9	**173.57**	

For **FDD**, one component carrier is able to provide peak data rate values up to 600 Mbps with SISO antenna configurations and **4.87 Gbps** with 8 layers in MIMO antenna configurations in FR1. Considering **TDD** techniques, peak data rates up to 1.80 Gbps for SISO and **10.85 Gbps** for MIMO can be achieved in FR2.

By **aggregating multiple component carriers (CC)**, higher peak data rate values can be achieved. Component carriers can be either contiguous or non-contiguous in the frequency domain. The number of component carriers has been set to the maximum, i.e. **16 component carriers**. With this configuration, peak data rates up to 9.75 Gbps and **78.05 Gbps** can be reached for **FDD** SISO and MIMO modes. In **TDD**, values up to 28.90 Gbps and **173.57 Gbps** can be reached with SISO and MIMO configurations, respectively. One can affirm that the use of **MIMO and carrier aggregation** is one of the main factors that **enables to meet the ITU-R peak data rate requirement**. By enabling just carrier aggregation in a SISO configuration, only TDD FR2 case meets this requirement.

B. Uplink

The peak data rate in the uplink is also provided for FDD and TDD techniques. Same SISO and MIMO configurations with single and aggregated component carriers are considered. The assumed parameter configuration is described in Annex B.

FDD

Considering an FDD mode where all resources are assigned to UL transmissions, peak data rate is calculated as follows:

Table 12. FDD UL peak data rate values

μ	BW_{max} (MHz)	γ_p SISO (Gbit/s)	Layers	γ_p MIMO (Gbit/s)	CA	γ_p SISO+CA (Gbit/s)	γ_p MIMO+CA (Gbit/s)	Req. (Gbit /s)
1	50	0.30	4	1.22	16	4.90	**19.60**	10
2	100	0.62	4	2.49	16	9.99	**39.99**	
3	100	0.62	4	2.49	16	9.99	**39.54**	

TDD

Following the same procedure, TDD UL peak data rate values are calculated:

Table 13. TDD UL peak data rate values

μ		BW_{max} (MHz)	γ_p SISO (Gbit/s)	Layers	γ_p MIMO (Gbit/s)	CA	γ_p SISO+CA (Gbit/s)	γ_p MIMO+CA (Gbit/s)	Req. (Gbit /s)
FR1	**0**	50	0.18	4	0.75	16	3.00	**12.03**	10
	1	100	0.38		1.52		6.11	**24.46**	
	2		0.37		1.50		6.02	**24.08**	
FR2	**2**	200	0.73		2.94		11.79	**47.16**	
	3	400	1.47		5.91		23.64	**94.57**	

For FDD, one component carrier is able to provide peak data rate values up to 620 Mbps with SISO antenna configurations and 2.49Gbps with MIMO 4 layers configuration in frequency ranges between 450 MHz and 6 GHz. Considering TDD techniques for frequency ranges of 450 MHz - 6 GHz and 24.25 GHz - 52.6 GHz, peak data rates up to 1.47 Gbps for SISO and 5.91 Gbps for MIMO 4 layers can be obtained.

By **aggregating multiple component carriers**, higher peak data rate values can also be reached for uplink transmissions. The number of component carriers has also been set to 16 component carriers. With this configuration, peak data rates up to 9.99 Gbps and 39.54 Gbps can be reached for **FDD** SISO and MIMO modes. In **TDD**, values up to 23.64 Gbps and 94.57 Gbps can be reached with SISO and MIMO configurations, respectively. As it can be seen, the use of **MIMO and carrier aggregation** techniques is also the **key for uplink since it allows meeting the 10 Gbps ITU-R requirement**.

4.1.3 Peak spectral efficiency

The peak spectral efficiency is the maximum data rate under ideal conditions normalised by channel bandwidth (in bit/s/Hz). Its expression is defined for DL and UL transmissions in both FDD and TDD as:

$$\eta_p = \frac{\gamma_p}{\alpha^{(j)} \cdot BW} \tag{7}$$

where:

- γ_p is the peak data rate value obtained for each evaluated configuration.
- $\alpha^{(j)}$ is the normalized scaling factor related to the proportion of resources used in the DL/UL ratio for the j component carrier, calculated as in section 4.1.2.
- BW is the bandwidth for each numerology, FR and duplexing technique.

A. Downlink

DL peak spectral efficiency is calculated for both FDD and TDD techniques. For FDD, peak spectral efficiency is only calculated for FR1 while for TDD, both FR1 and FR2 are considered. Peak spectral efficiency has been calculated per component carrier with

SISO and MIMO configurations. To enable the calculation, previous peak data rate values have been considered.

FDD

Table 14. Peak spectral efficiency for FDD DL.

	Numerology	BW_{max} (MHz)	η_p (bit/s/Hz) SISO	η_p (bit/s/Hz) MIMO
FR1	0	50	6.02	48.17
	1	**100**	**6.09**	**48.78**
	2	100	5.98	47.89

TDD

Table 15. Peak spectral efficiency for TDD DL.

	Numerology	Bandwidth (MHz)	η_p (bit/s/Hz) SISO	η_p (bit/s/Hz) MIMO
FR1	0	50	5.91	47.34
	1	**100**	**5.99**	**47.93**
	2	100	5.88	47.03
FR2	2	200	5.88	35.29
	3	400	5.91	35.48

As shown in Table 14 and Table 15, one component carrier is able to provide peak spectral efficiency values up to **48.78 bps/Hz** for **FDD** and up to **47.93 bps/Hz** for **TDD** techniques thanks to the use of MIMO 8 layers configuration. Both FDD and TDD configurations are able to **meet the ITU-R requirement** (30 bps/Hz) for all the evaluated bandwidths and numerologies.

B. Uplink

UL peak spectral efficiency is also calculated for both FDD and TDD. Same assumptions about frequency ranges and antenna configurations have been made. The previous UL peak data rate values have also been used for this calculation.

FDD

Table 16. Peak spectral efficiency for FDD UL. Numerologies from 0 to 2, with and without MIMO.

Frequency Band	Numerology	Bandwidth (MHz)	η_p (bit/s/Hz) SISO	η_p (bit/s/Hz) MIMO
FR1	0	50	6.12	24.51
	1	**100**	**6.24**	**24.99**
	2	100	6.17	24.71

TDD

Table 17. Peak spectral efficiency for TDD UL. Numerologies from 0 to 3, with and without MIMO.

Frequency Band	Numerology	Bandwidth (MHz)	η_p (bit/s/Hz) SISO	η_p (bit/s/Hz) MIMO
FR1	0	50	5.91	23.66

	1	**100**	**6.01**	**24.05**
	2	100	5.92	23.68
FR2	2	200	5.79	23.18
	3	400	5.81	23.24

As shown in Table 16 and Table 17**, one component carrier** is able to provide peak spectral efficiency values up to **24.99 bps/Hz** and **24.05 bps/Hz** for both **FDD** and **TDD** techniques thanks to the use of with MIMO 4 layers configurations. All the numerology and bandwidth combinations are able to provide values above the ITU-R requirement, which is fixed to 15 bps/Hz.

4.1.4 BICM spectral efficiency

This KPI indicates the number of data bits per channel used to provide a minimum carrier-to-noise ratio (CNR). The CNR is evaluated through link-level simulations. The spectral efficiency can by simply calculated as:

$$\eta_{BICM} = Q_m \cdot R \tag{8}$$

The selected Quality of Service (QoS) is a block error rate BLER < 0.1%. Ideal channel estimation is used in all cases. In this section, both PDSCH and PDCCH channels have been included.

4.1.4.1 Physical Downlink Shared Channel (PDSCH)

a) Technology Comparison: NR vs. LTE/ATSC 3.0

Figure 12 shows the BLER as a function of the required CNR (dB) for the different MCS available in NR, where each colour represents a specific modulation order. Curves with the same colour represent different MCS and therefore CRs. Note that both tables included in the TS 38.213 [11] have been considered. The BW selected is 5 MHz with numerology 0, i.e. a carrier spacing of 15 kHz.

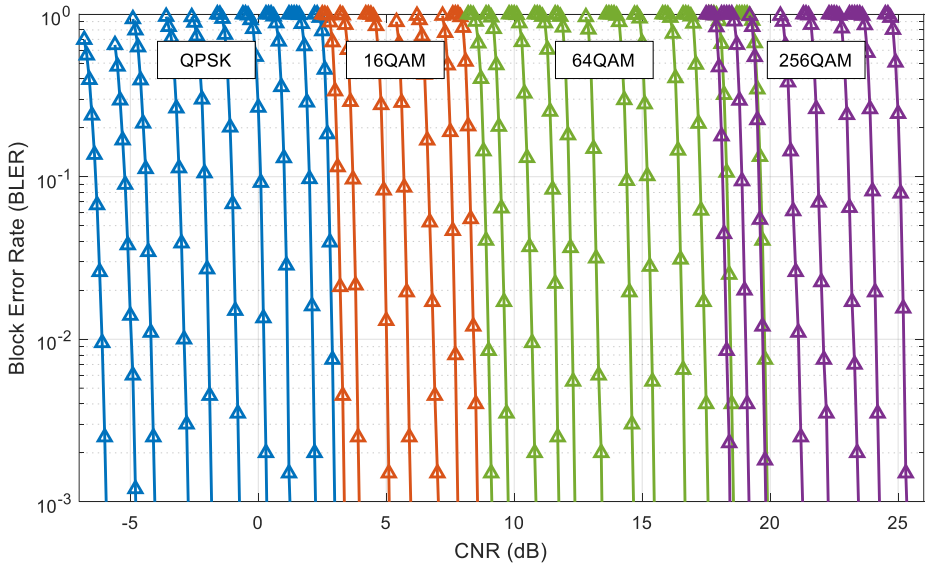

Figure 12. Block error rate vs CNR (dB) for SISO AWGN channel with NR.

As shown in the figure, NR Rel'15 provides a good granularity. In fact, only high CRs with 64QAM and low CRs with 256QAM provide similar performance. That is why they do not appear in both tables as specified in 3GPP.

Figure 13 shows the BICM spectral efficiency (bpc) as a function of the required CNR in an AWGN channel for NR, compared with other technologies such as ATSC 3.0, 4G LTE PTP, SC-PTM and MBSFN. The channel capacity is also shown for comparison. The performance of NR when using a single antenna port and layer is better than 4G LTE. The use of Low-Density Parity Check (LDPC) codes provides significant performance gains. However, there is room for improvement since the gap to ATSC 3.0 is still high, especially for high CNR values.

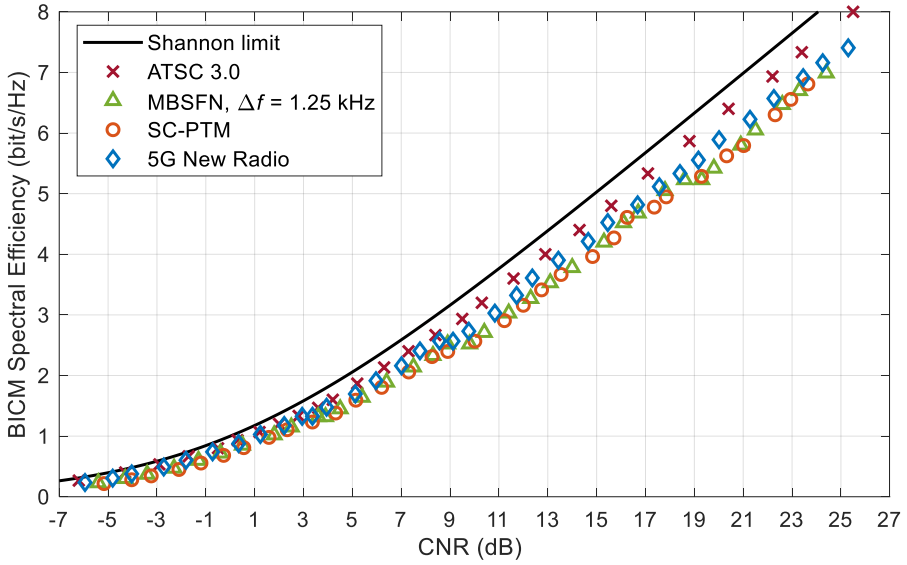

Figure 13. BICM spectral efficiency vs CNR (dB) for SISO AWGN channel. NR vs. LTE Rel'14 eMBMS and ATSC 3.0.

On the one hand, ATSC 3.0 employs Non-Uniform Constellations (NUC), which provide an important performance improvement due to the geometrical signal shaping. Note that no gains are obtained with QPSK, since this constellation does not have room for possible optimization. Additional gains are also obtained due to the use of longer codewords that in turn employ long LDPC lengths. The codeword in ATSC 3.0 has 64800 bits, while the maximum length in NR is 25344 bits and it is only used with high MCS indexes.

b) MIMO Performance

The following section shows the performance of 5G when using a MIMO configuration in an AWGN channel. This deliverable has considered two configurations: 2x2 and 4x4 antennas, with 2 and 4 layers respectively (note that NR implements up to 8 layers), as shown in Figure 14. The channel capacity is also shown for comparison.

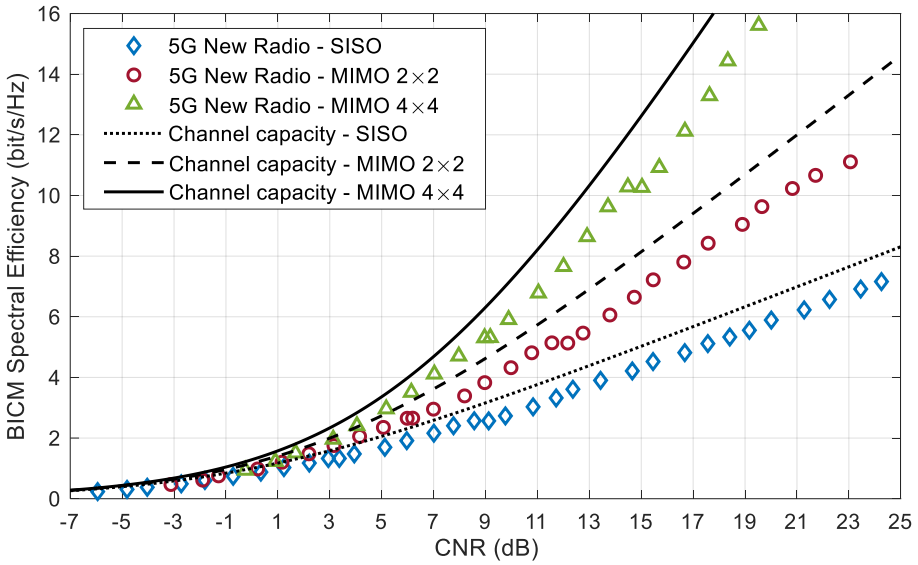

Figure 14. BICM spectral efficiency vs CNR (dB) with NR, AWGN MIMO channel.

The use of multiple antennas drastically increases the BICM spectral efficiency of the systems. For example, NR provides a capacity of approximately 5.1 bpc for a minimum CNR of 18 dB with a single antenna. If MIMO 2x2 is used, the capacity is increased to 8.4 bpc. With MIMO 4x4, this capacity reaches a value of 13.3 bpc.

Observing the results for MIMO 2x2, it is possible to affirm that NR exceeds the SISO capacity if the CNR is high enough, in this case from 2 dB. The same behaviour can be seen with MIMO 4x4, which exceeds the 2x2 MIMO channel capacity when the CNR is 7 or higher.

c) IMT-2020 Scenarios

Figure 15 shows the BICM spectral efficiency vs. CNR with NR for the IMT-2020 considered scenarios, i.e. indoor hotspot, dense urban and rural. All scenarios are evaluated considering Line-of-Sight (LoS) and compared with AWGN and the independent and identically distributed (i.i.d.) Rayleigh channels. The frequency selected is 700 MHz.

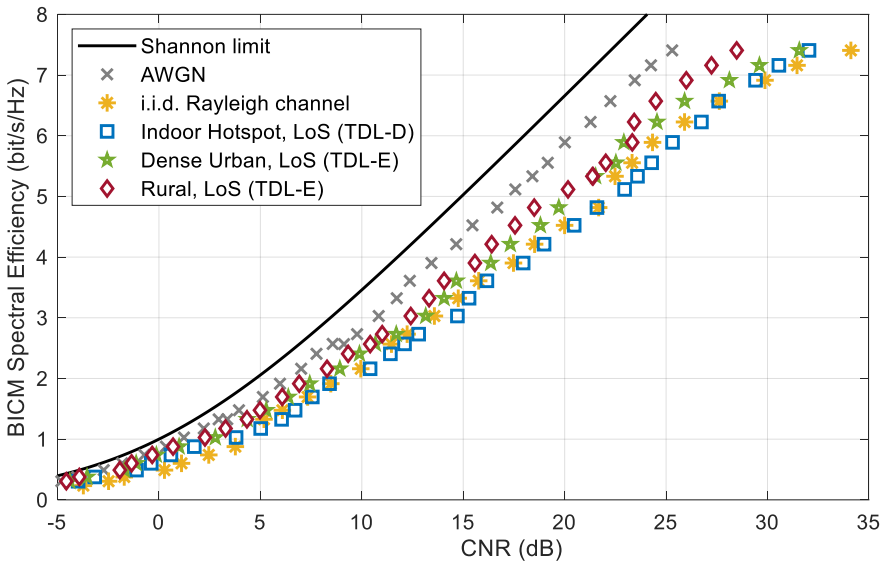

Figure 15. BICM spectral efficiency vs CNR (dB) for all considered scenarios.

The indoor hotspot scenario is modelled with the TDL-A channel model [44, 46]. The selected bandwidth is 10 MHz, with numerology 0. In this scenario, a user speed of 3 km/h is used. The delay spread is 20 ns. Particular indexes with low constellation orders and high CRs have been discarded. In this case, it is better to use a higher modulation order with a more robust CR that improves the performance while keeping the same BICM spectral efficiency. The dense urban scenario is modelled with the TDL-C channel model. In this scenario, a user speed of 30 km/h and a delay spread of 100 ns are used. Finally, the rural scenario is also modelled with the TDL-C channel, but in this case, the user speed is set to 120 km/h. The delay spread also changes for this scenario, having 30 ns in all cases.

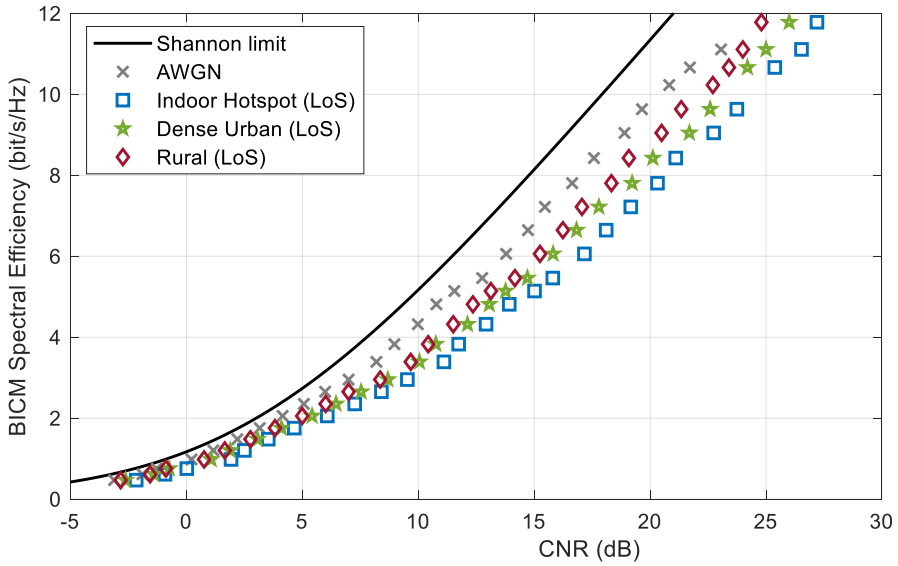

Figure 16. BICM spectral efficiency vs CNR (dB) for TDL scenarios with 2x2 MIMO.

Figure 16 depicts the BICM spectral efficiency vs. CNR for the IMT-2020 considered scenarios, i.e. indoor hotspot, dense urban and rural. All scenarios are evaluated with

and LoS and compared with the AWGN MIMO channel. Two transmitter and receiver antennas are used. A single codeword is transmitted by using two independent layers as specified in [12].

4.1.4.2 Physical Downlink Control Channel (PDCCH)

a) Technology Comparison: NR vs LTE

Figure 17 shows the BER and BLER as a function of the required CNR (dB) for the different aggregation levels (AL) of Control Channel Elements (CCE), including both New Radio configuration and LTE in AWGN channel.

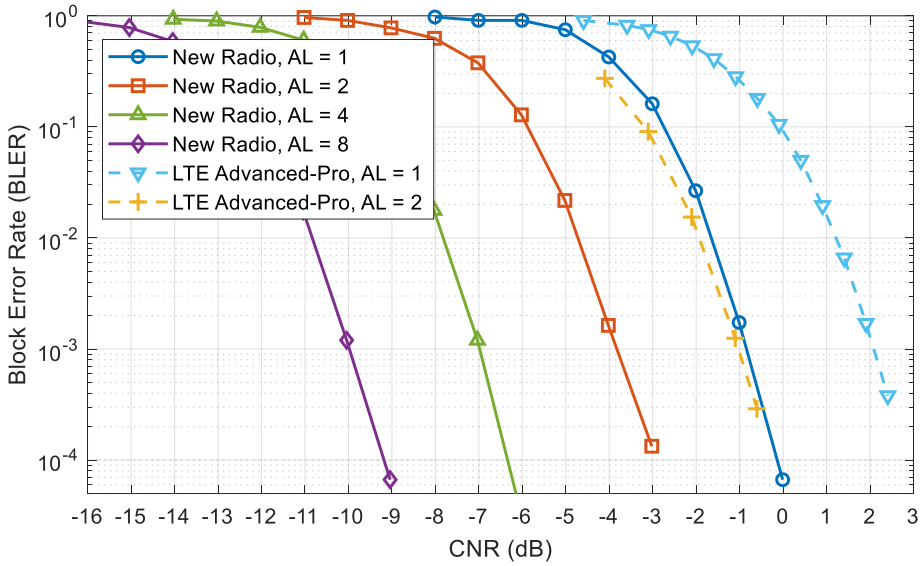

Figure 17. Block error rate vs CNR for AWGN channel with different ALs.

The simulation parameters include a channel BW of 5MHz, CFI = 3, 12 DCI bits in NR (smallest possible) and LTE (format 1C), CRC length of 16 and 24 bits with LTE and NR respectively, Tail Biting Convolutional Code (TBCC) with LTE: (mother code rate of 1/3) and polar codes with NR, AWGN channel, Maximum Likelihood (ML) demapper and QPSK as the only modulation order for both NR and LTE. The rate recovery process includes additively combining any repetitions to distinguish the performance difference of higher aggregation level.

The corresponding **effective code rate** for each aggregation level is:

- New Radio: $\left\{\frac{12}{144}, \frac{12}{288}, \frac{12}{576}, \frac{12}{1152}\right\}$ for AL 1, 2, 4, 8 respectively.
- LTE: $\left\{\frac{12}{72}, \frac{12}{144}\right\}$ for AL 1, 2 respectively.

The reason of choosing the number of DCI information bits 12 is because for higher numbers zeros shall be appended to the DCI format until the payload size equals 12 [12]. This means 12 bits is the smallest possible number of DCI information bits, which should be equivalent to the smallest possible CNR requirement for all conditions (different aggregation levels).

From the results in Figure 17, we can see that a higher aggregation level generally gives more protection to codewords, which is reflected in the required CNR for both LTE and NR situation, by trading more occupied bandwidth. Due to the different CRC and aggregation levels for LTE and NR, it is not easy to achieve a fair comparison. Generally,

Polar codes should outperform TBCC. If compared under the same AL with the parameters shown, NR requires about 2.3dB less than LTE to achieve BLER < 10^{-3}.

b) IMT-2020 Scenarios

In this section, the SISO performance for the IMT-2020 scenarios is presented and compared with AWGN, according to different scenarios described in subsection 4.1.5.1. Perfect channel estimation has been used in a frequency range of 700 MHz.

The following table shows the minimum CNR needed for:

- TDL-A channel model for indoor hotspot scenario with 30ns delay spread and 3km/h.
- TDL-C channel model for rural scenario with 300ns delay spread and 30km/h.

Table 18. Minimum CNR threshold of PDCCH in AWGN, TDL-A/C channels.

Scenario	AL 1	AL 2	AL 4	AL 8
AWGN	0.3 dB	-3.8 dB	-7 dB	-10 dB
Indoor hotspot	1.5 dB	-3.2 dB	-6.5 dB	-9.4 dB
Rural	-	-3.7 dB	-6.8 dB	-9.9 dB

From the results, we can see that under perfect channel estimation, the higher movement speed equivalent to better Doppler diversity which makes the CNR requirement for each aggregation level of the TDL-C channel (with 30km/h movement speed) outperform the corresponding point with TDL-A channel (with 3km/h movement speed).

Compared to the AWGN results, at lower aggregation level, which is equivalent to high data rates, the BLER performance for both TDL-A and TDL-C channels are worse than AWGN result. But because of the fixed code word length, when aggregation level goes higher, the code rate dramatically decreases and the TDL channel performances are almost aligned with the AWGN channel. For channel models with LOS path (results not shown here), it will give exactly the same results as the AWGN channel due to the large Rice factor (K) of the LOS path. (i.e. TDL-D and TDL-E).

4.2 Ultra-Reliable Low Latency Communications for Public Warning and Automotive

4.2.1 Mobility

4.2.1.1 Physical Downlink Shared Channel (PDSCH)

This section studies the speed tolerance with practical receiving algorithms in NR. The mobility KPI is a variant of the BICM spectral efficiency KPI, evaluated with link-level simulations by using a mobile channel model. In mobile environments, the channel realizations are a time variant function that depends on the relative speed of the transmitter and receiver pair.

a) Theoretical Doppler limit

The time dependent variation of the channel realizations produces frequency shifts in the received signal known as the Doppler. The maximum frequency shift f_D in the received signal due to the Doppler shift assuming ideal interpolation is:

$$f_D = \frac{v\, f_c \cos\alpha}{c} \tag{9}$$

where v is the receiver velocity c is the speed of light, f_c is the carrier frequency of the signal, and α is the angle between directions of the receiver velocity and the arriving signal. The Doppler limit can be theoretically estimated as:

$$f_{D_{limit}} = \frac{1}{2D_y(T_U + T_{CP})}\ Hz \tag{10}$$

where D_y is the length of the reference signal sequence in OFDM symbols, T_U is the useful symbol duration, and T_{CP} is the cyclic prefix length in time. Hence, the performance depends on the carrier spacing, system bandwidth, the operational frequency band and the accuracy of channel estimation. For this study, a wide range of Doppler shifts is evaluated. The obtained results can be easily mapped to the frequency bands under evaluation by using the previous formulas. Two frequency bands are here evaluated: 700 MHz and 4 GHz.

The theoretical Doppler limits for each frequency band depend on the DMRS signal used. Assuming Mapping Type A, DMRS configuration type 1 and *DL-DMRS-add-pos = 1,* i.e. 2 symbols ($D_y = 7$), the Doppler limit can be calculated as:

$$f_D = \frac{1}{2 \cdot 7 \cdot 10^{-6}(66.6 + 5.2)} = \mathbf{994.8\ Hz} \tag{11}$$

which corresponds to a user speed of 1534 km/h at 700 MHz and 268 km/h at 4 GHz. Note that a numerology 0 has been used in this calculation and higher numerologies will increase the speed, since lower $T_U + T_{CP}$ will be obtained. Likewise, using a different pattern will change the user speed limit as follows:

The IMT-2020 requirement is a user speed of 500 km/h [47]. As can be observed, every configuration at the 700 MHz band fulfils the selected criterion. This is not the case at 4 GHz, where using numerology 0 hampers the reception if only 2 DMRS symbols are used (**marked in bold**).

Table 19. Doppler limit (Hz) and related speed for 700 MHz and 4 GHz bands.

μ	DMRS Symbols	D_y	f_D	User limit (km/h) @ 700 MHz	User limit (km/h) @ 4 GHz
0	2	7	994.8	1534	**268**
	4	3	2319.3	3576	625
1	2	7	1992.6	3074	537.99
	4	3	4638.6	7155	1251
2	2	7	3982.7	6144	1075
	4	3	5566.4	14313.1	2496

These values are the maximum theoretical limits, which can be only reached if the transmitted configuration is robust enough. The use of modulation and coding will lower these values significantly, as the next section shows.

b) Link-level Evaluation

In order to evaluate the mobility performance of NR in the IMT-2020 evaluation context, several channel models with a range of different user speeds have been evaluated. The considered scenario is a Typical Urban (TU-6) with variable speed.

The three considered numerologies for frequency range 1 (450 MHz to 6 GHz) are evaluated, i.e. 15, 30 and 60 kHz. This parameter is important when evaluating mobility, since higher numerologies are more robust against Doppler shifts. Mapping Type A with DMRS configuration type 1 is assumed. Different pilot patterns, i.e. patterns with 2 and 4 symbols are also explored. Real channel estimation (linear in time, linear in frequency) with **MCS 3** is used in all cases.

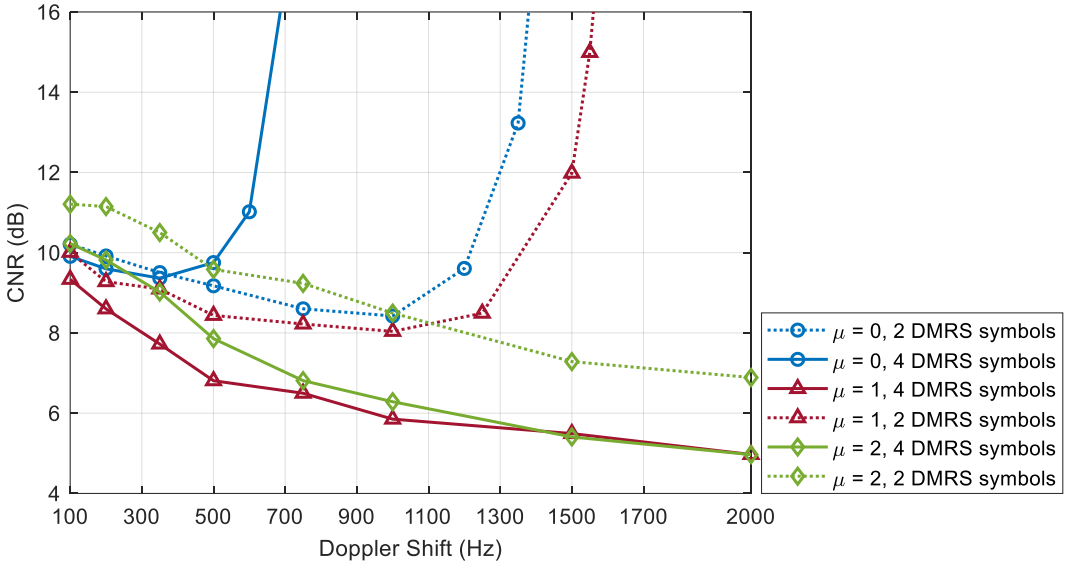

Figure 18. CNR against user speed for 5G New Radio in TU-6 mobile channel. Numerologies 0,1 and 2, MCS 3.

Results in Figure 18 show that for Doppler shifts up to 500 Hz, the performance with all configurations and real channel estimation is good enough to keep an acceptable CNR. In this case, the higher the speed the lower the CNR required. This behaviour is obtained because of the Doppler range used. At high Doppler shifts, it may increase as occurs with the rest of configurations. Then, degradation appears. For higher user speeds and some configurations, the Doppler shift starts to cause significant Inter-Carrier Interference (ICI) and channel estimation errors. This leads to performance degradation. The way to increase the Doppler shift limits is by using more DMRS symbols or by increasing the numerology.

Configurations with Doppler limits are:

- Numerology 0
  - 2 DMRS symbols: 600 Hz (925 km/h @ 700 MHz, 162 km/h @ 4 GHz).
  - 4 DMRS symbols: 1300 Hz (2005 km/h @ 700 MHz, 351 km/h @ 4 GHz).
- Numerology 1
  - 2 DMRS symbols: 1500 Hz (2314 km/h @ 700 MHz, 405 km/h @ 4 GHz).

The rest of configurations are good enough to support user speeds higher than 500 km/h at 4GHz. Therefore, **numerology 1 with more than 2 DMRS symbols is at least needed at 4 GHz** with this modulation and coding scheme. On the other hand, **all configurations fulfil the requirement at 700 MHz**. These results are slightly worse than the theoretical limits obtained in Table 19.

The use of a higher **MCS 15** further reduces these limits, as shown in Figure 19 for numerology 0.

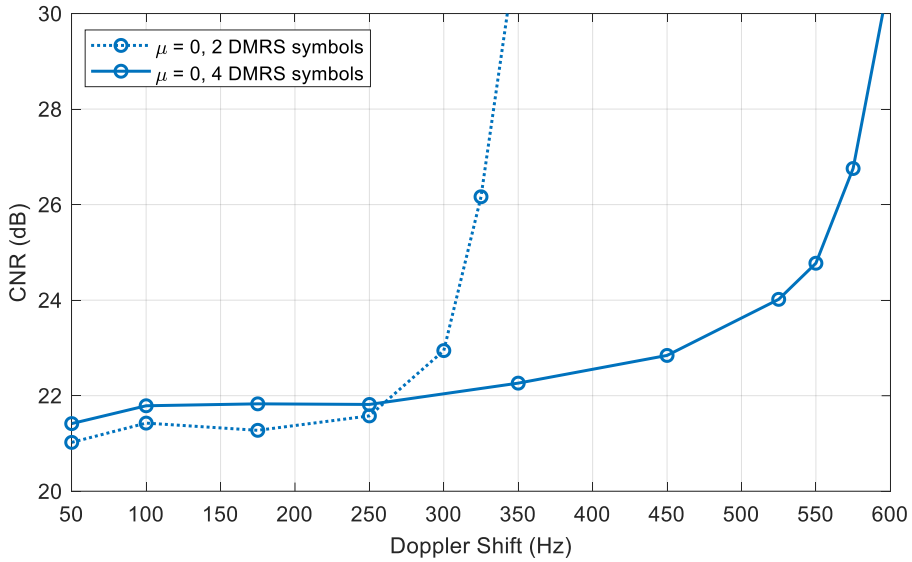

Figure 19. CNR against user speed for 5G New Radio in TU-6 mobile channel. Numerology 0, MCS 15.

Results in Figure 19 show that the degradation for the case of 2 DMRS symbols starts in this case at 300 Hz. The value is reduced to half compared to MCS 3. A similar behaviour can be observed when using 4 DMRS symbols. The Doppler limit is reduced to 600 Hz in this case, having 1200 Hz with MCS 3.

4.2.1.2 Physical Downlink Control Channel (PDCCH)

This section studies the speed tolerance of the NR PDCCH with practical channel estimation algorithms.

a) Theoretical Doppler limit

Considering the frame structure shown in Figure 2 and the CORESET allocation shown in Figure 4 (aligned with the frame structure in [12]), it can be observed that there is no gap between PDCCH DMRS symbols in the time domain. More specifically, for NR:

- In the frequency domain, PDCCH DMRS symbols are allocated in every 4 subcarriers;
- In the time domain, the number of PDCCH DMRS symbols is dependent on the value of $N_{symb}^{CORESET}$, which is determined by PCFICH and can be 1, 2 or 3.

In order to estimate the channel, a two-dimensional (i.e., frequency and time) sampling should satisfy:

- In the frequency domain, the sampling rate must be faster than or equal to the maximum delay spread of the channel;
- In the time domain, the sampling rate must be greater than or equal to the maximum Doppler spread of the channel.

The maximum distance between two PDCCH DMRS symbols in the time domain, n_{max}, is therefore given by:

$$n_{max} \leq \frac{1}{2(T_U + T_{CP})d_{max}} \quad (12)$$

where d_{max} represents the maximum Doppler spread of the channel. Due to the fact that the PDCCH DMRS symbols cover all the time domain REs on selected subcarriers, i.e., $D_y = 1$, thus the number of PDCCH DMRS symbols is sufficient enough to capture the time variation of the channel with potentially a wide range of user speeds, as given by:

$$f_D = \frac{1}{2 \cdot 1 \cdot 10^{-6}(66.6 + 5.2)} = \mathbf{6963.6\ Hz} \quad (13)$$

which corresponds to a user speed of 10743 km/h at 700 MHz and 1880 km/h at 4 GHz. As previously mentioned, the numerology 0 has been used in this calculation and higher numerologies will increase the speed, since lower $T_U + T_{CP}$ will be obtained.

b) Link-level Evaluation

To evaluate the performance of PDCCH in the mobile environments, link level simulations are performed to, first, verify if any error floor occurs in the BICM performance when the practical channel estimation applies and different user speeds are considered. If not, then the required CNR to achieve BLER < 0.1% against the Doppler shift or user speeds can be evaluated. The two-dimensional pilot-based estimation with the linear interpolation is used. Different aggregation levels have been considered.

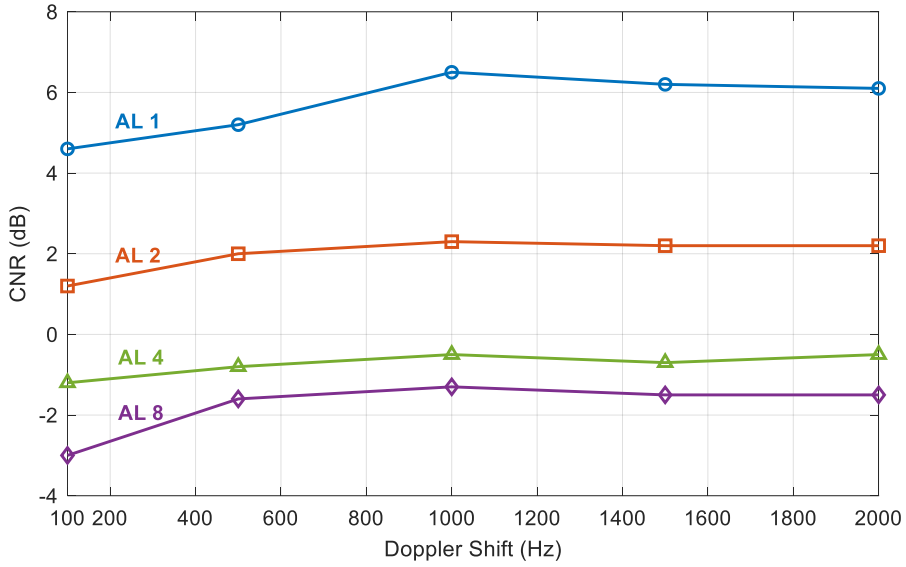

Figure 20. CNR against user speed for 5G New Radio in TDL-A mobile channel. PDCCH, real channel estimation.

As shown in the above figure, the **PDCCH can handle all required user speeds for all aggregation levels**, as in [3] for all the considered frequency bands. Also, the higher the aggregation level, the lower the required CNR, due to the better coding rate used (half with the next level).

4.2.2 User plane latency

The next section describes the **User Plane (UP) latency** that 5G NR Rel'15 introduces for different configurations. The user plane latency is defined as the delay necessary to transmit data between the gNB and the UE. It consists of the transmission (τ_1), HARQ request (τ_2) and retransmission (τ_3) between both entities as shown in Figure 21.

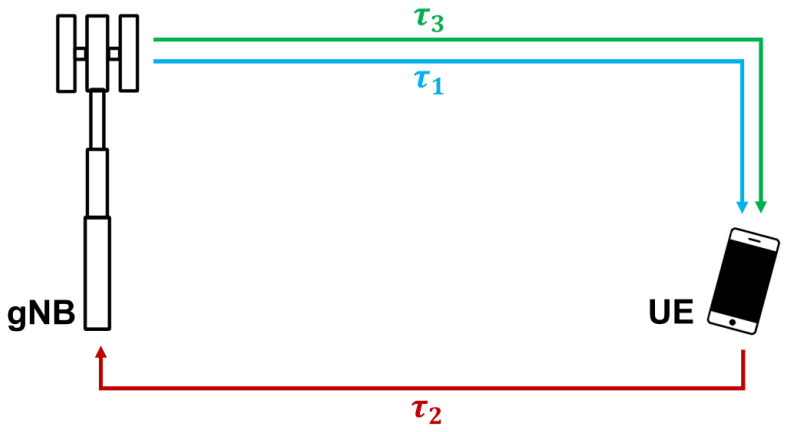

Figure 21. User plane latency calculation.

The requirements for this KPI are 1 ms for URLLC and 4 ms for eMBB services respectively. The transmission process can be modelled as follows:

$$T_{UP} = \tau_1 + p(\tau_2 + \tau_3) \quad (14)$$

where p is the probability of a retransmission. The latency in the first transmission, T_1, can be calculated as follows:

$$\tau_1 = t_{gNB,tx} + t_{FA1} + t_{TTI} + t_{UE,rx} \quad (15)$$

where $t_{gNB,tx}$ is the processing time in the gNB, t_{FA1} is the time needed for frame alignment, starting when permitted by the configuration, t_{TTI} is the time of data transmission and $t_{UE,rx}$ is the processing time in the UE. If the reception is correct, then $T_{UP} = \tau_1$. Otherwise, the UE needs to ask for a retransmission through a HARQ petition, as follows:

$$\tau_2 = t_{UE,tx} + t_{FA2} + t_{HARQ} + t_{gNB,tx} \quad (16)$$

where t_{FA2} is the time for frame alignment in this case and t_{HARQ} is the time of the petition (1 OFDM symbol in all cases). Then, the gNB retransmits the content as follows:

$$\tau_3 = t_{gNB,tx} + t_{FA3} + t_{TTI} + t_{UE,rx} \quad (17)$$

Example:

a) First transmission

We assume UE capability 2 [48], as it is representative of URLLC. As an example, this analysis presents first the case of numerology 0, with slot based scheduling of 14 symbols and probability of retransmission $p = 0.1$. First, the gBN needs some time to process the data. This step is calculated as follows:

$$t_{gNB,tx} = \frac{T_{proc,2}}{2} = \frac{\max(N_2(2048 + 144) \cdot \kappa \cdot 2^{-\mu} \cdot T_c/(SCS \cdot 2048),0)}{2} \quad (18)$$

where N_2 is a parameter that depends on the SCS. For numerology μ=0 and UE capability 2, N_2 is 5. Therefore, the processing time in the gNB, $t_{gNB,tx}$, is **178.4 *μ*s**. To start transmitting the content, the gNB needs to be aligned with the first possible symbol to transmit, in this case the symbol number 0. This value depends on the moment when the gNB starts the process. The gNB waits a minimum time t_{FA1} of 35.9 *μ*s and a

maximum time of 964.5 μs. On average, the time needed is **500 μs**. Then, the TTI is transmitted. 14 OFDM symbols with numerology 0 need **1 ms**, which is the time of a subframe. Finally, the UE processing time is calculated as follows:

$$t_{UE,rx} = \frac{T_{proc,1}}{2} = \frac{\max(N_1(2048+144)\cdot\kappa\cdot 2^{-\mu}\cdot T_c/(SCS\cdot 2048),0)}{2} \quad (19)$$

The value of N_1 also depends on the SCS. In this case, N_1 is 8, and therefore the processing time, $t_{UE,rx}$, is **107 μs**. The total time needed for the data transmission without HARQ,τ_1 is therefore **1.8 ms**.

b) HARQ request

If the data is not correctly received, then the UE sends the HARQ petition. Note that processing times in the UE and BS are the same in this case. The UE then needs **107 μs** to process the petition, and does not need to wait for this particular case, as Figure 22 shows. Therefore, t_{FA2} is **0 μs**. The time for the HARQ petition is 1 OFDM symbol, and thus t_{HARQ} is **71.4 μs**. The gNB the processes the request in **178.4 μs**. In total, the HARQ petition needs a time T_2 of **356.4 μs**.

c) HARQ retransmission

The gNB then needs time to process the retransmission, with the same value of **178.4 μs**. The time for frame alignment in this case is **357 μs** in any case, to reach the symbol number 0 and retransmit. Then, the TTI is retransmitted in **1 ms**, and the UE processes the data again in **107 μs**. The total time of retransmission T_3 is **1.59 ms**. The total user plane latency with a probability of retransmission $p = 0.1$ is therefore **1.98 ms**.

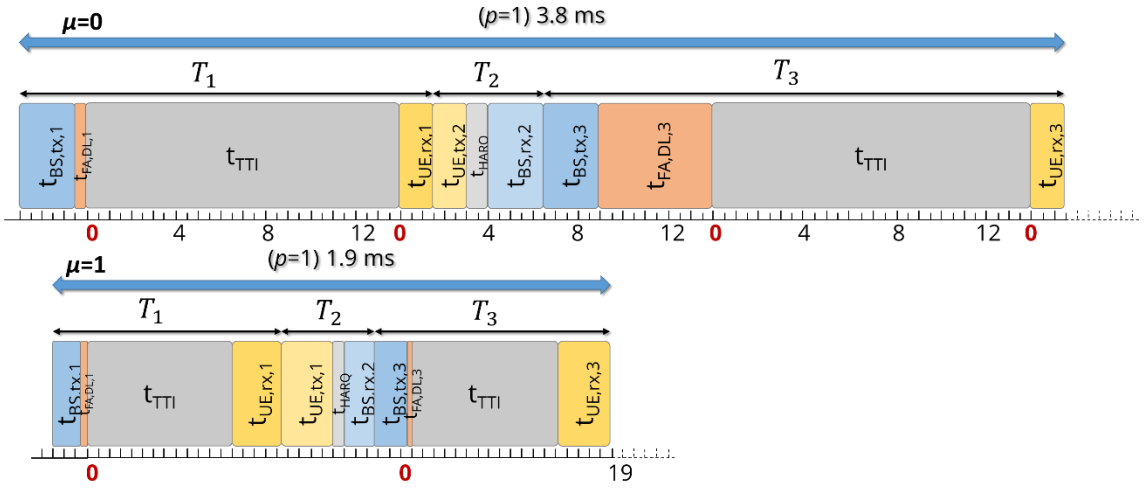

Figure 22. User plane latency for numerologies 0 and 1, with slot based scheduling of 14 symbols. Minimum frame alignment.

Extrapolation to all configurations:

The process can be easily extrapolated to all numerologies, as well as different slot configurations. In this deliverable, we assume FDD for the latency calculation. The results are summarized in Table 20.

Table 20. User plane latency (ms) for all considered configurations.

Slot configuration	HARQ probability	μ=0	μ=1	μ=2
2 symbols	$p = 0$	0.50	0.27	**0.23**
	$p = 0.1$	0.58	0.32	0.27
	$p = 1$	1.35	0.77	0.66
4 symbols	$p = 0$	0.71	0.38	0.28
	$p = 0.1$	0.82	0.44	0.34
	$p = 1$	1.85	0.95	0.78
7 symbols	$p = 0$	1.03	0.54	0.36
	$p = 0.1$	1.18	0.62	0.41
	$p = 1$	2.53	1.29	0.86
14 symbols	$p = 0$	1.80	0.92	0.55
	$p = 0.1$	1.98	1.02	0.63
	$p = 1$	3.78	1.91	1.30

4.2.3 Control plane latency

The control plane (CP) latency in 5G NR refers to the UE transition time required from idle to active state. The UE will naturally require some time to go from a battery efficient state to a starting point with continuous data transfer [8]. The IMT-2020 requirement is 20 ms. The procedure is divided into several stages, as Figure 23 shows.

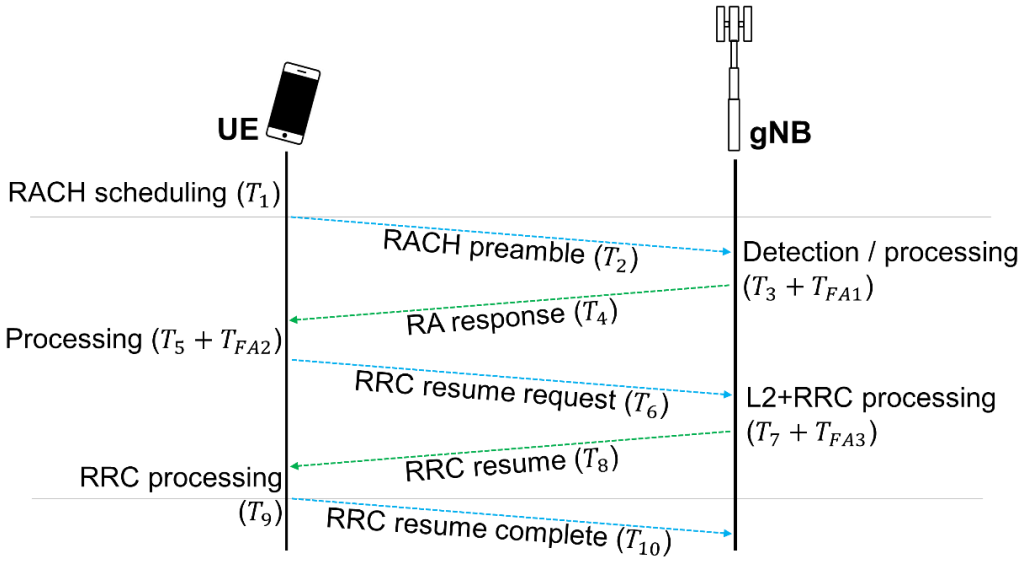

Figure 23. Control Plane latency calculation.

As it can be observed, the CP latency calculation process is divided into 10 steps related to scheduling, processing and transmissions aspects, and 3 additional steps related to additional frame alignments. Equation (20) describes the CP latency calculation:

$$T = \sum_{i=1}^{10} T_i + \sum_{j=1}^{3} T_{FA,j} \quad (20)$$

The transmission process can only start in OFDM symbols where a PRACH preamble is used. The first step is related to the delay due to the RACH scheduling period. Since the transition from idle to a different state does not start until the transmission of the RACH preamble, this step is considered irrelevant and therefore $T_1 = 0$ ms. The RACH preamble delay T_2 logically depends on the preamble length as specified in [12]. The third step is the preamble detection and processing in the gNB. The delay is calculated as $T_3 = t_{gNB}/2$, with t_{gNB} as calculated in (18). After time for frame alignment, $T_{FA,1}$, the gNB sends the RA response, which takes the length of 1 slot or non-slot, depending on the configuration used, that includes PDCCH and PDSCH. Hence, $T_4 = T_s$. The UE processing delay comprehends the decoding of scheduling grant, timing alignment, C-RNTI assignment and L1 encoding of the Radio Resource Control (RRC) resume request. It is calculated as follows:

$$T_5 = N_{T,1} + N_{T,2} + T_{wait} \quad (21)$$

where $N_{T,1}$ is the time to transmit N_1 symbols for PDSCH reception with processing capability 1 and additional DMRS configuration; $N_{T,2}$ is the time to transmit N_2symbols for PUSCH reception with processing capability 1; and $T_{wait}$is the average waiting time between the reception and transmission of data, which is assumed 0.5 ms. These values can be obtained from tables 5.3-1 and 6.4-1 in [43] respectively. After frame alignment $T_{FA,2}$, the next step is the transmission of the RRC resume request, which takes $T_6 = T_s$. The gNB then processes the L2 and RRC request. Following the procedure given in [48], it is assumed that $T_7 = 3$ ms. The following step is the slot alignment $T_{FA,3}$ and transmission of RRC resume, which takes $T_8 = T_s$. Finally, the UE processes the RRC. As done in step 7, we assume $T_9 = 7$ ms. The step 10 is considered to be the start of the data transfer, since it includes the transmission of RRC resume complete signal but user plane data. Therefore, it is assumed that $T_{10} = 0$ ms.

Example:

Following the same methodology than the UP latency, in this calculation we first provide a particular example to explain the CP procedure. The results are then extrapolated to a wider range of configurations. In this example, resource mapping type A, UE capability 2, numerology μ=0 with mini-slot based scheduling of 7 symbols, PRACH length of 1 ms and FDD mode have been selected. Figure 24 illustrates the assumed configuration for a better understanding.

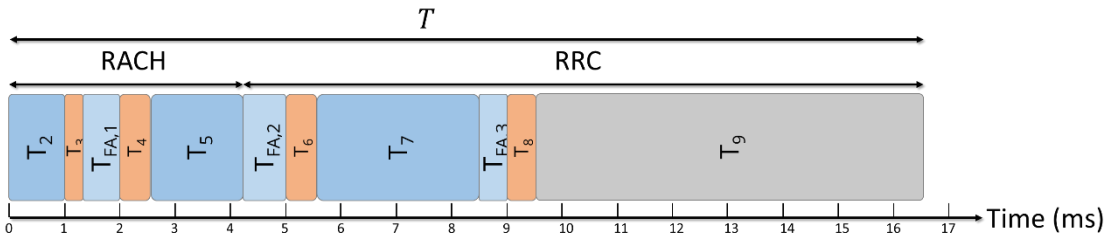

Figure 24.Control plane latency for μ=0, PRACH of 1 ms, mini-slot based scheduling of 7 symbols, resource mapping type A and UE capability 1.

The first delay to consider is $T_2 = 1$ ms, which is related to the PRACH length selected. Then, T_3 is calculated according to the methodology as $t_{gNB}/2$. As a result, $T_3 = 0.357$ ms. Since T_4 cannot cross any slot boundary, the gNB needs to wait $T_{FA,1} = 0.714$ ms, as shown in Figure 24. The transmission of a RA response takes $T_4 = T_s = 0.5$ ms. From

[43], the UE processing delay T_5 is calculated for this particular configuration with values $N_1 = 8$ and $N_2 = 10$ and therefore $N_{T,1} = 0.57$ ms, $N_{T,2} = 0.71$ ms and $T_5 = 1.785$ ms.

The UE waits until the next slot is available to start the RRC resume request, with $T_{FA,2} = 0.714$ ms. The transmission of the RRC resume request needs one mini-slot, equivalent to the PUSCH allocation length, i.e. $T_6 = T_s = 0.5$ ms. As denoted in the methodology, the processing delay in the gNB takes $T_7 = 3$ ms and the UE waits $T_{FA,3} = 0.5$ ms. Finally, the gNB transmits the RRC resume signal, which takes $T_8 = T_s = 0.5$ ms, and the UE processes it in $T_9 = 7$ ms. The total CP latency in this example is then $T = 16.5$ ms.

Assuming UE capability 2, the process in this work is extrapolated to all possible numerologies in FR1, both resource mapping types, all slot configurations and different PRACH lengths. The results are summarized in Table 21. The lowest CP value achieved is 11.6 ms, which fulfills the IMT-2020 requirement of 20 ms.

Table 21. Control plane latency (ms) for all considered configurations.

Mapping	Slot	PRACH 1 ms		PRACH 2 symbols		
		μ=0	μ=1	μ=0	μ=1	μ=2
Type A	4 symbols	16.3	13.6	15.3	12.6	12.1
	7 symbols	16.5	14.3	15.5	13.3	12.1
	14 symbols	17	14.5	-	-	-
Type B	4 symbols	13.7	12.7	12.9	11.8	**11.6**
	7 symbols	14.4	13	13.6	12	11.7
	14 symbols	15	13.5	14	12.8	11.9

4.3 Massive Machine Type Communications

4.3.1 Energy efficiency

The energy efficiency can be evaluated from both network and device perspectives. It is considered in IMT-2020 as a qualitative measure [47]. The network energy efficiency is defined in [48] as the capability of a Radio Interface Technology (RIT) or a set of RITs (SRIT) to minimize the RAN energy consumption in relation to the provided traffic capacity. On the other hand, the device energy efficiency is the capability of the RIT/SRIT to minimize the device power consumption in relation to the traffic characteristics. Note that this KPI can be in turn calculated as the sleep ratio, i.e. fraction of unoccupied resources in a period of time (%); or the sleep duration, i.e. the absolute value or continuous period of time with no transmission and reception. In this deliverable, network energy efficiency has been evaluated, since it demands requirements that are more stringent.

When no data transfer takes place (unloaded case), NR networks perform periodical transmission of SS/PBCH blocks and Remaining Minimum System Information (RMSI) paging signals, so that UEs can access the RAN. The sleep ratio per slot is calculates as follows:

$$E_{slot} = 1 - \frac{\lceil L/2 \rceil}{2^{\mu} \cdot P_{SSB}} \quad (22)$$

where L is the number of SS/PBCH blocks in a SS Burst set, and P_{SSB} is the SSB periodicity. The sleep duration can be easily derived by just multiplying the sleep ratio, E_{slot}, by P_{SSB}. Additionally, the sleep ratio can be calculated per symbol as:

$$E_{symbol} = 1 - \frac{L(2/7)}{2^{\mu} \cdot P_{SSB}} - \beta \frac{L/7}{2^{\mu} \cdot P_{RMSI}} \quad (23)$$

where β is a flag variable ($\beta = 1$ for FR1 and $\beta = 0$ for FR2) and P_{RMSI} is the RMSI periodicity.

Since FR1 has been assumed in the following calculations, $\beta = 1$. Additional assumptions need to be considered in the calculation. Each SS/PBCH block is assumed to occupy 4 OFDM symbols with 20 RBs in one slot. One or multiple SS/PBCH blocks compose an SSB, which is confined in half radio frame window, i.e. 5 ms. The SSB periodicity (P_{SSB}) can be 5, 10, 20, 40, 80 or 160 ms [43]. On the other hand, the RMSI occupies 2 OFDM symbols in one slot, with a slot accommodating two RMSI transmissions. RMSI is usually time-division multiplexed with SS/PBCH and therefore it can be transmitted in the same slot. The RMSI periodicity is 20 ms if $P_{SSB} \leq 20$ ms and P_{SSB} ms otherwise. Given the different SSB periodicity values, and assuming numerology μ=0, Table 22 shows the network energy efficiency in terms of sleep ratio (%) for the selected configurations at both slot and symbol levels. As observed, efficiencies up to 99.73% are achieved in 5G NR. Since the minimum value obtained is 80%, it is considered that all possible values fulfil the IMT-2020 requirement.

Table 22. Energy efficiency or Sleep ratio (%) in 5G NR for μ=0 and FR1.

	L	5 ms	10 ms	20 ms	40 ms	80 ms	160 ms
Slot	1	80	90	95	97.5	98.75	99.38
	2						
Symbol	1	93.57	96.43	97.86	98.93	99.46	**99.73**
	2	87.14	92.86	95.71	97.86	98.93	99.46

5 Performance Evaluation of 5G PTM Air Interface

This section evaluates the performance of the 5G PTM air interface solutions described in Section 3. This section redefines the KPIs analysed in Section 4 and additionally includes a new KPI related to SFN coverage simulations, specific to multicast and broadcast services. The methodology is structured around the IMT-2020 evaluation types, i.e. analytical, link-level and coverage simulations [44]. Table 23 shows the list of KPIs and methodologies used to evaluate each of the 5G PTM air interface solutions:

Table 23. Assessment method used per KPI and associated technology.

KPI	Scenario	Methodology	5G NR PTP	SC-MM	MC-MM	TB
Bandwidth	eMBB, URLLC	Inspection	✓			
Peak data rate	eMBB	Analytical	✓	✓	✓	✓
Peak spectral eff.	eMBB	Analytical	✓	✓	✓	✓
BICM spectral eff.	eMBB	Link Level	✓		✓	✓
SFN coverage	eMBB	Coverage / Link Level			✓	✓
Mobility	URLLC, eMBB	Link Level	✓		✓	✓
User Plane Latency	URLLC	Analytical	✓	✓	✓	✓

Control Plane Latency	URLLC	Analytical	✓	✓	✓	✓
Energy Efficiency	mMTC	Analytical	✓	✓	✓	✓

As shown in Table 23, depending on the PTM air interface solution, a set of different KPIs has been considered, due to the different nature and type of service that these modes were created for.

SC-MM introduces the design of a new multicast CORESET, which is used to convey all the control information for all users in the cell. When the number of users in the cell is high, it allows reducing the PDCCH overhead from 50% up to 90%. Consequently, the use of a new multicast CORESET has an impact on the peak data rate and peak spectral efficiency calculation.

MC-MM includes the design of a SFN operation mode that allows covering ISDs up to 20 km thanks to the design of negative numerologies combined with extended CP. According to that, BICM Spectral Efficiency is calculated in SFN scenarios for the different numerology options. In addition, SFN coverage is obtained through link-level simulations for different echo delays. Finally, mobility tolerance is analysed for the new SCS, related to the new negative numerology design.

TB extends the SFN coverage up to 100 km thanks to the use of the new narrow numerologies and extended CP. As it has been explained in Section 3.4, TB introduces new CP lengths, DMRS patterns and control regions that may have an impact on the peak data rate and peak spectral efficiency. BICM spectral efficiency and coverage are also analysed for the new SFN operation mode. Finally, Terrestrial Broadcast mobility tolerance is also evaluated.

5.1 Enhanced Mobile Broadband for Media & Entertainment

5.1.1 Bandwidth

The maximum bandwidth for SC-MM, MC-MM and TB modes is 50 MHz. This value has been inherited from numerology 0 and FR1 in PTP, see section 4.1.1. Since all proposed PTM numerologies provide lower or the same SCS than numerology 0, the maximum bandwidth cannot exceed this value.

5.1.2 Data Rate

As explained in Section 4, the peak data rate is calculated depending on the overhead introduced by the different 5G NR physical channels and signals. While in 5G NR PTP the variation in the number of users affects the overhead and the peak data rate value, the overhead associated to the number of users in PTM systems is fixed. Due to this parameter variability, from now on the KPI is simply referred as data rate. Figure 25 shows the PTP and PTM data rate achieved when changing the number of users sharing the same spectrum. As can be observed, the variation in the number of users has an impact in the total overhead. In this case, numerology μ = 0 and 50 MHz of bandwidth are configured. PTM results can be linked to the SC-MM and MC-MM designed in this project and extended to all the possible numerology and bandwidth configurations. The parameter γ in the figure refers to the fixed data rate obtained thanks to the use of a fixed CORESET.

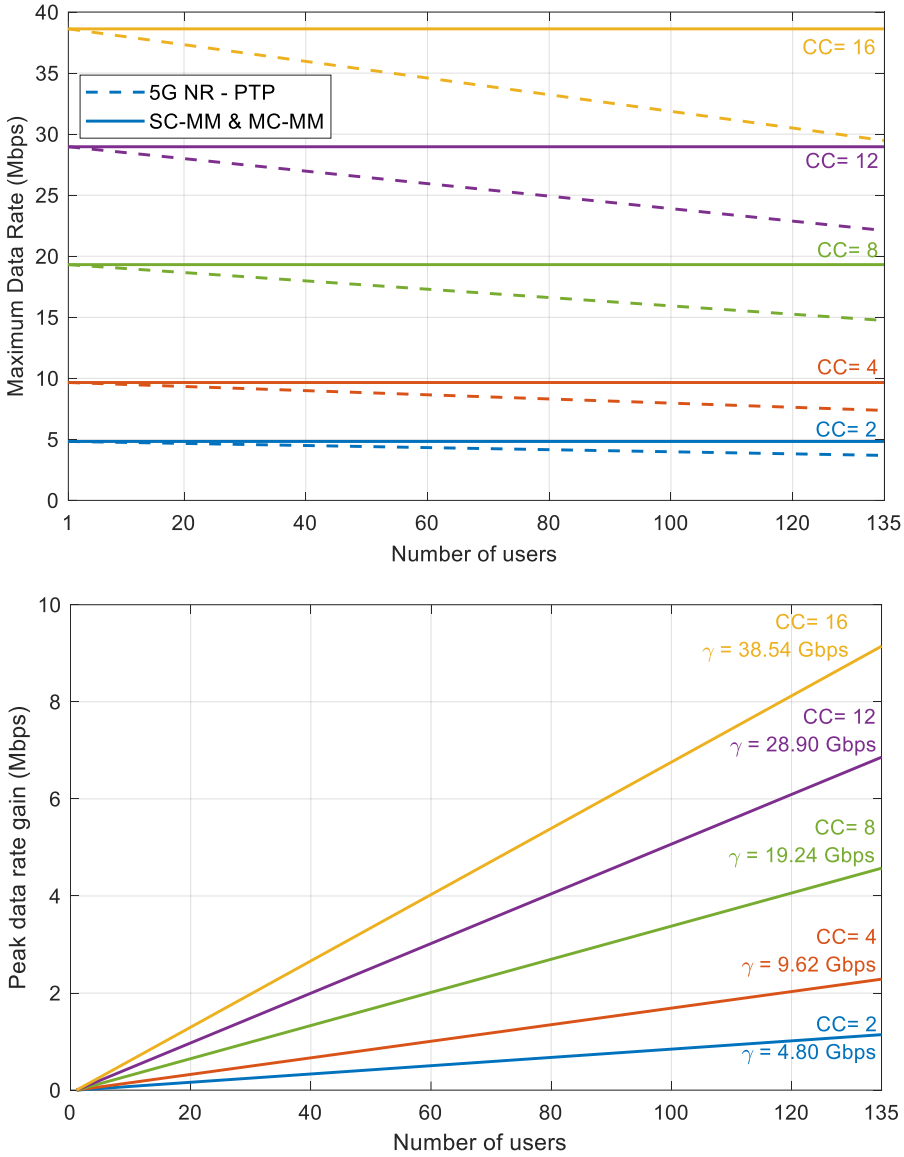

Figure 25. Peak data rate (top) and gain obtained (bottom) with SC-MM and MC-MM compared to PTP, for different numbers of users and different number of CCs.

There is a **clear data rate gain compared to PTP** services, especially for high numbers of users. This is due to the use of a single CORESET, saving 72 REs per user. Results show that the use of unicast is not efficient in this scenario, and the data rate gain becomes even higher when multiple carriers (by means of carrier aggregation) are used. For example, with 16 CC and 135 users, the maximum rate gain is **9.15 Gbps**, since it is fixed to 38.62 Gbps with the MM regardless of the number of users.

5.1.3 Spectral Efficiency

The spectral efficiency can be easily calculated by following the procedure described in section 4.1.3 for PTP. There is a direct relationship between spectral efficiency and data rate, and therefore the **PTM gain** has similar behaviour. The specific spectral efficiency values and gains for both modes are shown in Table 24. A numerology μ = 0 and 50 MHz of bandwidth are used.

Table 24. Spectral efficiency vs number of users.

Number of users	PTP (bit/s/Hz)	MM (bit/s/Hz)	Gain (%)
1	48.17	48.17	0
5	47.93		0.48
10	47.51		1.37
25	46.23		4.03
50	44.09		8.45
100	39.83		17.31
135	36.84		23.51

Gains **up to 23.51%** are achieved when a single multicast CORESET is transmitted in SC-MM and MC-MM, if the number of users is high enough. These percentages can be applied also to peak data rate. In the case of TB, the maximum spectral efficiency is 38.47 bit/s/Hz.

5.1.4 BICM Spectral Efficiency

The BICM spectral efficiency is calculated for both PDSCH and PDCCH channels in SFN scenarios through link-level simulations, as specified in Section 4.

SFN scenarios are modelled with 0 dB echo channel, which is defined in the DVB-T2 implementation guidelines [49] as a channel model composed of two paths with the same amplitude and a time delay equivalent to 90% of the CP duration. In this study, the channel has been modified and extended to enable different delays. The selected Quality of Service (QoS) is a block error rate BLER < 0.1%. Real channel estimation is used in all cases. In particular, channel estimation is performed by interpolating linearly in time domain and with a DFT-based method in frequency domain [50]. DFT method offers an additional accuracy in multipath environments with respect to linear interpolation

5.1.4.1 Multi-Cell Mixed-Mode

Figure 26 shows the BICM spectral efficiency (bit/s/Hz) as a function of the required CNR for the different MCS available in NR. Different negative numerologies have been simulated for an echo delay equal to 16.67 µs (ISD = 5 km) and compared with LTE SC-PTM. The channel capacity is also shown for comparison.

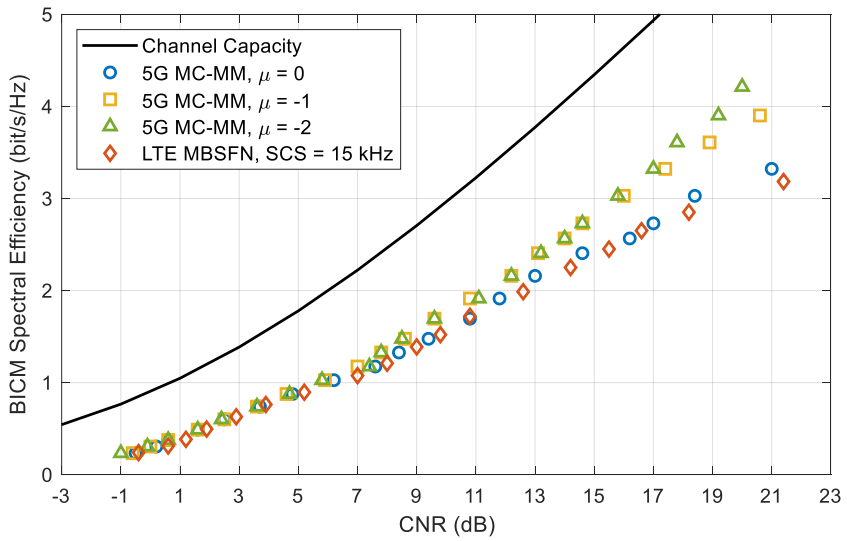

Figure 26. BICM spectral efficiency vs. CNR for MC-MM with 0 dB echo channel.

As discussed previously, the use of LDPC codes in 5G NR provides a BICM spectral efficiency gain with respect to turbo-codes in LTE. For this reason, the MC-MM with numerology 0 and therefore same carrier spacing as LTE, provides better performance. As expected, **additional gains are obtained with lower numerologies**. This impact is obtained because of the subcarrier density increase, which better helps to estimate the frequency variation of the SFN channel model.

5.1.4.2 Terrestrial Broadcast

Figure 27 shows the BICM spectral efficiency for different MCS indexes of the 5G NR Terrestrial Broadcast mode. In this case, the performance is compared with eMBMS enTV Rel'14. As occurred with the MC-MM, the **TB provides higher BICM spectral efficiency than LTE enTV** thanks to the use of LDPC coding.

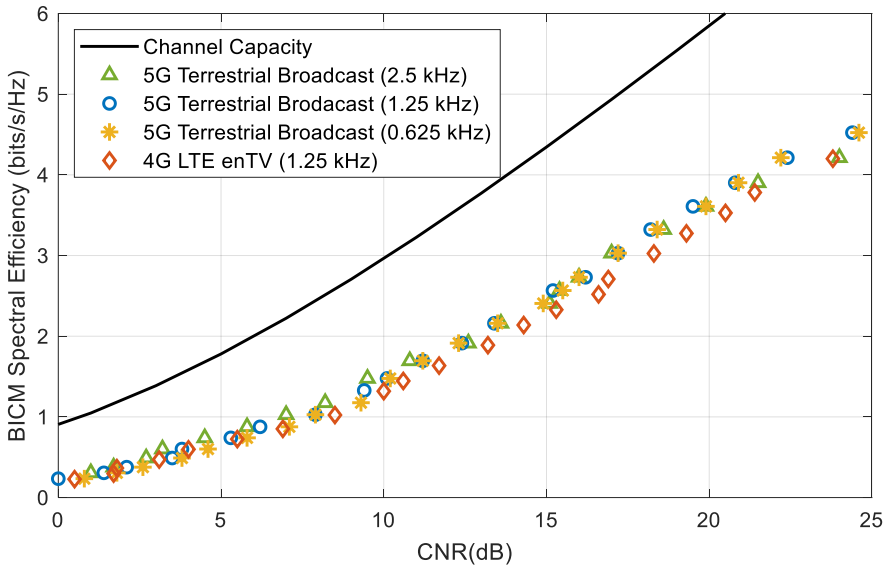

Figure 27. BICM spectral efficiency vs. required CNR, TB with 0 dB echo channel.

5.1.5 SFN Coverage

SFN coverage is expressed as the variation of the required CNR depending on the relative echo delay. To carry out its evaluation, the channel model has been extended to allow the configuration of multiple echo delays inside and outside the CP region. Coverage has been analysed by means of link-level simulations for all the physical channels involved in SFN transmissions, i.e. PDSCH and PDCCH. QoS requirements and channel estimation techniques from previous sections are reused. For each physical channel, different SCS and CP configurations are evaluated.

5.1.5.1 Multiple Cell Mixed Mode

The PDSCH coverage has been evaluated for different CP lengths associated to negative numerologies in MC-MM, i.e. 16.66 µs (ISD = 5 km), 33.33 µs (ISD = 10 km) and 66.66 µs (ISD = 20 km). All configurations have been simulated with MCS 2.

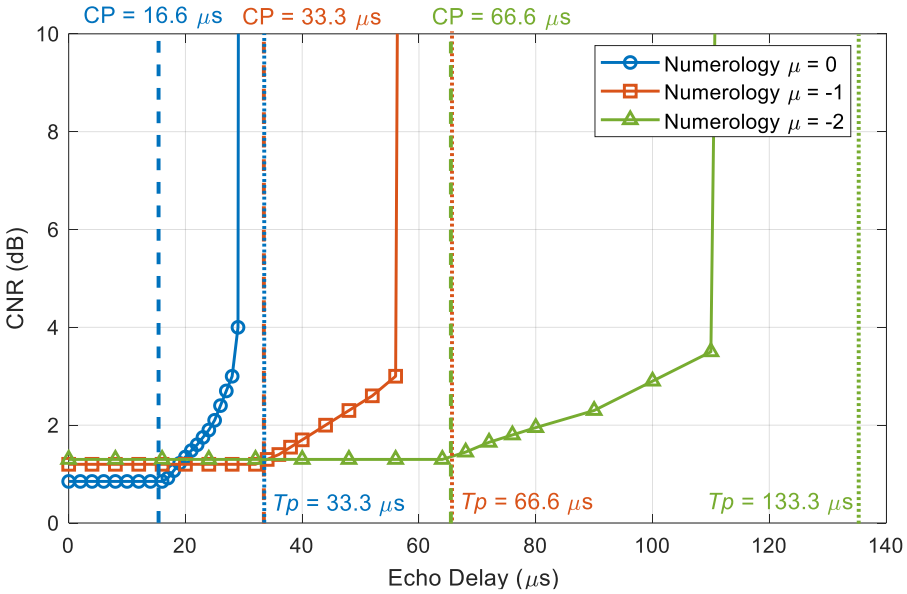

Figure 28. Required CNR with different echo delays using MC-MM.

As Figure 28 depicts, the performance remains constant for all the evaluated configurations when echoes arrive inside the CP. Otherwise, degradation due to multipath effect is introduced. In particular, when echoes arrive between the CP and the Nyquist limit, the degradation depends on the robustness of the MCS selected. On the other hand, echoes outside the Nyquist limit produce a total degradation of the system.

Therefore, **the MC-MM coverage in SFN scenarios is limited by the Cyclic Prefix and the Nyquist limit**. Configurations with longer CP and longer Nyquist limits provide higher coverage. When transmitters are deployed with ISD equal to the CP length, there is no degradation. If the ISD is set up to the Nyquist limit, longer coverage is introduced at the expense of introducing more degradation to the system [51].

5.1.5.2 Terrestrial Broadcast

The performance for the designed CP lengths in TB, i.e.100 μs (ISD = 30 km), 200 μs (ISD = 60 km) and 400 μs (ISD = 120 km) is shown in Figure 29. LTE enTV coverage, with CP 200 μs, is also used as a reference. Same MCS index is also evaluated.

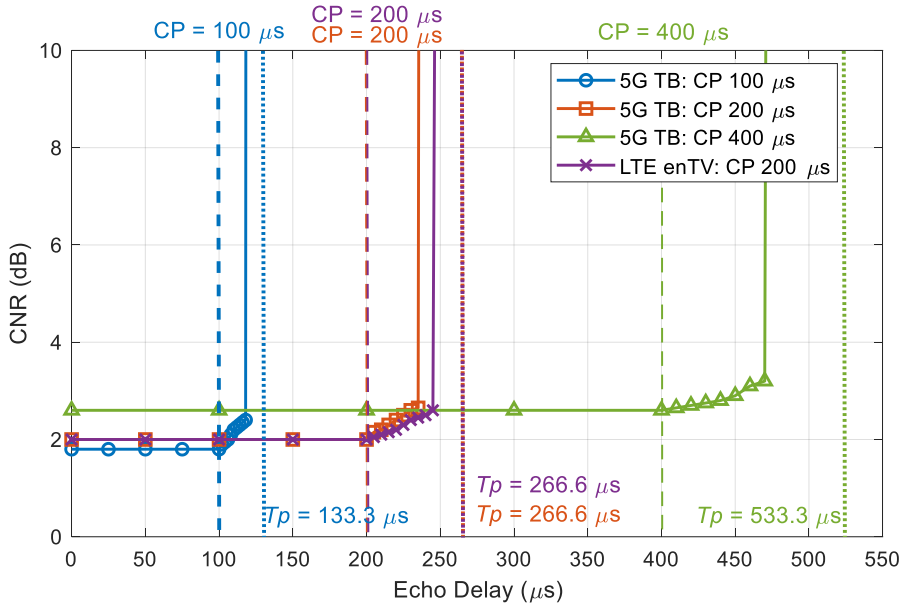

Figure 29. Required CNR with different echo delays using the 5G TB mode.

Figure 29 shows how **5G TB outperforms LTE enTV** in terms of SFN coverage thanks to the definition of CP = 400 μs (ISD = 120 km). In addition, TB also introduces a new CP = 100 μs that enables to cover smaller ISD = 30 km. As described previously, CNR degradation appears when the echo delay arrives beyond the CP region. As a particularity, the percentage of Nyquist limit region where degradation is acceptable gets reduced when the highest coverage mode is selected.

5.1.5.3 Physical Downlink Control Channel (PDCCH)

In this section, the performance of the NR-PDCCH channel with different coverage settings has been evaluated. In theory, with a specific μ and therefore a fixed useful symbol duration T_U, the maximum channel delay spread is highly dependent on the DMRS pattern, or to be specific, the pilot granularity in the frequency domain D_x. The maximum distance between two frequency domain PDCCH DMRS symbols, m_{max}, is given by:

$$m_{max} \leq \frac{T_U}{\tau_{max}} \tag{24}$$

where τ_{max} represents the maximum delay spread of the channel. Take the 15kHz subcarrier spacing as an example, also as shown in the frame structure in Figure 2 and the CORESET allocation in Figure 4, $D_x = 4$, one can derive $T_U = 1/\Delta_f = 66.7\mu s$. Therefore, the maximum channel delay spread that can be tolerated would be $\tau_{max} \leq T_U/D_x \approx 16.66\mu s$, greater than the one from the channel such as TDL-A and TDL-C. Thus, similar to the NR-PDSCH, the 0dB echo channel has been modified and extended to include different delays.

Differently from PDSCH, there is no need to perform interpolations in time domain due to the tight pilot distribution as discussed in section 4.2.1.2. The DFT-based interpolation is applied in frequency domain, which is a widely-used channel estimator and shows promise in the literature [50], compared with the estimator with the other types of interpolations such as the linear interpolation. Two set of simulations are considered:

- Re-use of CP/FFT relationship in the PTP scenario, i.e., normal CP length with 7% FFT size (only for μ = 0).
- Extended CP with 25% of FFT size. Note that due to the increase of CP length, the number of OFDM symbol in the control region decreases (μ = 0, -1 and -2)

The pilot granularity remains the same in both scenarios, and the aggregation level 2 is considered. The corresponding simulation results are presented in Figure 30.

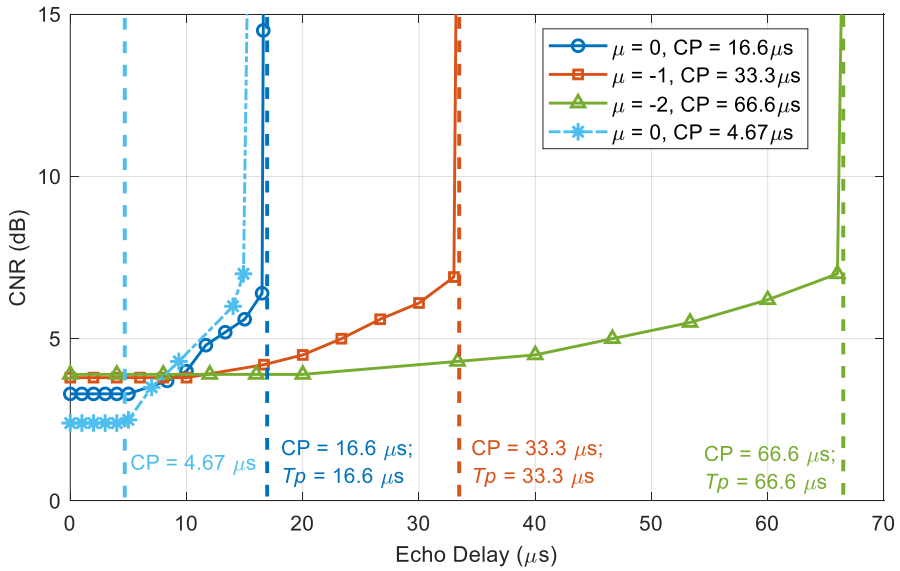

Figure 30. Required CNR vs corresponding echo delay (PDCCH, AL = 2)

With numerology 0, both normal and extended CPs can work properly with the time delay equivalent to the normal CP duration. Then the larger the time delay, the higher the required CNR for normal CP, due to the increased ISI. However, the required CNR for the extended CP is increased even within the CP duration. Regarding the maximum channel delay spread to be tolerated, both normal CP and extended CP can support up to around 16μs, aligned with the theoretical limit as calculated previously.

Considering the different values of μ, due to the increased useful symbol duration, the case with the extended CP can tolerate the maximum channel delay spread up to the corresponding theoretical limits. Beyond those limits, the required CNR for the PDCCH with the Rel-15 DMRS pattern (i.e., $D_x = 4$) immediately raises to a considerably high level. In the following, we provide an analysis of these results and discuss possible solutions.

a) Analysis

Focusing on the numerology 0, the usage of extended CP does not help to increase the PTM coverage and the required CNR to achieve the same BLER is increased with extended CP. Two aspects can be highlighted:

- **CNR loss with increased CP**

The insertion of CP disperses the transmitter energy (the amount of consumed power depends on how large the CP length), where the signal-to-noise (SNR) lost due to the CP introduction indicates the loss of transmission energy. The loss factor is given as:

$$\mathrm{CNR}_{loss} = -10log_{10}(1 - \frac{T_{CP}}{T_U + T_{cp}}) \quad (25)$$

which is equivalent to the increase of noise variance (if fixed symbol energy), thus yields an increased channel estimation error at the pilot position. As we can see the comparison in Figure 31, with a relatively short 2nd path delay, both normal and extended CP scenarios can still reconstruct the channel within an acceptable offset range. However, in

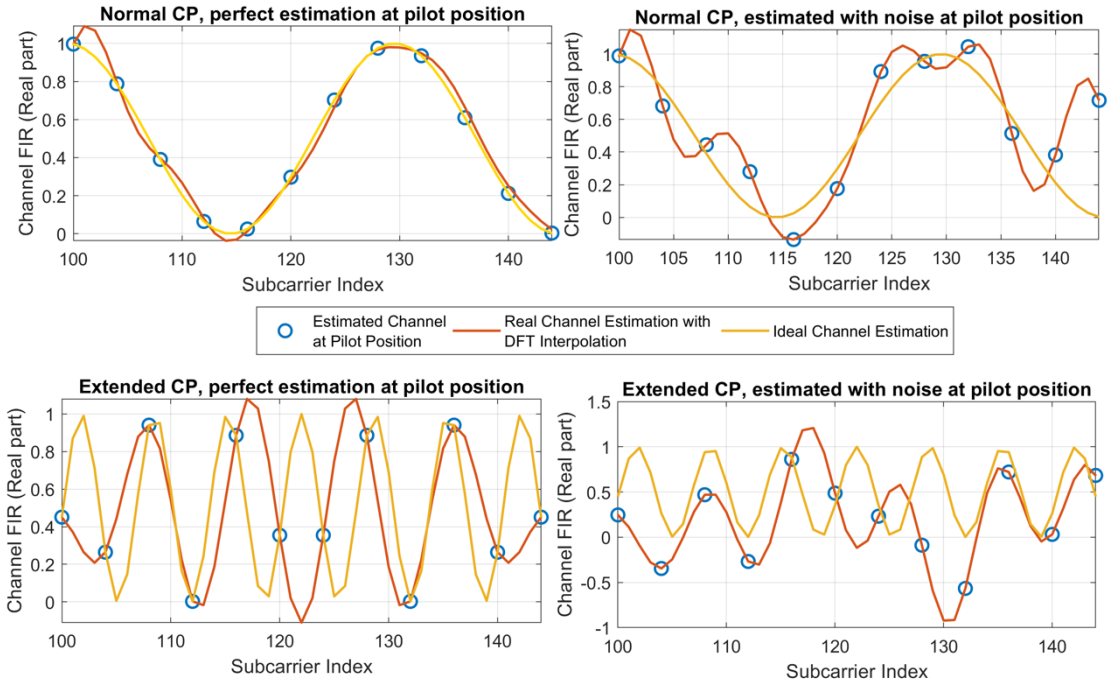

Figure 32, with higher 2nd path delay (but still inside the CP duration), with normal CP, the channel can be reconstructed, which is not the case for the extended CP. Combining with the second aspect, the setting with the extended CP results in that the channel almost unable to be reconstructed.

- **Not enough pilots to catch the channel variation**

When the delay of the second path increases, we obtained the simulation results for estimated and ideal channel as well. Comparing the two figures at the left side of

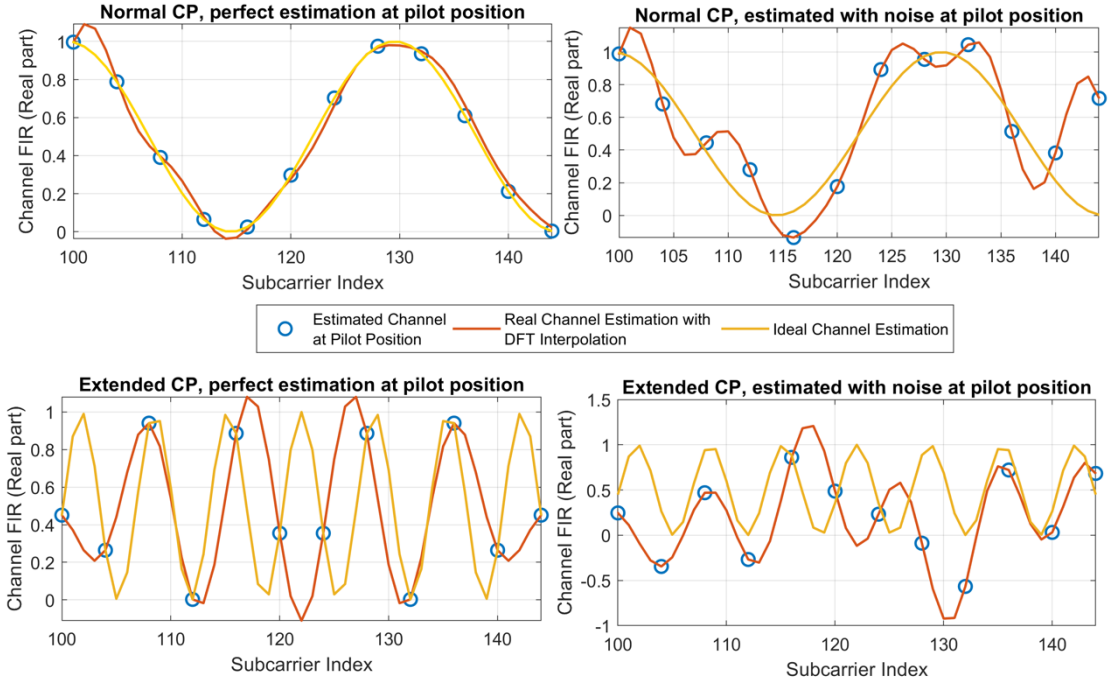

Figure 32, with normal CP, the interpolation almost perfectly captures the channel variation. However, with extended CP, even with perfect channel estimation at the pilot position, the interpolation cannot reconstruct the channel due to the low pilot granularity. This can cause that the corresponding channel estimation error is further amplified by the increased noise due to the increase of CP (see last point in the figure), as shown in the right two figures in

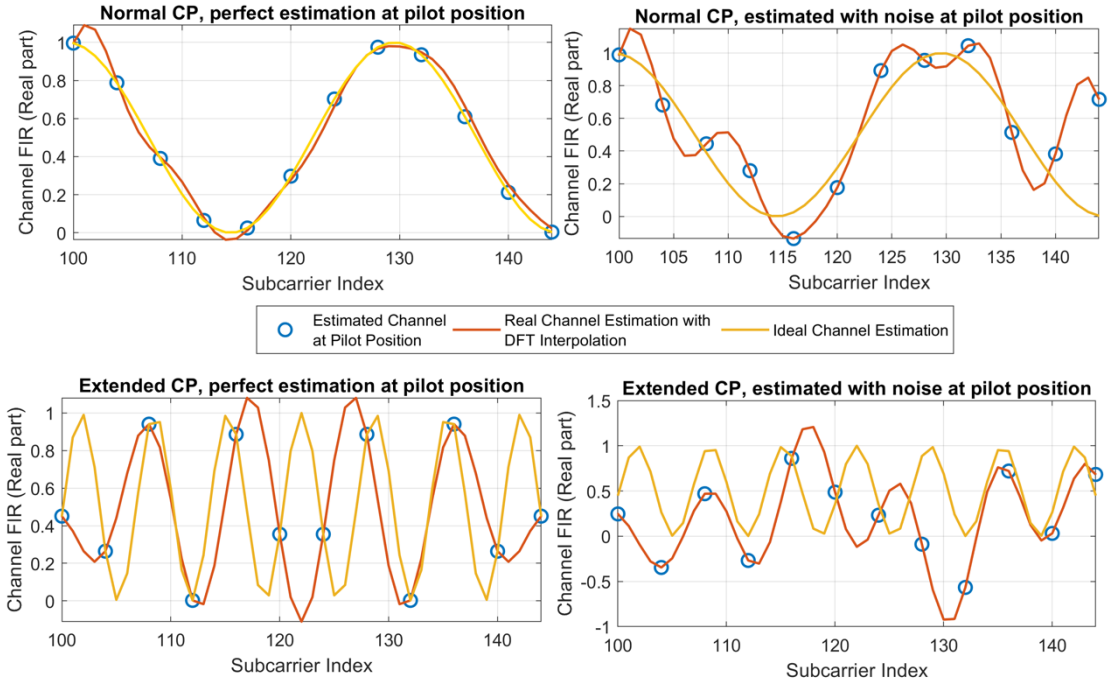

Figure 32.

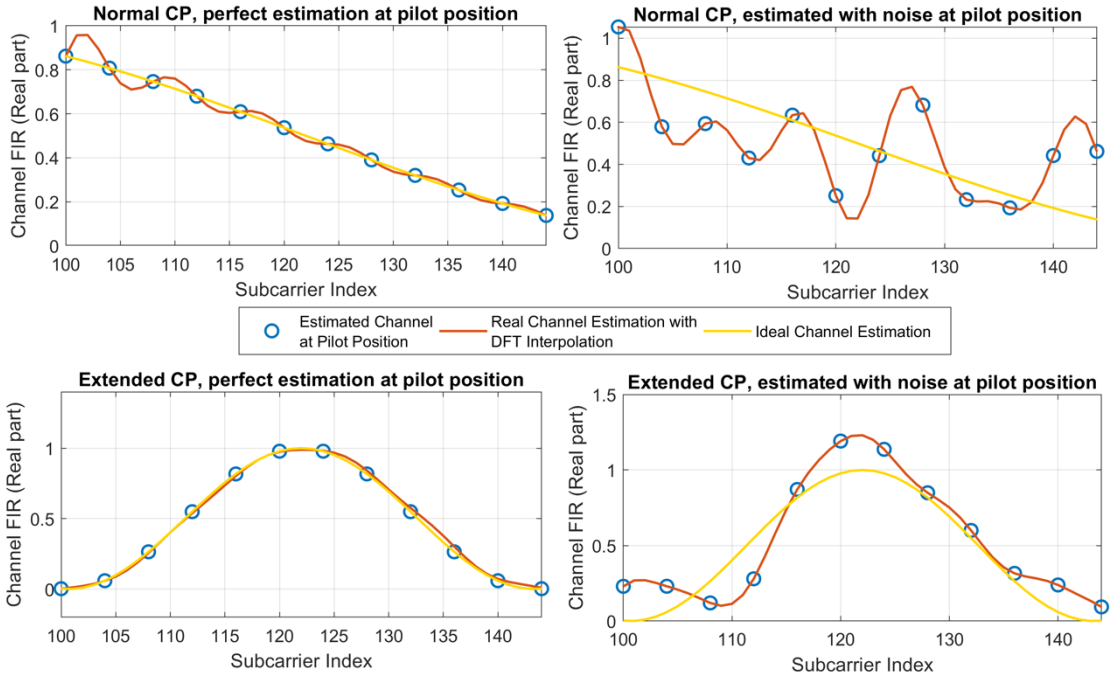

Figure 31. Normal & extended CP with $0.1 * T_{cp}$ as delay for the second path.

To elaborate more on the relationship between the pilot granularity in the frequency domain and the supported maximum delay spread of the channel, we consider the requirement of the DFT-based channel estimation/interpolation. As discussed in [50] and its related works, one requirement should be fulfilled in order to ensure that the DFT-based interpolation can work properly: The number of pilots should be much greater than the channel delay spread (counted as the number of the channel delay taps in the time domain). The frequency domain pilot granularity in the PDCCH DMRS pattern cannot meet this requirement in the certain scenarios (see the time delay of $0.6 * \mathrm{T_{cp}}$ in the Figure 27 and 25), which causes the imperfection of the DFT-based channel estimation, thus the performance degradation of the system.

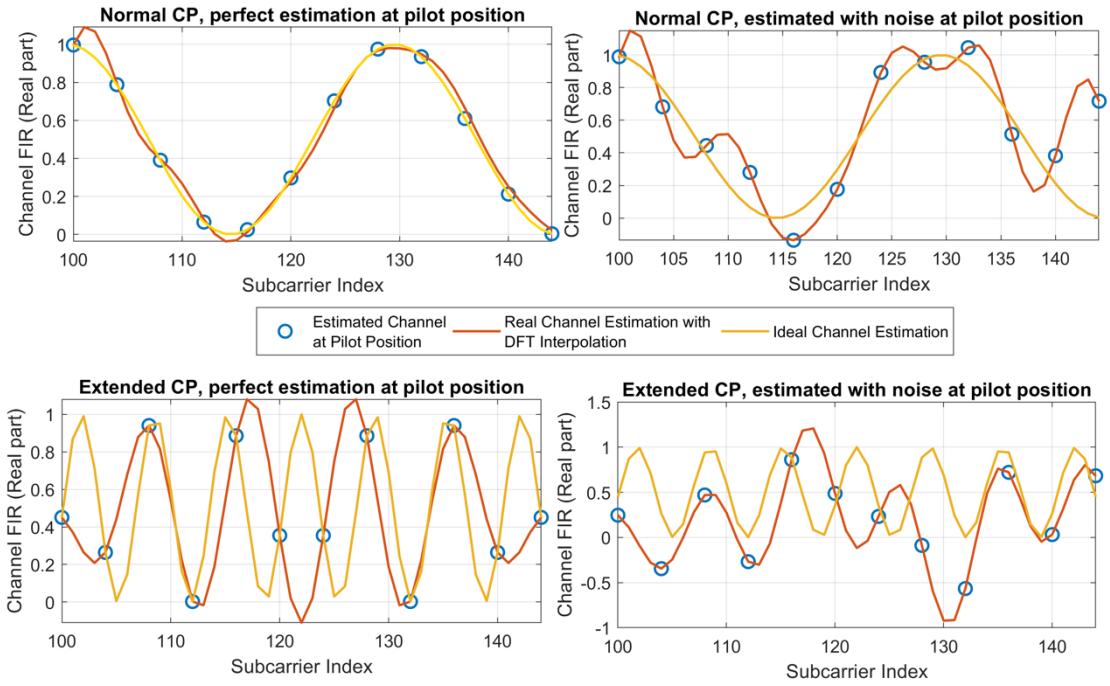

Figure 32. Normal & extended CP with $0.6 * T_{cp}$ as delay for the second path.

b) Solutions to increase coverage

One solution to enhance the coverage capability is to use the negative numerology as proposed previously. Another possible solution is to design new PDCCH DMRS pattern, especially for the extended CP. Recall the relationship between the distance between two frequency domain PDCCH DMRS symbols and the supporting delay spread of the channel, one can design the control channel frame or the DMRS pattern by decreasing D_x. This, however, can result in the significantly decreased number of available REs for the control channel payload transmission, considering the limited number of available radio resources and very low spectral efficiency in the control channel.

5.1.5.4 Coverage Evaluations of Different Numerologies

This subsection provides coverage simulations in fixed rooftop and mobile environments for different numerology options. The simulation parameters are aligned with [52] and a summary is presented in Table 25 and Table 26.

Table 25 Network Parameters

Parameter	MPMT	HPHT-1	HPHT-2	LPLT
ISD	50km	125km	173.2km	15km
BS Power	60dBm	70dBm	70dBm	46 dBm
Carrier frequency	700MHz			
Channel BW	10MHz as baseline			
BS antenna gain	10.5dBi	13dBi	13dBi	15dBi
Cellular Layout	Hexagonal grid, 61 cell sites, 1 sector per site	Hexagonal grid, 61 cell sites, 1 sector per site	Hexagonal grid, 61 cell sites, 1 sector per site	Hexagonal grid, 61 cell sites,3 sector per site

Table 26 Channel characteristics for considered environments

Parameter	Rooftop	Car-mounted
Propagation model	ITU-R P.1546-5 50% / 1% (serving / interfering)	ITU-R P.1546-5 50% / 1% (serving / interfering)
Receiving antenna height	10m	1.5m

5.1.5.4.1 Fixed rooftop environment

This section presents the results for the fixed rooftop receiving environment with a directional receiving antenna where the evaluation methodology is detailed in [53-54]. The simulation results appear in the plots below where each curve represents a specific numerology with the CP/Tu fraction shown. Only the 200/800 (i.e., 800μs Tu, 200 μs CP) numerology has been standardised in LTE Rel'14 – the other numerologies have been hypothesised in order to show the benefit of increasing the CP and/or Tu. In all cases the reference signal pattern of the existing 200 μs CP numerology has been assumed. Under this assumption, increasing Tu similarly increases the equalisation interval (EI) - the interval over which echoes with long delays may be correctly equalised. As the results show, increasing Tu may significantly increase a network's capacity.

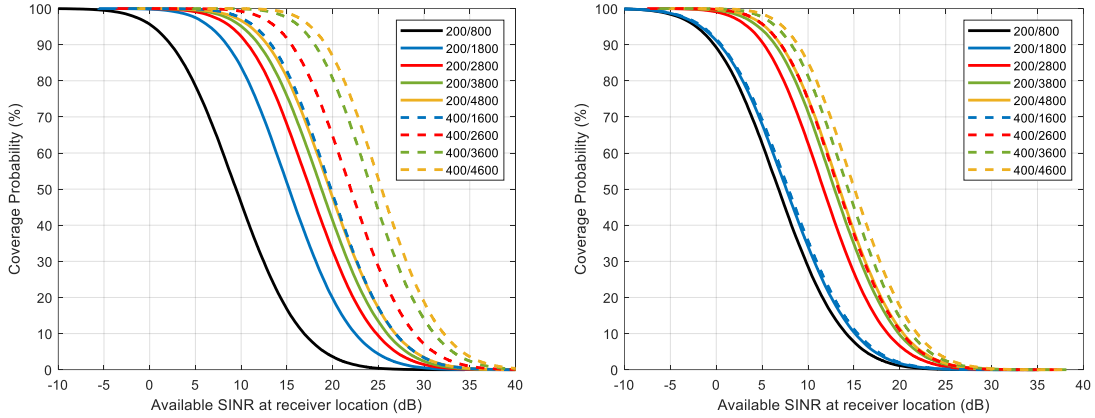

Figure 33. SINR vs Coverage Probability at the location of minimum capacity for the network configurations. Fixed rooftop reception. HPHT1 (left) and HPHT2 (right).

The SINR achieved for 95% locations is summarised in the Table 27.

Table 27 Achievable SINR (dB) at 95% locations. Fixed rooftop reception.

CP/ T_u (μs)	200/ 800	200/ 1800	200/ 2800	200/ 3800	200/ 4800	400/ 1600	400/ 2600	400/ 3600	400/ 4600
HPHT1	0.35	6.55	8.86	10.06	10.99	11.52	13.76	16.42	17.6
HPHT2	-2.19	-1.71	3.42	4.57	5.32	-1.53	5.35	6.5	7.28

Table 27 shows that, for HPHT1 and HPT2, increasing the CP to 400 μs would significantly increase the achievable SINR compared with the existing 200 μs CP. It can also be seen that simultaneously increasing the useful symbol duration (Tu) up to 4.6 μs would be similarly beneficial. Increasing Tu in order to reduce LTE's conventional Cp/(Tu

+ CP) ratio of 20% would also reduce the overhead given over to the CP, as Table 28 shows.

Table 28 Carrier spacing and CP overhead for numerologies used in simulations

CP/ T_u (µs)	200/ 800	200/ 1800	200/ 2800	200/ 3800	200/ 4800	400/ 1600	400/ 2600	400/ 3600	400/ 4600
Carrier Spacing (Hz)	1250	556	357	263	208	625	385	278	217
CP/(T_u + CP) Overhead	20%	10%	6.7%	5%	4%	20%	13.3%	10%	8%

5.1.5.4.2 Mobile environments

This section presents the results for the mobile reception environment with an omni-directional receiving antenna where the methodology is detailed in [53-54].

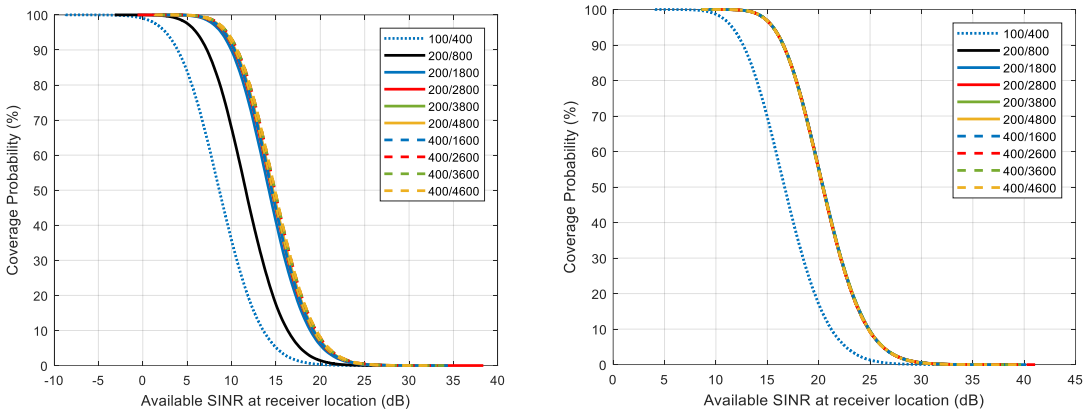

Figure 34. SINR vs Coverage Probability at the Location of Minimum Capacity for car mounted reception. MPMT (left), LPLT (right).

The SINR achieved for 95% locations is summarised in the Table 29.

Table 29 Achievable SINR (dB) at 95% locations. Car mounted reception

CP/ T_u (µs)	100/ 400	200/ 800	200/ 1800	200/ 2800	200/ 3800	200/ 4800	400/ 1600	400/ 2600	400/ 3600	400/ 4600
MPMT	2.1	6.0	8.8	9.2	9.2	9.3	9.2	9.5	9.5	9.5
LPLT	11.6	15.6	15.6	15.6	15.6	15.6	15.6	15.6	15.6	15.6

Table 29 shows that there may be some merit in introducing an additional numerology for the 200 µs CP with a longer Tu (e.g. 1800 or 2800 µs) in order to improve the capacity in this reception mode for MPMT networks. However, the Doppler performance of such a numerology would have to be carefully considered.

The table also shows that there would be no benefit in increasing the CP or the Tu for this reception mode from LPLT networks. Furthermore, shortening the CP would reduce the achievable SINR – it would degrade from 15.6 dB to 11.6 dB.

However, the degradation is tolerable as a usefully high SINR would still be achievable. Most importantly, the 100µs would improve the Doppler performance of the system by approximately a factor of two relative to the existing 200µs numerology. Thus the shorter, 100µs CP would be a good compromise between Doppler performance and coverage for LPLT networks.

5.2 Ultra-Reliable Low Latency Communications for Public Warning and Automotive

5.2.1 Mobility

This section follows the same procedure than section 4.2.1 and evaluates the PTM modes for a TU-6 scenario with variable speed.

All designed numerologies, both in the MM and TB, are evaluated in order to observe their influence on the maximum user speed tolerated. The DMRS configurations developed in section 3 are here assumed. Real channel estimation (linear in time, FFT in frequency) with **MCS 3** is used in all cases.

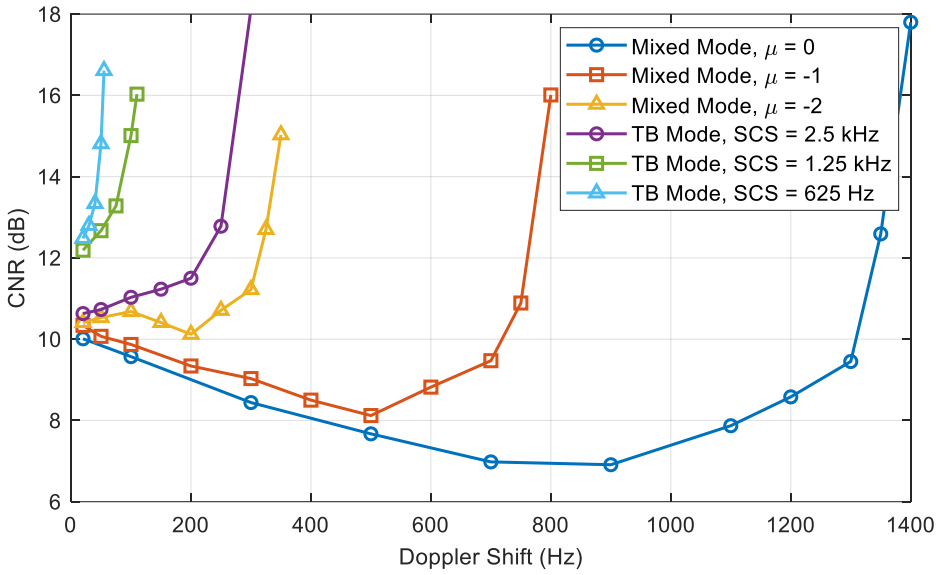

Figure 35. CNR vs user speed for 5G-Xcast PTM modes in TU-6 mobile channel.

Results in Figure 18 show that the use of a different numerology has a great impact on the mobility tolerance. The MM has been designed with higher SCS and therefore the maximum user speed permitted is much higher than the TB, originally designed for fixed reception.

The mixed mode allows Doppler shifts of up to 1350 Hz with numerology 0, equivalent to 2080 km/h in a frequency band of 700 MHz, typical from multicast and broadcast scenarios. The other two numerologies, i.e. -1 and -2 reduce the maximum speed to 775 and 330 Hz, equivalent to 1200 and 510 km/h. Therefore, **all numerologies in the MM fulfil the mobility requirement at 700 MHz,** if the MCS selected is robust enough. In the **4 GHz** frequency band**, only the numerology 0** provides user speeds higher than 250 km/h. The rest of numerologies are well below this value.

Compared to the MM, the user speeds permitted with TB mode are considerably lower. TB has been designed to support high-demanding coverage requirements in fixed reception scenarios, which implies the use of long CPs that in turn, require, narrow a carrier spacing. This considerably limits the use of 5G for mobility scenarios. **The SCS of 2.5 kHz represents a compromise** between both options. In this case, the coverage is limited, but the mobility is still relatively high, i.e. 260 Hz equivalent to 400 km/h at 700 MHz. As main drawback, this is only valid for low throughputs that are not ideal for these type of scenarios. **The SCS 1.25 kHz and 625 Hz are not suitable for mobility**

conditions, since these modes only permit user speeds of 150 and 80 km/h respectively with MCS 3. If a less robust mode is selected, maximum speeds are even lower.

5.2.2 User Plane Latency

The next section describes the **user plane latency** for the MM and the TB, for all configurations designed in Section 3.

5.2.2.1 Mixed Mode

As done in section 4, we assume UE capability 2. This analysis presents first an example for numerology -2, extended CP (3 symbols) with non-slot based scheduling of 2 symbols and probability of retransmission $p = 0.1$. It is also necessary to define values for N_1 and N_2, since they are only defined in 3GPP for positive numerologies. We assume N_1=2 and N_2=2,5 for numerology -2 and N_1=2,5 and N_2=4 for numerology -1.

a) First transmission

The processing time in the gNB, $t_{BS,tx}$, in this case is **356.8 µs**. To start transmitting the content, the gNB needs to be aligned with the first possible symbol to transmit. The gNB waits a minimum time t_{FA1} of 309.9 µs and a maximum time of 643.2 µs. On average, the time needed is **476.6 µs**. Then, the TTI is transmitted in **666.6 µs**. Finally, the processing time in the UE, $t_{UE,rx}$, is **285.4 µs**. The total time needed for the data transmission without HARQ, T_1, is **1.78 ms**.

b) HARQ petition

If the data is not correctly received, then the UE sends the HARQ petition. The UE then needs **285.4 µs** to process the petition, and waits an average time t_{FA1} of **95.8 µs**. The time for the HARQ petition is 1 OFDM symbol, having that t_{HARQ} is **333.3 µs**. The gNB then processes the request in **356.8 µs**. In total, the HARQ petition needs a time T_2 of **1.1 ms**.

c) HARQ retransmission

The gNB processes the retransmission in **356.8 µs** and, on average, needs **286.5 µs** to be aligned with the TTI and retransmit. Then, the data is retransmitted in **666.6 µs**, and the UE processes the data again in **285.4 µs**. The total time of retransmission T_3 is **1.6 ms**. The total user plane latency with a probability of retransmission $p = 0.1$ is therefore **2.05 ms**.

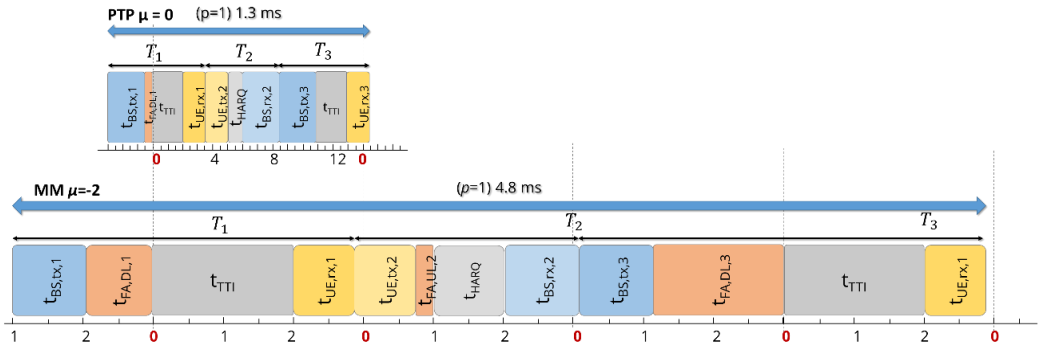

Figure 36. User plane latency for numerology -2, with non-slot based scheduling of 2 symbols. Minimum frame alignment. Comparison with PTP µ=0.

The process can be easily extrapolated to all numerologies, as well as different slot configurations. In this deliverable, we assume FDD for the latency calculation. The results are summarized in Table 30.

Table 30. User plane latency (ms) with the Mixed Mode.

Slot configuration	HARQ probability	*μ = -2*	*μ = -1*	*μ = 0*
2 symbols	$p = 0$	1.78	0.93	**0.56**
	$p = 0.1$	2.08	1.09	0.66
	$p = 1$	4.78	2.60	1.56
4 symbols	$p = 0$	-	1.43	0.82
	$p = 0.1$	-	1.66	0.95
	$p = 1$	-	3.76	2.14
7 symbols	$p = 0$	-	-	1.19
	$p = 0.1$	-	-	1.34
	$p = 1$	-	-	2.77

5.2.2.2 Terrestrial Broadcast

This analysis presents first an example for a **SCS of 625 kHz**, with extended CP (1 symbol), slot based scheduling of 1 symbol and probability of retransmission $p = 0$. It is important to note that the TB mode is a DL-only configuration, and therefore there is no possible retransmission in the process. It is also necessary to define values for N_1 and N_2, since they are only defined in 3GPP for positive numerologies. We assume N_1=1 and N_2=1 for all configurations.

The processing time in the gNB, $t_{BS,tx}$, in this case is **856.2 μs**. The gNB waits a time t_{FA1} that is always **143.8 μs**. This is because of the use of a single symbol per TTI. Then, the TTI is transmitted in **1 ms** and the processing time in the UE, $t_{UE,rx}$, is **856.2 μs**. The total time needed for a TB transmission is **2.85 ms**. The process can be easily extrapolated to all numerologies, as shown in Table 31.

Table 31. User plane latency (ms) with 5G Terrestrial Broadcast.

Slot configuration	*625 Hz (μ = -4.5)*	*1.25 kHz (μ = -3.5)*	*2.5 kHz (μ = -2.5)*
1 symbol	2.85	2.42	**1.21**
2 symbols	-	-	1.96

5.2.3 Control Plane Latency

As it occurred with user plane latency, control plane latency is affected by the subcarrier spacing and, hence of the numerology adopted. Therefore, this KPI differs among NR unicast, MC-MM and TB. As done in section 4, we assume UE capability 2.

5.2.3.1 Mixed Mode

Following similar procedure as in Section 4.2.3, Table 32 presents the control plane latency for the two negative numerologies adopted in the MC-MM. Following the same values that in the user plane calculation, we assume N_1=2 and N_2=2.5 for numerology -2 and N_1=2.5 and N_2=4 for numerology -1, with UE capability 2. Note that extended CP is used with Mixed Mode and therefore some of the possibilities, initially designed for PTP, are not available in this case.

Table 32. Control plane latency (ms) for the 5G Mixed Mode.

Mapping	Slot	PRACH 1 ms			PRACH 2 symbols		
		μ = 0	μ= -1	μ= -2	μ= 0	μ= -1	μ= -2
Type A	4 symbols	16.3	17.6	-	15.3	16.6	-
	7 symbols	16.5	-	-	15.5	-	-
Type B	2 symbols	14	15.6	18.3	13.2	15	18.3
	4 symbols	14.6	17.6	-	13.7	17	-
	7 symbols	16.3	-	-	15.1	-	-

As expected, the MM introduces some additional latency compared to unicast. In numerology 0, this is due to the use of extended CP. Numerologies -1 and -2 have even large symbol durations and therefore the latency introduced is larger. In any case, the control plane latency is below 20 ms.

5.2.3.2 Terrestrial Broadcast

The Terrestrial Broadcast mode has been designed as a receive-only mode, where there media content is transmitted via DL from the gNB to the users. There is no petition from the UE to connect the gNB and therefore the control plane latency analysis done for PTP and the MM does not apply in this case.

5.3 Massive Machine Type Communications

5.3.1 Energy Efficiency

The next section describes the **energy efficiency** for the MM and the TB, for all configurations designed in Section 3.

5.3.1.1 Mixed Mode

As done in unicast, the MM performs periodical transmission of SS/PBCH blocks and RMSI paging signals, so that UEs can access the RAN. In this deliverable, we assume FR1 and *L*=1.

Each SS/PBCH block occupies 4 OFDM symbols and 20 RBs. One or multiple SS/PBCH blocks compose an SSB, which is confined in half radio frame window, i.e. 5 ms. The SSB periodicity (P_{SSB}) can be 5, 10, 20, 40, 80 or 160 ms [43]. RMSI is usually time-division multiplexed with SS/PBCH and therefore it can be transmitted in the same slot.

Since the SS/PBCH block occupies 4 OFDM symbols, it cannot be transmitted if the numerology is lower than -1. The numerology -2 only provides 3 OFDM symbols per slot and subframe. For the sake of simplicity, we could assume that SS/PBCH blocks are transmitted using numerology 0. Therefore, the energy efficiency from 5G NR is maintained, as Table 33Table 22 shows.

Table 33. Energy efficiency (%) in 5G Mixed Mode for different SSB periodicities.

	5 ms	10 ms	20 ms	40 ms	80 ms	160 ms
Slot	80	90	95	97.5	98.75	99.38
Symbol	93.57	96.43	97.86	98.93	99.46	**99.73**

Another option would be the adoption of SS/PBCH blocks to the new numerologies. In such case, block would expand $4 \times 2^{\mu}$ OFDM symbols, fitting the current window for a

slot. Since the periodicity would still be the same, the energy efficiency would be also maintained.

5.3.1.2 Terrestrial Broadcast

In the Terrestrial Broadcast mode, control channels are assumed to convey SS/PBCH Block, MIB signalling via the PDCCH and a series of SIBs via the PDSCH. These control channels are transmitted using regular unicast numerology every specific number of subframes. Assuming the same periodicity that LTE enTV, the PBCH data may be transmitted every 40 ms. In this case, the energy efficiency obtained would be **97.5%**, in any case and for all numerologies considered.

6 Conclusions

6.1 Air Interface Design of 5G Mixed Mode and Terrestrial Broadcast

The 5G-Xcast air interface has been divided into three modes, Single-Cell Mixed Mode (SC-MM), Multi-Cell Mixed Mode (MC-MM) and Terrestrial Broadcast (TB).

6.1.1 Single-Cell Mixed Mode (SC-MM)

This mode has been designed as a flexible single-cell solution that enables the dynamic allocation of unicast and multicast services in both the downlink and the uplink. SC-MM has **a common air interface** with 5G NR Rel'15 in order to keep backwards compatibility. However, some modifications have been defined to enable group communications in both physical downlink and uplink channels:

- **Group-RNTI (G-RNTI):** SC-MM includes the use of the G-RNTI. G-RNTI is based on C-RNTI, but it **enables group communications**. It is acquired during RRC connections in order to descramble the CRC sequence encoded for the control information allocated in the DCI. The definition of a common RNTI identifier permits the simultaneous discovery of scheduling information by groups of users interested in the same content over the same cell.

- **Multicast CORESET:** the transmission of a common DCI message implies the transmission of a common CORESET. Depending on the number of UEs requesting the same content, the transmission of a common multicast CORESET introduces a PDCCH overhead reduction **from 50% up to 90%.**

- **Feedback evaluation:** SC-MM has also evaluated the use of feedback mechanisms in multicast communications. In particular, **uplink mechanisms** such as AMC and HARQ feedback have been considered. If few UEs request feedback transmissions, link adaptation schemes and HARQ retransmissions can provide considerable **performance improvements.** However, if many UEs send requests, feedback schemes may introduce considerable overheads and even collapse the PUCCH.

6.1.2 Multi-Cell Mixed Mode

MC-MM is an extension of SC-MM. It has been proposed as a scalable PTM solution to deliver unicast and multicast content dynamically in **multiple cells**. Among all possible multiple cell coordination mechanisms, 5G-Xcast has considered the inclusion of an **SFN operation mode**. To enable SFN transmissions, the following air interface parameters have been proposed:

- **Common cell scrambling sequence**: In SFN deployments, the same content has to be transmitted from different sites. Since, the control and data location as well as DMRS values are determined according to the scrambling sequence, the MC-MM initialises the same scrambling sequence for all the serving cells. This configuration provides **SFN gains** in multi-cell deployments, mitigating interferences between adjacent cells, especially at the coverage edge.

- **Negative numerologies and extended CP**: the MC-MM solution has defined the use of negative numerologies combined with extended CPs to increase the coverage in SFN scenarios. These numerologies have been proposed for the same **PDSCH** channel. In 5G-Xcast, **numerologies μ = {-1, -2}, which corresponds to subcarrier**

spacing Δf = {7.5, 3.75} kHz respectively, have been considered as compatible solutions. The narrower subcarrier spacing, the longer de CP length and, hence, the larger the Inter-Site Distance (ISD). Whereas with Rel'15 numerologies, the maximum ISD is 1.4 km, the proposed subcarrier spacings allow up to **ISD of 30 km**.

- **Channel estimation mechanisms:** new numerologies need new DMRS patterns. Therefore, additional DMRS have been designed to enable a proper channel estimation for MC-MM. The designed DMRS allow tracking user speeds higher than 500 km/h in all cases, fulfilling the IMT-2020 mobility requirement.

- **Feedback evaluation:** MC-MM has also considered the design of feedback coordination between multiple cells.

6.1.3 Terrestrial Broadcast

A TB mode has been additionally proposed to enable dedicated transmissions of multimedia and TV services in a static manner. It is a DL-only mode, and therefore UEs do not need to register to the network. This mode goes from more cellular-oriented LPLT to **traditional broadcast HPHT** deployments. The proposed modifications are the following:

- **New extended CPs and longer subframes:** to allow very large ISDs, very narrow subcarrier spacing (more than those provided in the Mixed Mode) are introduced, leading to new CP lengths. For instance, the specific case of 400 μs is crucial to cover the 5G-broadcast requirement from [5].

- **Channel estimation mechanisms:** As previously done for MC-MM, additional DMRS patterns have been designed to enable channel estimation in large SFN areas. Dense patterns increase the SFN equalization interval and mobility tolerance at the expense of introducing larger overheads.

6.2 Performance Evaluation of 5G NR (PTP)

The 5G-Xcast project is involved in the 5G PPP IMT-2020 Evaluation Working Group[6]. This deliverable evaluates the KPIs defined in the IMT-2020 guidelines [44] and analyses them against the requirements defined in [47]. The analysed KPIs are categorized following the three use case families introduced by ITU: eMBB KPIs, which englobe the M&E vertical of the project, are addressed in Section 6.2.1; URLLC KPIs that cover the Automotive and PW verticals, are analysed in Section 6.2.2, and mMTC KPIs, which address the IoT vertical, are provided in Section 6.2.3.

6.2.1 Enhanced Mobile Broadband (eMBB)

The following KPIs have been considered for **inspection and analysis**: bandwidth, peak data rate and peak spectral efficiency. The main outcomes are:

- The maximum supported bandwidth depends on the numerology and frequency range (FR). By aggregating 16 component carriers, transmission bandwidths **up to 6.4 GHz** are supported in NR Rel'15 when transmitting in FR2 with numerology 3.
- The peak data rate also has a strong dependency on the numerology and the FR used. It also depends on the frame structure, the OH introduced, the number of MIMO

[6] In particular, 5G-Xcast has contributed or plans to contribute to the following KPIs: bandwidth, peak data rate, peak spectral efficiency, mobility and latency.

layers or the component carriers. The peak data rate is **173.57 Gbps** with 8 layers, numerology 3, FR2 and a total BW of 6.4 GHz (16 component carriers).

- The peak spectral efficiency is obtained for numerology 1 and FR1[7] leading to **6.09 bit/s/Hz** for SISO and **48.78 bit/s/Hz** for MIMO with 8 layers.

Table 34 presents the analysed KPIs and demonstrates that they **fulfil with the IMT-2020 requirements** as defined in [46].

Table 34. KPI analysis and the associated IMT-2020 requirements.

KPI	5G-Xcast analysis	IMT-2020 requirement
Bandwidth	6.4 GHz	100 MHz / 1 GHz
Peak data rate	173.57 Gbps	20 Gbps
Peak spectral efficiency	48.78 bit/s/Hz	30 bit/s/Hz

Additionally, the **BICM performance** of both PDSCH and PDCCH channels has been evaluated through link-level simulations. It has been shown that the PDSCH performance in 5G NR for AWGN in SISO transmissions is better than 4G LTE, achieving **gains from 0.5 to 1 dB**, thanks of using more efficient Low-Density Parity Check (LDPC) codes. However, there is room for improvement since the gap with ATSC 3.0 is still high, especially for high CNR values because of the use of non-uniform constellations [55-58]. The use of **MIMO** drastically increases the BICM spectral efficiency. In fact, 5G NR exceeds the SISO capacity if the CNR is high enough. The throughputs provided in this case are extremely high compared to SISO for the same minimum CNR requirement. The main conclusion from **PDCCH** results is that a higher aggregation level (AL) generally gives more protection to the codewords, which is reflected on the required CNR. The minimum CNR in this case is obtained with AL 8, obtaining -10 dB. This value is lower than any possible value obtained with PDSCH, which facilitates the demodulation in real scenarios.

6.2.2 Ultra-Reliable Low Latency Communications (URLLC)

The 5G-Xcast PW and Automotive verticals are more related to URLLC communications. For this family, the mobility, user plane and control plane latency KPIs have been evaluated. The IMT-2020 requirement are 500 km/h, 1 ms, and 20 ms, respectively [47].

For the mobility KPI, link-level simulations for PDSCH in FR1 with three numerologies have been evaluated, μ={0, 1, 2}. Following IMT-2020 guidelines, real channel estimation with **MCS=3** is used in all cases. Results have shown that **all possible numerologies and DMRS fulfil the requirement at 700 MHz**. On the other hand, **at 4 GHz, numerology μ = 1 with more than 2 DMRS is at least required**. The use of a higher MCS**,** e.g. **MCS=15,** reduces speed limits to half, compared to MCS=3. Following these results, the PDCCH has been evaluated for numerology μ=0, which is the most demanding configuration in terms of mobility. Results have shown that the **PDCCH meets the mobility requirements for any AL** and for all considered FR. Hence, all PDCCH numerologies available in 5G NR fulfil this requirement.

This deliverable has also evaluated both user and control plane latencies. The results on user plane latency have shown that this KPI is highly dependent on the numerology and the number of HARQ retransmissions. Without retransmission, the analysis has provided a **minimum user plane latency of 0.23 ms**, with numerology μ=2. This number

7 The peak data rate for this configuration is 78.05 Gbps, extracted from Table 10.

increases to 0.27 ms if the probability of a retransmission is p=0.1. With one complete retransmission (p=1), the user plane latency goes up to 0.66 ms. In any case, the IMT-2020 requirement of 1 ms is met with 5G NR. On the other hand, results have also shown that assuming UE capability 2 and FR1, **the lowest control plane latency achieved is 11.6 ms**, which clearly fulfils the IMT-2020 requirement of 20 ms. Furthermore, all evaluated configurations fulfil this criterion.

6.2.3 Massive Machine Type Communications (mMTC)

IoT is the vertical associated to mMTC in 5G-Xcast. This particular technology has been evaluated via the energy efficiency KPI. The requirement is defined in [47] as a qualitative measure: “The system shall have the capability to support a high sleep ratio and long sleep duration”. Hence, the energy efficiency has been evaluated from a network perspective in terms of sleep ratio (%). **Efficiencies up to 99.73% are achieved in 5G NR**. Since the minimum value obtained is 80%, it is considered that all possible values fulfil the IMT-2020 requirement.

6.3 Performance Evaluation of 5G Mixed Mode and Terrestrial Broadcast

The KPIs evaluated for the unicast component of 5G NR have been also analysed for the new designed MM and TB modes. A comparison among the different configurations in the considered scenarios of interest have been carried out. In addition, coverage KPI has been evaluated, as it is exclusive from multicast and broadcast deployments.

6.3.1 Enhanced Mobile Broadband (eMBB)

The main outcomes for this scenario are the following:

- Since the use of these modes has been restricted only to FR1, the maximum bandwidth is **50 MHz** in a single carrier, for all the proposed numerologies. This value applies to both MM and TB. The use of carrier aggregation increases the BW up to 800 MHz with 16 component carriers.
- **SC-MM and MC-MM provide a clear data rate gain compared to unicast**, especially for high numbers of users, due to the use of a single CORESET that saves 72 REs per user. This gain is even further increased when using multiple carriers. While the same peak data rate than unicast can be achieved with MM with a single carrier, i.e. 2.40 Gbps using a single carrier and **38.54 Gbps** with 16 CCs, the control overhead reduction for more than 100 served users can lead to data rate gains up to **9.15 Gbps**. There is a trade-off in data rate and coverage with the **TB** mode. The data rate is 1.92 Gbps with a single RF carrier, and **30.78 Gbps** when using 16 CCs. Although this data rate is lower than 5G NR and MM, it enables large SFN coverage areas up to 120 km ISD.
- Regarding spectral efficiency analysis, same conclusions as for data rate are obtained.

The BICM performance has been evaluated against the CNR in specific SFN scenarios for PDSCH. These scenarios have been modelled with a 0 dB echo channel. The **MC-MM** with numerology µ=0 provides better performance than LTE thanks again to the more efficient LDPC code designs of 5G NR. **Additional gains are obtained with the new numerologies for MC-MM and TB**, due to the longer CP lengths.

The SFN coverage KPI studies have revealed that the MC-MM coverage with longer CP lengths provide higher coverage. Moreover, **the TB mode outperforms LTE enTV** by employing the CP length of 400 µs.

Regarding the PDCCH, it has been shown that with numerology μ=0, limits **both normal and extended CPs** can tolerate the maximum channel delay spread up to the corresponding theoretical, **allowing proper SFN scenarios**. However, the required CNR for extended CP duration is increased.

6.3.2 Ultra-Reliable Low Latency Communications (URLLC)

This section assumes similar mobility results for control than those obtained for PTP and focuses only on data. The new numerologies defined for both MC-MM and TB modes have been evaluated in terms of user speed. Real channel estimation with **MCS=3** is used again in all cases. **All numerologies in the MC-MM fulfil the mobility requirement at 700 MHz,** for the MCS under consideration, having 510 km/h as the more limited requirement with numerology μ=-2. In the frequency band of **4 GHz, only the numerology μ=0** provides user speeds higher than 250 km/h. User speeds permitted with the TB mode are considerably lower, since the designed SCS are initially designed for fixed reception and therefore considerably narrower. **The SCS of 2.5 kHz is the only option** where the mobility is still relatively high, i.e. 400 km/h at 700 MHz. **The SCS 1.25 kHz and 625 Hz are not suitable for mobility conditions**, since these modes only permit user speeds of 150 and 80 km/h in this representative band.

The **minimum user plane latency for MM obtained has been 0.56 ms**, with numerology μ=0. This number increases to 0.66 ms if the probability of a retransmission is p=0.1. With p=1 complete retransmission, the user plane latency goes up to 1.56 ms. Therefore, **the requirement of 1 ms is only fulfilled if no retransmission takes place.** With the TB mode, since it is aimed at DL-only transmissions, there is no space for retransmission delays. The lowest possible value has been achieved with the narrowest SCS of 2.5 kHz. The **latency obtained is 1.21 ms, which unfortunately does not fulfil the URLLC requirement. However, it is below the required 4 ms for eMBB use cases**.

Regarding the control plane latency, the MM introduces some additional latency compared to unicast. In numerology μ=0, this is due to the use of extended CP. Numerologies μ=-1 and μ=-2 have even longer symbol durations and therefore the latency introduced is larger. **The minimum control plane latency obtained is thus, 14 ms** with numerology μ=0, configuration type B and 2 symbols for slot configuration. In all cases evaluated, the values are below the IMT-2020 requirement of 20 ms. Note that **the control plane evaluation does not apply to the TB mode**, since it has been designed as a DL-only mode, where media content is transmitted from the gNB to the users, so that the methodology agreed does not apply here.

6.3.3 Massive Machine Type Communications (mMTC)

A **minimum energy efficiency of 99.73%** has been obtained with the MM. Regarding the TB mode, and assuming an SS/PBCH block transmission periodicity of 40 ms, the **energy efficiency obtained is 97.5%**, for all the designed numerologies. Since the minimum value obtained is 80%, both MM and TB modes fulfil the IMT-2020 requirement.

A Physical Layer Transmitter Block Diagrams

A.1 Physical Downlink Control Channel (PDCCH)

In this section, the PDCCH processing chain is introduced, including the effective code rate calculation. Control information for one or multiple UEs is contained in a Downlink Control Information (DCI) message and is transmitted through the Physical Downlink Control Channel (PDCCH). Different DCI formats are defined with respect to different purpose of the DCI message.

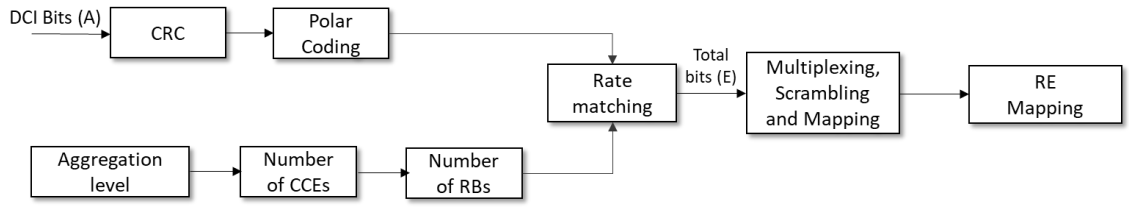

Figure 37. PDCCH block diagram.

For NR, in the 3GPP document TS 38.212 [42], the available formats specifically for scheduling of PDSCH are:

- **Format 1_0:** used for the scheduling of PDSCH in **one DL cell.**
- **Format 1_1:** used for the scheduling of PDSCH in **one cell.**

Taking format 1_0 with CRC scrambled by C-RNTI, the information and corresponding occupied bit positions are summarized as follows:

Table 35. DCI Format 1_0 content.

Field	Bits	Comments
Identifier for DCI formats	1	Always set to 1, indicating a CL format
Frequency domain resource assignments	Variable	Depending on the Resource Blocks inside the downlink bandwidth part (BWP)
Time domain resource assignment	-	
VRB-to-PRB mapping	1	Interleaved or non-interleaved RB
Modulation and coding scheme	5	
New data indicator	1	
Redundancy version	2	
HARQ process number	4	
Downlink assignment index	2	
TPC command assignment for scheduled PUCCH	2	
PUCCH resource indicator	3	
PDSCH-to-HARQ feedback timing indicator	3	

This format is for the unicast purpose, and some of the fields do not have strong relations with PTM, such as fields related to PUCCH and for the HARQ process. Moreover, there

is no format that supports CRC (Cyclic Redundancy Check) scrambled by m-RNTI (MBMS-RNTI) or g-RNTI (group-RNTI).

a) DCI coding

After deciding the DCI format, for example, the DCI includes A bits of information bits. To form the PDCCH payload, the DCI has to undergo coding processes, including:

- CRC attachment: The parity bits are generated by one of the six available cyclic generator polynomials [42], where the generator polynomial $g_{CRC24C}(D)$ is used, which makes the DCI bits now has a length of $(A + 24)$ bits.
- Code block segmentation and code block CRC attachment: depending on the length of the input bit sequence i.e.A, it will be segmented into at most 2 code blocks, and each of them will be attached with 24 bits of CRC parity check bits.
- Channel Coding: the details of polar encoding can be found in [42]. Given the length of the polar encoded bits N, where $N = 2^n$, and the value of *n* is a positive integer between 5 and 9 (including 5 and 9). Therefore, the maximum length of the encoded bits is fixed at $2^9 = 512$.
- Rate Matching: defined per coded block and consists of sub-block interleaving, bit collection, and bit interleaving. However, according to the 3GPP document, the flag of doing bit interleaving is set to be 0. Denoting the length of DCI message after rate matching as E.

b) PDCCH processing

Before being mapped onto the resource elements, the coded DCI bits have to be further processed, including:

- Multiplexing and Scrambling: blocks of coded bits for each control channel are multiplexed and scrambled in order to create a block of data.
- Modulation: the available modulation for control channel bits is only QPSK.
- Layer Mapping and Precoding: these processes mapped the complex-valued modulation symbols for each of the codewords onto one or several layers and transmitted by different antenna ports. The mapping logistics are covered in [42].

c) Extra: Matching PDCCH to CCE Positions

As occurred in LTE, PDCCH is still categorised into Common and UE-specific PDCCH. Each type supports a specific set of search spaces. Each search space consists of a group of consecutive CCEs, which could be allocated to a PDCCH called a PDCCH candidate. Some of the LTE resource allocation unit remains in NR, which includes:

- Resource Element (RE)
- Resource Element Group (REG)
- Control Channel Element (CCE)
- Aggregation Level (AL), with additional supported level, i.e., aggregation level 16.

The relation between REG and CCE has changed in NR, i.e., 1 CCE is now made up 6 REGs and 1 REG is now made up of one resource block (12 REs in the frequency

domain) and one OFDM symbol in the time domain. In addition, some new units are added in NR, including:

- REG Bundle: One REG bundle is made up of multiple REGs.
- Control Resource Set (CORESET): A CORESET is made up of multiples RBs (i.e., multiples of 12 REs) in the frequency domain and '1' or '2' or '3' OFDM symbols in the time domain. CORESET is equivalent to the control region in LTE subframe. A UE can be configured with multiple CORESETs and each CORESET is associated with one CCE-to-REG mapping only [42].

Figure 38 gives an example of the mapping procedure from RE (REG) to CCE with aggregation level of 1. In this example, 3 OFDM symbols in the time domain are used for the control region, and there are totally two CCEs in the CORSET.

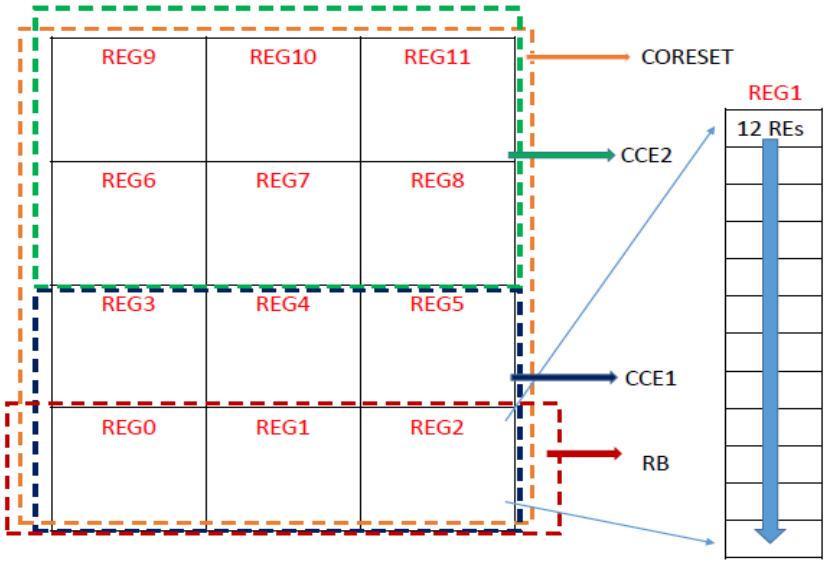

Figure 38. RE mapping procedure in PDCCH for aggregation level 1

In Figure 38, the total available REs inside one CCE of this CORESET is given by:

$$RE_{avail} = AL * (REG\ per\ CCE) * (RE\ per\ REG) = 1 * 6 * 12 = 72$$

which means the total available bits position in one CCE equals to $72 * 2 = 144$ bits (QPSK modulation) i.e., the length of bits after rate matching.

A.2 Physical Downlink Shared Channel (PDSCH)

In the transmitter block, the input variables, i.e. the information bits from upper layers are channel encoded, mapped, interleaved, and OFDM modulated, according to the configuration under evaluation. Figure 39 illustrates the LTE transmitter block diagram.

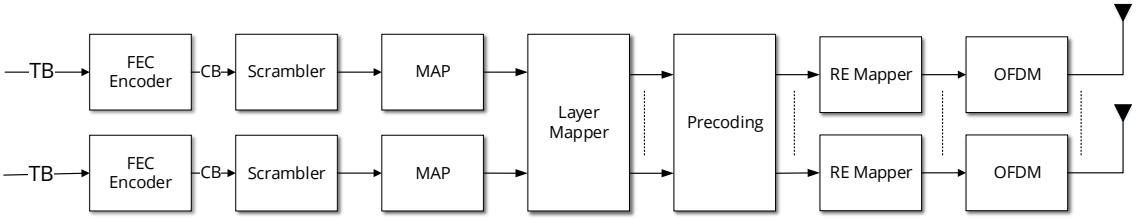

Figure 39. NR Link-level transmitter block diagram.

The channel FEC encoder is formed by segmentation, CRC attachment, LDPC coding and rate matching. The transmission of the input data bits *A* is divided into the following stages:

A.2.1 Segmentation + CRC attachment

1. A first set of CRC parity bits is generated by a cyclic generator polynomial, with size *L* = 24 if *A* > 3824 and size *L* = 16 otherwise.
2. The output bits *B* are segmented into several CBs with size *K* if *B* is higher than the maximum code block size, which depends on the LDPC Base Graph (BG) used.
3. An additional CRC sequence with always size *L* = 24 is attached to each CB.
4. Filler bits *F* are inserted to fit the size *K*.

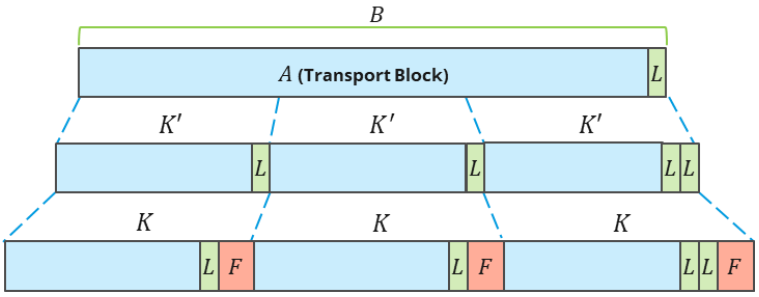

Figure 40. Segmentation and CRC attachment process in PDSCH.

A.2.2 LDPC coding

Each CB with size *K* is coded using a LDPC matrix, which is generated as follows:

1. Initial H_{BG} matrix generated with all zeros.
2. The elements with row and column indices given in Tables 5.3.2-2 (BG1) and 5.3.2-3 (BG2) in [43] are set to 1.
3. H is obtained by replacing each element of H_{BG} with a $Z_c \times Z_c$ matrix.
   a. Elements in H with value 0 are replaced by a zero matrix of size $Z_c \times Z_c$.
   b. Elements in H with value 1 are replaced by a circular permutation matrix $I(P_{i,j})$ of size $Z_c \times Z_c$, obtained by circularly shifting the identity matrix I of size $Z_c \times Z_c$ to the right $P_{i,j}$ times. Values of $P_{i,j}$ are given in [42].
4. Generate the parity bits w with size *N* such that $H \times \begin{bmatrix} c \\ w \end{bmatrix} = 0$, where c is the code block with size K.

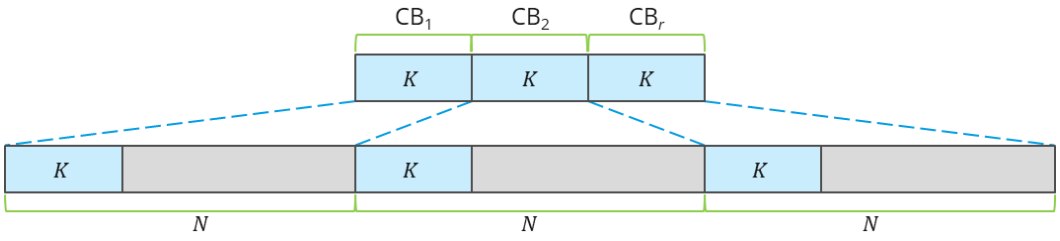

Figure 41. LDPC coding in PDSCH.

A.2.3 Rate matching

The bits of each CB are interleaved, circular buffered and punctured to provide the real CR fixed by the MCS. The rate matched bits of all CBs are finally concatenated into a single codeword.

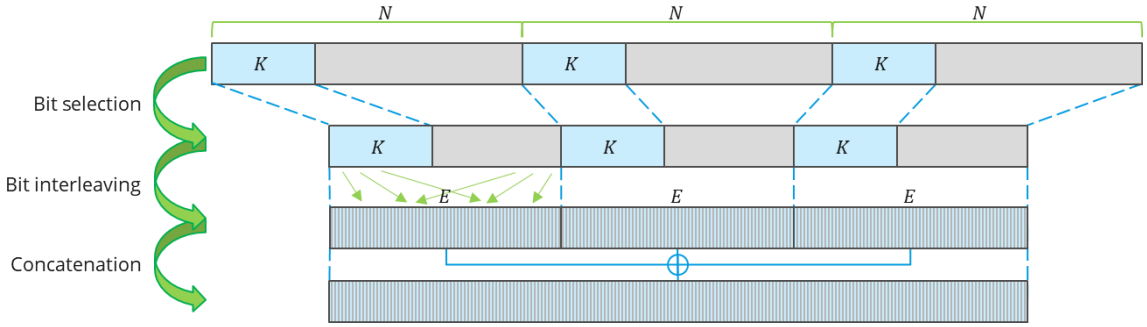

Figure 42. Rate matching and concatenation in PDSCH.

A.2.4 Scrambling

Input bits are scrambled prior to modulation for protection against burst errors. Bits are multiplied by a scrambling sequence $\tilde{b}(i) = \left(b(i) + c(i)\right) \bmod 2$.

A.2.5 Modulation

Bits are transformed into complex-valued symbols using Quadrature Amplitude Modulation (QAM). Constellation orders used are QPSK, 16QAM, 64QAM and 256QAM. The selection of the constellation depends on the MCS index provided.

A.2.6 Layer mapping

The complex-valued modulation symbols are next mapped onto one or several transmission layers and precoded for transmission on the antenna ports.

A.2.7 Resource Element (RE) mapping and waveform

The data symbols are located in the available elements in the resource grid for each antenna port. Finally, the OFDM signal is generated by means of an inverse Fast Fourier Transform and the Cyclic Prefix is inserted.

B Detailed Assumptions Data Rate and Spectral Efficiency Calculations

B.1 Downlink

Parameters	Downlink Configuration			Details
	FDD FR1	TDD FR1	TDD FR2	
Total number of aggregated carriers J	16			Maximum allowed value
$\alpha_{DL}^{(j)}$	1	0.7643	0.7643	**Note 1**
Max. number of layers $v_{Layers}^{(j)}$	8			Maximum value allowed for DL
Highest modulation order $Q_m^{(j)}$	8			256 QAM
Scaling factor of modulation $f^{(j)}$	1			No capability mismatch between baseband and RF.
Max. coding rate R_{max}	984/1024 = 0.9258			Maximum CR
μ	0,1,2,3			According to [12]
T_s^{μ}	$T_s^{\mu} = \frac{10^{-3}}{14 \cdot 2^{\mu}}$			Depending on the numerology.
$N_{PRB}^{BW(j),\mu}$	- 270 for BW 50 MHz, SCS 15 kHz - 273 for BW 100 MHz, SCS 30 kHz - 135 for BW 100 MHz, SCS 60 kHz		- 264 for BW 200 MHz, SCS 60 kHz - 264 for BW 400 MHz, SCS 120 kHz	Depending on the available bandwidth [10] and the numerology.
$OH^{(j)}$	- 0.1037 for BW 50 MHz, SCS 15 kHz - 0.1036 for BW 100 MHz, SCS 30 kHz - 0.1076 for BW 100 MHz, SCS 60 kHz	- 0.1192 for BW 50 MHz, SCS 15 kHz - 0.1193 for BW 100 MHz, SCS 30 kHz - 0.1235 for BW 100 MHz, SCS 60 kHz	- 0.1033 for BW 200 MHz, SCS 60 kHz - 0.0999 for BW 400 MHz, SCS 120 kHz	**Note 2**

Note 1: FDD/TDD Frame Structure

- For FDD DL, all subframes, slots and OFDM symbols in the 5G NR frame are assigned to DL transmissions.

- For TDD DL, frame structure: DDDSUDDDSU (6D: Downlink, 2U: Uplink, 2S: Mixed Downlink and Uplink) and SFI = 31 with a slot structure allocating 14 OFDM symbols as: 11 DL, 1 GP an 2 UL. Half of the GP symbols are considered as DL resources.

Note 2: Overhead Assumptions

- For FDD FR1:
  - **Total REs:** 10 subframes with 14 OFDM symbols per slot assigned to DL transmissions.
  - **SS/PBCH:** 1 blocks transmitted each 20 slots. Each block is composed of 240 subcarriers x 4 OFDM symbols.
  - **PDCCH:** 1 CORESET per slot with 2 CCEs (12 RB) in all subframes with DL content (All the subframes).
  - **PDSCH:**
    - DMRS: 16 RE/RB/slot in all RBs in all slots in all subframes.
    - CSI-RS NZP: 8 RE/RB/slot in all RBs each 20 slots.
    - CSI – IM: 4 RE/RB/slot in all RBs each 20 slots.
    - CSI-RS (TRS): 12 RE/RB/slot in 52 RBs each 20 slots.
- For TDD FR1:
  - **Total REs:** 6 DL subframes with 14 OFDM symbols per slot and 1 Mixed subframe with 12 OFDM symbols (11 DL and 1 GP) per slot and 1 Mixed subframe with 12 OFDM symbols (11 DL) assigned to DL transmissions.
  - **GP:** 1 OFDM symbol in each slot in 1 Mixed UL/DL subframe.
  - **SS/PBCH:** 1 block transmitted each 20 slots. Each block is composed of 240 subcarriers x 4 OFDM symbols.
  - **PDCCH:** 1 CORESET per slot with 2 CCEs (12 RB) in all subframes with DL content (8 out of 10 subframes).
  - **PDSCH:**
    - DMRS: 16 RE/RB/slot in all RBs in all slots in 8 out of 10 subframes.
    - CSI-RS NZP: 8 RE/RB/slot in all RBs each 20 slots.
    - CSI – IM: 4 RE/RB/slot in all RBs each 20 slots.
    - CSI-RS (TRS): 12 RE/RB/slot in 52 RBs each 20 slots.
- For TDD FR2:
  - **Total REs:** 6 DL subframes with 14 OFDM symbols per slot and 1 Mixed subframe with 12 OFDM symbols (11 DL and 1 GP) per slot and 1 Mixed subframe with 12 OFDM symbols (11 DL) assigned to DL transmissions.
  - **GP:** 1 OFDM symbol in each slot in 1 Mixed UL/DL subframe.
  - **SS/PBCH:** 8 blocks transmitted each 20 slots. Each block 240 subcarriers x 4 OFDM symbols.
  - **PDCCH:** 1 CORESET per slot with 4 CCEs (24 RB) in all subframes with DL content (8 out of 10 subframes).
  - **PDSCH:**
    - DMRS: 12 RE/RB/slot in all RBs in all slots in 8 out of 10 subframes.
    - CSI-RS NZP: 8 RE/RB/slot in all RBs each 20 slots.
    - CSI – IM: 4 RE/RB/slot in all RBs each 20 slots.
    - CSI-RS (TRS): 12 RE/RB/slot in 52 RBs each 20 slots.
    - PT-RS: 4 RB in 1 OFDM symbol in all slots in 8 out of 10 subframes.

B.2 Uplink

Parameters	Uplink Configuration			Details
	FDD FR1	TDD FR1	TDD FR2	
Total number of aggregated carriers J	16			Maximum value allowed
$\alpha_{UL}^{(j)}$	1	0.6375	0.6375	**Note 1**
Max. number of layers $v_{Layers}^{(j)}$	4			Maximum value allowed for UL
Highest modulation order $Q_m^{(j)}$	8			256 QAM
Scaling factor of modulation $f^{(j)}$	1			No capability mismatch between baseband and RF.
Max. coding rate R_{max}	984/1024 = 0.9258			Maximum CR
μ	0,1,2,3			According to [12]
T_s^{μ}	$T_s^{\mu} = \frac{10^{-3}}{14 \cdot 2^{\mu}}$			Depending on the numerology.
$N_{PRB}^{BW(j),\mu}$	- 270 for BW 50 MHz, SCS 15 kHz - 273 for BW 100 MHz, SCS 30 kHz - 135 for BW 100 MHz, SCS 60 kHz		- 264 for BW 200 MHz, SCS 60 kHz - 264 for BW 400 MHz, SCS 120 kHz	Depending on the available bandwidth [10] and the numerology.
$OH^{(j)}$	- 0.0834 for BW 50 MHz, SCS 15 kHz - 0.0815 for BW 100 MHz, SCS 30 kHz -0.0826 for BW 100 MHz, SCS 60 kHz	- 0.1194 for BW 50 MHz, SCS 15 kHz - 0.1163 for BW 100 MHz, SCS 30 kHz - 0.1174 for BW 100 MHz, SCS 60 kHz	- 0.1163 for BW 200 MHz, SCS 60 kHz - 0.1155 for BW 400 MHz, SCS 120 kHz	**Note 2**

Note 1: FDD/TDD Frame Structure

- For FDD UL, all subframes, slots and OFDM symbols in the 5G NR frame are assigned to UL transmissions.
- For TDD UL, frame structure: UUUSDUUUSD (6U: Uplink, 2D: Downlink, 2S: Mixed Downlink and Uplink) and SFI = 31 with a slot structure allocating 14 OFDM symbols as: 11 DL, 1 GP and 2 UL.

Note 2: Overhead Assumptions

- For FDD FR1:
  - **Total REs:** 10 subframes where all slots convey 14 OFDM symbols for UL transmissions.
  - **PRACH:** Preamble #71, 12 RB in 6 OFDM symbols in each slot in 2 out of 10 subframes.
  - **PUCCH:** Format 3 to convey CSI, HARQ ACK/NACK and SR. 2 RB in 2 OFDM Symbols in each slot in 10 out of 10 subframes.
  - **PUSCH:**
    - DMRS: 12 RE/RB/slot in all RBs in all slots in all subframes.
    - SRS: 12 RE/RB in all RBs of 1 OFDM symbol each 10 slots.
- For TDD FR1:
  - **Total REs:** 6 UL subframes with 14 OFDM symbols per slot, 1 Mixed subframe with 2 OFDM symbols per slot and 1 Mixed subframe with 3 OFDM symbols per slot assigned to UL transmissions.
  - **PRACH:** Preamble #71, 12 RB in 6 OFDM symbols in 2 out of 10 subframes.
  - **PUCCH:** Format 3 to convey CSI, HARQ ACK/NACK and SR. 2 RB in 2 OFDM Symbols in each slot in 6 out of 10 subframes.
  - **PUSCH:**
    - DMRS: 12 RE/RB/slot in all RBs in all slots in all subframes.
    - SRS: 12 RE/RB in all RBs of 1 OFDM symbol each 10 slots.
- For TDD FR2:
  - **Total REs:** 6 UL subframes with 14 OFDM symbols per slot, 1 Mixed subframe with 2 OFDM symbols per slot and 1 Mixed subframe with 3 OFDM symbols per slot assigned to UL transmissions.
  - **PRACH:** Preamble #71, 12 RB in 6 OFDM symbols in 2 out of 10 subframes.
  - **PUCCH:** Format 3 to convey CSI, HARQ ACK/NACK and SR. 2 RB in 2 OFDM symbols each slot in 6 out of 10 subframes.
  - **PUSCH:**
    - DMRS: 12 RE/RB/slot in all RBs in all slots in 8 out of 10 subframes.
    - SRS: 12 RE/RB in all RBs of 1 OFDM symbol each 10 slots.
    - PT-RS: 4 RB in 1 OFDM symbol in all slots in 8 out of 10 subframes.

B.3 Terrestrial Broadcast

Parameters	Downlink Configuration FDD FR1	Details
Total number of aggregated carriers J	16	Maximum allowed value
$\alpha_{DL}^{(j)}$	1	**Note 1**
Max. number of layers $v_{Layers}^{(j)}$	8	Maximum value allowed for DL
Highest modulation order $Q_m^{(j)}$	8	256 QAM
Scaling factor of modulation $f^{(j)}$	1	No capability mismatch between baseband and RF.
Max. coding rate R_{max}	984/1024 = 0.9258	Maximum CR
SCS, CP length	2.5 kHz (CP: 100 μs), 1.25 kHz (CP: 200 μs), 0.625 kHz (CP: 400 μs)	According to TB design
T_s^{μ}	1 ms (SCS 1.25 kHz or SCS 0.625 kHz), 0.5 ms (SCS 2.5 kHz)	Depending on the SCS.
$N_{PRB}^{BW(j),\mu}$	- 1666 for BW 50 MHz, SCS 2.5 kHz - 3333 for BW 50 MHz, SCS 1.25 kHz - 6666 for BW 50 MHz, SCS 0.625 kHz	Depending on the available bandwidth [10] and the SCS.
$OH^{(j)}$	- 0.1875 for BW 50 MHz and all SCS configurations	**Note 2**

Note 1: FDD/TDD Frame Structure

- For Terrestrial Broadcast, all resources are considered as DL (FDD).

Note 2: Overhead Assumptions

- For FDD FR1:
  - **Total REs:** 10 subframes with 1 OFDM symbol (SCS 1.25 kHz or SCS 0.625 kHz) or 2 OFDM symbols (SCS 2.5 kHz) per slot assigned to TB transmissions.
  - **CAS:** 1 out of 40 subframes assigned to convey PSS, SSS, PDCCH, PDSCH.
  - **TB:**
    - DMRS (SCS 2.5 kHz): 2 RE/RB/slot in all RBs in all slots in all subframes except CAS.
    - DMRS (SCS 1.25 kHz or 0.625 kHz): 4 RE/RB/slot in all RBs in all slots in all subframes except CAS.

C Link-Level Simulator Calibration Results

This annex describes the calibration procedure performed to demonstrate the correct operation of the link-level simulator used in this deliverable. In particular, calibration results have been obtained to evaluate the NR PDSCH performance.

C.1 Methodology and Parameter Configuration

Calibration procedure is fully aligned with the evaluation process followed in 3GPP RAN WG4. As described in [59], 3GPP calibrates the PDSCH performance by evaluating the maximum throughput provided for FR1 and FR2 scenarios and FDD and TDD techniques. For each scenario and duplexing technique, different specific cases are enumerated. According to the simulations performed in this deliverable, calibration is only performed for the FR1 FDD combination.

As shown in Table 36, 3GPP defines up to 14 different FDD FR1 evaluation cases where different channel model, MCS indexes and MIMO configurations are considered. For simplicity, 5G-Xcast calibration has only been performed for cases 4 and 5.

Table 36. FDD FR1 cases.

Case Number	BW/ SCS	MIMO	PDSCH mapping and MCS	Number of layer	Channel Model
1	10MHz/15 kHz	2Tx 2Rx ULA Low 2Tx 4Rx ULA Low	Type A QPSK MCS 4	1 layer	TDL-B 100ns, 400Hz
2	10MHz/15 kHz	2Tx 2Rx ULA Low 2Tx 4Rx ULA Low	Type A QPSK MCS 4	1 layer	TDL-C 300ns, 100Hz
3	10MHz/15 kHz	2Tx 2Rx ULA Low 2Tx 4Rx ULA Low	Type A 256QAM MCS 24	1 layer	TDL-A 30ns, 10Hz
4	10MHz/15 kHz	2Tx 2Rx ULA Low 2Tx 4Rx ULA Low	Type A 16QAM MCS 13	2 layers	TDL-C 300ns, 100Hz
5	10MHz/15 kHz	2Tx 2Rx ULA Low 2Tx 4Rx ULA Low	Type A 64QAM MCS 19	2 layers	TDL-A 30ns, 10Hz
6	10MHz/15 kHz	4Tx 4Rx ULA Low	Type A 16QAM MCS 13	3 layers	TDL-A 30ns, 10Hz
7	10MHz/15 kHz	4Tx 4Rx ULA Low	Type A 16QAM MCS 13	4 layers	TDL-A 30ns, 10Hz
8	10MHz/15 kHz	2Tx 2Rx ULA Med	Type A 16QAM MCS 13	2 layers	TDL-A 30ns, 10Hz
9	10MHz/15 kHz	4Tx 4RX ULA Med A	Type A 16QAM MCS 13	3 layers	TDL-A 30ns, 10Hz
10	10MHz/15 kHz	2Tx 2Rx ULA Low 2Tx 4Rx ULA Low	Type A 16QAM MCS 13	1 layers	TDL-C 300ns, 100Hz
11	10MHz/15 kHz	2Tx 2Rx ULA Low	Type B QPSK MCS 2	1 layers	TDL-A 30ns, 10Hz
11	10MHz/15 kHz	2Tx 2Rx ULA Low	Type B QPSK, MCS 2	1 Layer	TDL-A 30ns, 10Hz
12 (LTE-NR #1)	10MHz/15 kHz	4Tx 2Rx ULA Low	Type A QPSK, MCS 4	1 Layer	TDL-A 30ns, 10Hz
13 (LTE-NR #2)	10MHz/15 kHz	4Tx 2Rx ULA Low	Type A QPSK, MCS 4	1 Layer	TDL-A 30ns, 10Hz

14 (LTE-NR #3)	10MHz/15 kHz	4Tx 2Rx ULA Low	Type B QPSK, MCS 4	1 Layer	TDL-A 30ns, 10Hz

To evaluate the selected cases, 5G-Xcast adopts the following 3GPP parameter configuration:

- SSB/PBCH: Allocation in slot 0 in each second frame. 1 slot per 20 ms.
- CORESET configuration: Full BW allocation, 2 control symbols.
- PDSCH configuration:
  - Time domain: Mapping type A: Start symbol 2, duration 12 symbols.
  - Frequency domain: Full BW allocation.
  - Scheduling in all slots except SSB/PBCH slot. 19 out of every 20 subframes contain data.
  - HARQ assumptions: RV sequence {0, 2, 3.1}. 4 HARQ processes.
- DMRS configuration: 2 DMRS symbols.

C.2 Calibration Results

PDSCH throughput results have been obtained and compared with the calibration results provided by 3GPP companies in different contributions [59-62].

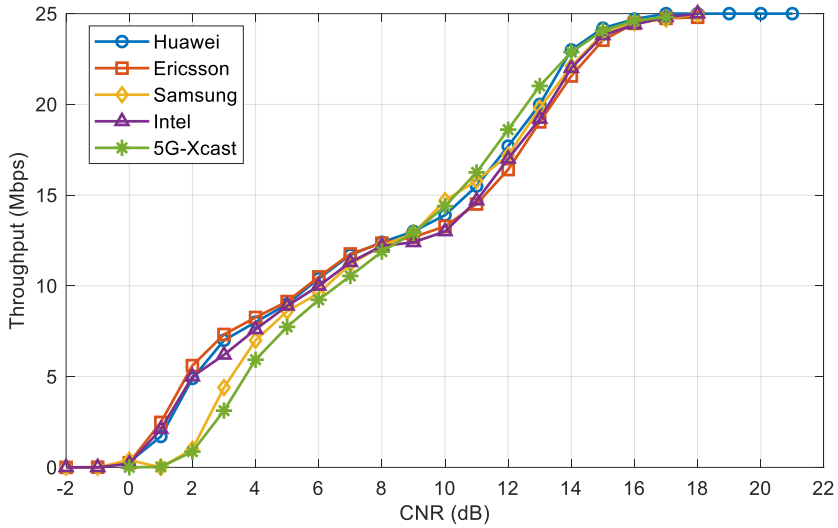

Figure 43. PDSCH Throughput: Case 4.

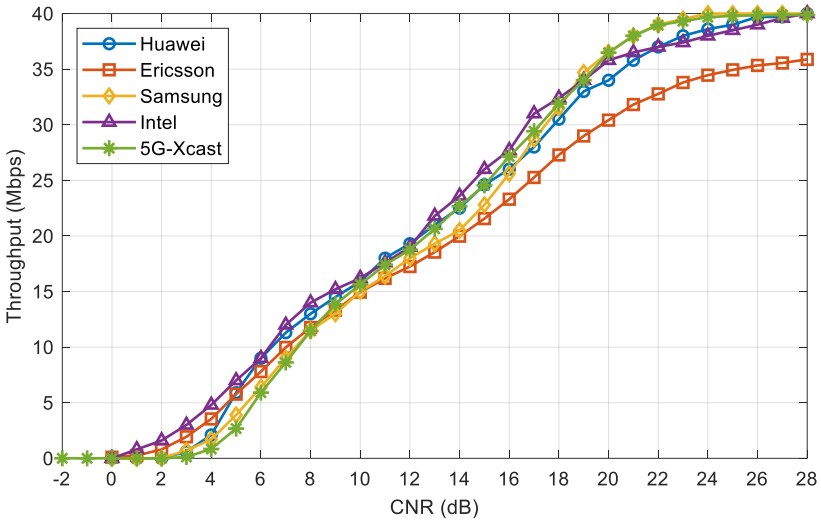

Figure 44. PDSCH Throughput: Case 5.

As shown in Figure 43 and Figure 44, the 5G-Xcast calibration results are fully aligned with those obtained by different companies in 3GPP RAN WG4. As a result of this calibration, the reliability of the simulation results provided in this deliverable is ensured.

References

[1] S. Parkvall, E. Dahlman, A. Furuskar and M. Frenne, "NR: The New 5G Radio Access Technology," *IEEE Communications Standards Magazine*, vol. 1, no. 4, pp. 24-30, December 2017.

[2] D. Gomez-Barquero, D. Navratil, S. Appleby and M. Stagg, "Point-to-Multipoint Communication Enablers for the Fifth-Generation of Wireless Systems", *IEEE Communications Standards Magazine*, vol. 2, no. 1, pp. 53-59, March 2018.

[3] D. Ratkaj and A. Murphy, Eds., "Definition of Use Cases, Requirements and KPIs," Deliverable D2.1, 5G-PPP 5G-Xcast project, October 2017.

[4] 3GPP TR 22.261 v16.3.0, "Service requirements for next generation new services and markets", April 2018.

[5] 3GPP TR 38.913 v14.3.0: "Study on Scenarios and Requirements for Next Generation Access Technologies", August 2017.

[6] D. Vargas and D. Mi, Eds., "LTE-Advanced Pro Broadcast Radio Access Network Benchmark," Deliverable D3.1, 5G-PPP 5G-Xcast project, November 2017.

[7] M. Fuentes *et. al.*, "Physical Layer Performance Evaluation of LTE-Advanced Pro Broadcast and ATSC 3.0 Systems", *accepted for IEEE Transactions on Broadcasting*, 2018.

[8] 3GPP RP-180672: "WID on LTE-based 5G Terrestrial Broadcast", June 2018.

[9] 3GPP RP-180669: "SID on NR Mixed Mode Broadcast/Multicast", June 2018.

[10] 3GPP TR 38.817-01 v1.0.0: "General Aspects for UE RF for NR", March 2018.

[11] 3GPP TS 38.213 v15.1.0: "NR; Physical Layer Procedures for Control", April 2018.

[12] 3GPP TS 38.211 v15.1.0: "NR; Physical Channels and Modulation", April 2018.

[13] 3GPP TS 38.331 v15.1.0: "NR; Radio Resource Control (RRC); Protocol Specification", April 2018.

[14] 3GPP R2-166852: "SC-PTM feedback scheme for link adaptation and retransmission", October 2016.

[15] X. Zhu, D. Yang, J. Wang and X. Zhang, "Small area broadcast in LTE," 2015 *International Conference on Wireless Communications & Signal Processing (WCSP)*, Nanjing, China, 2015, pp. 1-5.

[16] F. Tesema and V. Pauli, Eds., "RAT Protocols and Radio Resource Management in 5G-Xcast", Deliverable D3.4, 5G-PPP 5G-Xcast project, November 2018.

[17] 3GPP TR 36.890 v13.0.0: "Study on Single-Cell Point-to-Multipoint Transmission for E-UTRA (Release 13)", July 2015.

[18] 3GPP R1-1712879: "Forward Compatibility Consideration for ECP Design and NR-MBMS", August 2017.

[19] 3GPP TR 38.912 v14.1.0, Release 14, "5G; Study on new radio access technology", October 2017.

[20] G. K. Walker, X. Zhang and X. F. Wang, "Extended duration cyclic prefix with low overhead for LTE Broadcast" U.S. Patent 2015/0078292 A1, issued March 19, 2015.

[21] M. Joham, W. Utschick, and J. A. Nossek, "Linear Transmit Processing in MIMO Communications Systems," *IEEE Transactions on Signal Processing*, vol. 53, no. 8, pp. 2700-2712, Aug 2005.

[22] V. Stankovic and M. Haardt, "Generalized Design of Multi-User MIMO Precoding Matrices," *IEEE Transactions on Wireless Communications*, vol. 7, no. 3, pp. 953-961, March 2008.

[23] T. K. Y. Lo, "Maximum Ratio Transmission," *IEEE Transactions on Communications*, vol. 47, no. 10, pp. 1458-1461, Oct 1999.

[24] T. Yoo and A. Goldsmith, “Optimality of Zero-forcing Beamforming with Multiuser Diversity,” in *IEEE International Conference on Communications (ICC)*, vol. 1, May 2005, pp. 542-546 Vol. 1.

[25] E. Bjornson, M. Bengtsson, and B. Ottersten, “Optimal Multiuser Transmit Beamforming: A Diffcult Problem with a Simple Solution Structure [Lecture Notes],” *IEEE Signal Processing Magazine*, vol. 31, no. 4, pp. 142-148, July 2014.

[26] Y. Sun and K. J. R. Liu, “Transmit Diversity Techniques for Multicasting Over Wireless Networks,” in *IEEE Wireless Communications and Networking Conference*, vol. 1, March 2004, pp. 593-598.

[27] Q. Spencer, A. Swindlehurst, and M. Haardt, “Zero-forcing Methods for Downlink Spatial Multiplexing in Multiuser MIMO Channels,” *IEEE Transactions on Signal Processing*, vol. 52, no. 2, pp. 461-471, Feb 2004.

[28] Q. Spencer, C. Peel, A. Swindlehurst, and M. Haardt, “An Introduction to The Multi-User MIMO Downlink,” *IEEE Communications Magazine*, vol. 42, no. 10, pp. 60-67, Oct 2004.

[29] Y. C. B. Silva and A. Klein, “Linear Transmit Beamforming Techniques for the Multigroup Multicast Scenario,” *IEEE Transactions on Vehicular Technology*, vol. 58, no. 8, pp. 4353-4367, Oct 2009.

[30] W. Weichselberger, M. Herdin, H. Ozcelik, and E. Bonek, “A Stochastic MIMO Channel Model with Joint Correlation of Both Link Ends,” *IEEE Transactions on Wireless Communications*, vol. 5, no. 1, pp. 90-100, Jan 2006.

[31] M. Tomlinson, “New Automatic Equaliser Employing Modulo Arithmetic,” *Electronics Letters*, vol. 7, no. 5, pp. 138-139, March 1971.

[32] N. D. Sidiropoulos, T. N. Davidson, and Z.-Q. Luo, “Transmit Beamforming for Physical-layer Multi- casting,” *IEEE Transactions on Signal Processing*, vol. 54, no. 6, pp. 2239-2251, June 2006.

[33] E. Karipidis, N. D. Sidiropoulos, and Z. Luo, “Quality of Service and Max-Min Fair Transmit Beam- forming to Multiple Cochannel Multicast Groups,” *IEEE Transactions on Signal Processing,* vol. 56, no. 3, pp. 1268-1279, March 2008.

[34] M. Schubert and H. Boche, “Solution of the Multiuser Downlink Beamforming Problem with Individual SINR Constraints,” *IEEE Transactions on Vehicular Technology*, vol. 53, no. 1, pp. 18-28, Jan 2004.

[35] M. Sadeghi, E. Bjornson, E. G. Larsson, C. Yuen, and T. L. Marzetta, “Max-Min Fair Transmit Precoding for Multi-Group Multicasting in Massive MIMO,” *IEEE Transactions on Wireless Communications*, vol. 17, no. 2, pp. 1358-1373, Feb 2018.

[36] D. Christopoulos, S. Chatzinotas, and B. Ottersten, “Weighted Fair Multicast Multigroup Beamforming Under Per-antenna Power Constraints,” *IEEE Transactions on Signal Processing*, vol. 62, no. 19, pp. 5132-5142, Oct 2014.

[37] Y. Gao and M. Schubert, “Group-oriented Beamforming for Multi-stream Multicasting Based on Quality- of-service Requirements,” in *IEEE International Workshop on Computational Advances in Multi-Sensor Adaptive Processing (CAMSAP)*, Dec 2005, pp. 193-196.

[38] O. T. Demir and T. E. Tuncer, “Antenna Selection and Hybrid Beamforming for Simultaneous Wireless Information and Power Transfer in Multi-Group Multicasting Systems,” *IEEE Transactions on Wireless Communications*, vol. 15, no. 10, pp. 6948-6962, Oct 2016.

[39] D. Vargas, D. Gozalvez, D. Gomez-Barquero and N. Cardona, "MIMO for DVB-NGH, the next generation mobile TV broadcasting," in IEEE Communications Magazine, vol. 51, no. 7, pp. 130-137, July 2013.

[40] D. Gómez-Barquero et al., "MIMO for ATSC 3.0," in IEEE Transactions on Broadcasting, vol. 62, no. 1, pp. 298-305, March 2016.
[41] D. Vargas, “Transmit and Receive Signal Processing for MIMO Terrestrial Broadcast Systems,” Ph.D. dissertation, Universitat Politecnica de Valencia, May 2016.
[42] 3GPP TS 38.212 v15.1.1: “NR; Multiplexing and Channel Coding”, April 2018.
[43] 3GPP TS 38.214 v15.1.0: “NR; Physical Layer Procedures for Data”, April 2018.
[44] ITU-R M2412-0: “Guidelines for Evaluation of Radio Interface Technologies for IMT-2020”, October 2017.
[45] ITU-R WP5D: “Initial Description Template of 3GPP 5G Candidate for Inclusion in IMT-2020”, January 2018.
[46] 3GPP TR 38.901 v14.3.0: “Study on Channel Model for Frequencies from 0.5 to 100 GHz”, January 2018.
[47] ITU-R M.2410-0: “Minimum Requirements Related to Technical Performance for IMT-2020 Radio Interface(s)”, November 2017.
[48] 3GPP TR 37.910 v1.0.0, “Study on Self Evaluation towards IMT-2020 Submission (Release 15)”, September 2018.
[49] ETSI TS 102 831 v1.2.1, “Digital Video Broadcasting (DVB); Implementation guidelines for a second generation digital terrestrial television broadcasting system (DVB-T2)”, August 2012.
[50] L. Zhang, Y. Wu, W. Li, Z. Hong, K. Salehian, H. M. Kim, S. I. Park, J. Y. Lee, P. Angueira, J. Montalban, and M. Velez, “Enhanced DFT based channel estimation for LDM systems over SFN channels,” in *Proceedings IEEE International Symposium on Broadband Multimedia Systems and Broadcasting (BMSB)*, Ghent, Belgium, June 2015.
[51] J. L. Carcel, J. J. Gimenez and D. Gomez-Barquero, "Zero-guard OFDM performance in SFN with ATSC 3.0 ultra-robust transmission modes," *2017 IEEE International Symposium on Broadband Multimedia Systems and Broadcasting (BMSB)*, Cagliari, 2017, pp. 1-5.
[52] 3GPP TR 36.776 v0.0.3 “Study on LTE-based 5G terrestrial broadcast (Release 16)” November 2018.
[53] R1-1811588, Scenarios and simulation assumptions for the LTE based terrestrial broadcast gap analysis, EBU, BBC, IRT; 3GPP RAN WG1 #94-Bis, Chengdu, China, October 2018.
[54] R1-1812430, Evaluation Results for LTE-Based 5G Terrestrial Broadcast, EBU, BBC, IRT; 3GPP RAN WG1 #95, Spokane, USA, November 2018.
[55] L. Fay, L. Michael, D. Gómez-Barquero, N. Ammar and M. W. Caldwell, "An Overview of the ATSC 3.0 Physical Layer Specification," *IEEE Trans. Broadcast.*, vol. 62, no. 1, pp. 159-171, March 2016.
[56] L. Michael and D. Gómez-Barquero, "Bit-Interleaved Coded Modulation (BICM) for ATSC 3.0," *IEEE Trans. Broadcast.*, vol. 62, no. 1, pp. 181-188, March 2016.
[57] K. J. Kim et al., "Low-Density Parity-Check Codes for ATSC 3.0," *IEEE Trans. Broadcast.*, vol. 62, no. 1, pp. 189-196, March 2016.
[58] N. S. Loghin, J. Zöllner, B. Mouhouche, D. Ansorregui, J. Kim and S. I. Park, "Non-Uniform Constellations for ATSC 3.0," *IEEE Trans. Broadcast.*, vol. 62, no. 1, pp. 197-203, March 2016.
[59] 3GPP R4-1812164, “Normal PDSCH demodulation alignment simulation results,” Intel Coorporation, October 2018.
[60] 3GPP R4-1812461, “Simulation results for NR UE PDSCH in FR1,” Samsung, October 2018.
[61] 3GPP R4-1813632, “Simulation results for NR PDSCH demodulation performance requirements,” Huawei, HiSilicon, October 2018.

[62] 3GPP R4-1813439, “Simulation results for NR UE PDSCH demodulation tests,” Ericsson, October 2018.